THE BEHAVIOUR OF STIRRED, TWO AND THREE PHASE SYSTEMS

Andrew Peter Kruszewski

A thesis submitted for the degree of Doctor of Philosophy at the University of London.
(1985)

The Department of Chemical Engineering and
Chemical Technology,
Imperial College of Science and Technology, London.

ABSTRACT :

The aim of the project has been to examine the factors influencing the performance of an agitated tank for two phase (gas-liquid) and three phase (gas-liquid-solid) systems. This was done by measuring the power consumption of the stirrer and the (gas-liquid) interfacial area produced for a number of impeller designs and for a range of gas flowrates. Both single tube and ring spargers were used as gas inlets.

Organic and aqueous liquid phases were studied using the chemical method to determine the active interfacial area. For an aqueous system, the oxidation of sodium sulphite was employed, whilst several amine-CO_2 reactions were tried in the case of organic liquids. Kinetic data for all of these were obtained from experiments with a quiescent interface cell.

As well as demonstrating the considerable importance of impeller and gas sparger design, the results also show the effect of gas flowrate, stirrer speed and mass of solids upon the major parameters : power requirement, gas dispersion and solids suspension.

Although the sulphite-air reaction was used successfully to obtain values of interfacial area in aqueous systems, none of the organic reactions considered was sufficiently slow for the chemical method to be applicable quantitatively. However, it was found that one of them (di-isopropanolamine-CO_2) could be used to make qualitative comparisons between the various operating conditions.

(continued overleaf)

ABSTRACT : (contd.)

In view of the results, it is suggested that future work might include :

- a further search for a more appropriate organic chemical reaction,
- the collection of data for a wider range of solid particle sizes,
- measurements of interfacial area using a suitable physical method,

and, perhaps most importantly :

- experiments in one or more larger vessels in order that scale-up rules may be determined.

With many thanks to my supervisor, Professor H.Sawistowski, for his help and guidance throughout the project; to the workshop and glass-blowers of our department for their manufacture of the apparatus and to I.Drummond of analytical services for his advice.

I am very grateful to the Science and Engineering Research Council for their financial support of my post-graduate studies.

Dla Mamusi.

INDEX :

Title Page	1.
Abstract	2.
Acknowledgement	4.
Index	5.
List of Figures	13.
Glossary	15.

INDEX :

1. INTRODUCTION	17.
2. LITERATURE SURVEY (THEORY)	20.
2.1 Mass transfer Rates	20.
2.1.1 Physical Methods	20.
2.1.2 Chemical Methods	21.
2.2.1 Sulphite Method	22.
2.2.2 Amine-CO_2 Method	24.
2.3 Gas Flowrate, Gas Sparger	25.
2.4 Power Input, Stirrer Speed	26.
2.5 Stirrer Configuration	27.
2.6 Solids	29.
2.7 Liquid Viscosity	32.

INDEX :

3. EXPERIMENTAL 33.

3.1 Agitated Vessel : Description 33.
3.1.1 Experimental Procedure 36.
3.1.2 Sulphite Method 36.
3.1.3 Amine-CO_2 Method 37.
3.1.4 Aims 38.

3.2 Quiescent Interface Cell : Description 39.
3.2.1 Experimental Procedure 39.
3.2.2 Aims 41.

3.3 Analysis of Samples 41.
3.3.1 Sulphite Method : Analysis 41.
3.3.2 Amine-CO_2 Method : Analysis 42.

3.4 Safety 43.

INDEX :

4. RESULTS	45.
4.1 Physical Measurements : Two Phase	45.
4.1.1 Stirrer Speed v Power	45.
4.1.2 Gas Flowrate v Power	45.
4.1.3 Stirrer Configuration	54.
4.1.4 Liquid Phase	55.
4.1.5 Flow Patterns, Gas Distribution	56.
4.1.6 Correlation and Comparison of Results	57.
4.2 Physical Measurements : Three Phase	68.
4.2.1 Solids Concentration v Suspension	68.
4.2.2 Gas Flowrate v Suspension	68.
4.2.3 Stirrer Configuration	77.
4.2.4 Comparison with Our Previous Results	78.
4.2.5 Correlation with Other Results	80.
4.3 Quiescent Interface Cell	85.
4.3.1 CHA-CO_2	85.
4.3.2 DEA-CO_2	87.
4.3.3 DIPA-CO_2	89.
4.3.4 Sodium Sulphite - O_2	91.

INDEX :

4. RESULTS (contd.)

4.4 Agitated Vessel : Organic Liquid Phase	92.
4.4.1 CHA-CO_2	92.
4.4.2 DEA-CO_2	92.
4.4.3 DIPA-CO_2	94.
4.5 Agitated Vessel : Inorganic Liquid Phase	98.
4.5.1 Ring Sparger, Disc Turbines	98.
4.5.2 Ring Sparger, Propellers	101.
4.5.3 Single Tube Sparger, Propellers	104.
4.5.4 Correlation and Comparison of Results	108.

INDEX :

5. CONCLUSIONS	115.
5.1 Power Consumption	115.
5.2 Gas Sparger	115.a
5.3 Solids	116.
5.4 Organic Systems	118.
5.5 Interfacial Areas	118.
5.6 Optimum Conditions	120.
5.7 Assessment of Methods and Apparatus	121.
5.8 Future Work	122.

INDEX :

APPENDICES :

A 3.1.1 : Calculation of Power Input 124.

A 3.1.2 : Sulphite Reaction :
Variation of Rate with Temperature 125.

A 3.3.1 : Analysis of Sulphite Samples 127.

A 3.3.2 : Analysis of Amine Samples 129.

A 3.4 : Safety 132.

B 4.1 : Two Phase Physical Measurements 135.

C 4.2 : Three Phase Physical Measurements 148.

INDEX :

APPENDICES : (contd.)

D 4.3	: Quiescent Interface Cell	152.
D 4.3.1	: CHA-CO_2	152.
D 4.3.2	: DEA-CO_2	153.
D 4.3.3	: DIPA-CO_2	155.
E 4.4	: Agitated Vessel : Amine-CO_2 Reactions	157.
E 4.4.1	: CHA-CO_2	157.
E 4.4.2	: DEA-CO_2	158.
E 4.4.3	: DIPA-CO_2	159.
F 4.5	: Agitated Vessel : Sulphite Oxidation	161.
F 4.5.1	: Ring Sparger : Disc Turbines	161.
F 4.5.2	: Ring Sparger : Propellers	171.
F 4.5.3	: Single Tube Sparger : Propellers	180.

REFERENCES : 188.

LIST OF FIGURES :

1.	: Four types of slurry reactor	18.
3.1a	: Agitated vessel apparatus	34.
3.1b	: Disc turbine and propeller design	35.
3.2a	: Quiescent interface cell	40.
4.1.1a	: P v N Downflow Disc	46.
4.1.1b	: " " Upflow "	47.
4.1.1c	: " " Downflow Propeller	48.
4.1.1d	: " " Upflow " "	49.
4.1.2a	: P v Q_G Downflow Disc	50.
4.1.2b	: " " Upflow "	51.
4.1.2c	: " " Downflow Propeller	52.
4.1.2d	: " " Upflow " "	53.
4.1.6a	: Ne v N Downflow Disc, Upflow Propeller	59.
4.1.6b	: P_G v $(P_0ND^3/G^{0.56})^{0.45}$ Downflow Disc	62.
4.1.6c	: $\log(P_G)$ v $\log(P_0ND^3/G^{0.56})$ " "	63.
4.1.6d	: (P_G/P_0) v N Upflow Propeller	64.
4.1.6e	: " " Downflow Disc	65.
4.1.6f	: " v G Upflow Propeller	66.
4.1.6g	: " " Downflow Disc	67.
4.2.1a	: N_{JS} v X Downflow Disc	69.
4.2.1b	: " " Upflow "	70.
4.2.1c	: " " Downflow Propeller	71.
4.2.1d	: " " Upflow " "	72.
4.2.2a	: N_{JS} v Q_G Downflow Disc	73.
4.2.2b	: " " Upflow "	74.
4.2.2c	: " " Downflow Propeller	75.
4.2.2d	: " " Upflow " "	76.

LIST OF FIGURES :

4.2.5a : log(N_{JS}) v log(M) Disc Turbines, 3-phase 82.
4.2.5b : " " Propellers, 3-phase 83.
4.2.5c : ΔN_{JS} v Q_G Disc Turbines, 3-phase 84.

4.3.1a : Quiescent Interface Cell : CHA-CO_2 rate 86.
4.3.2a : " " " : DEA-CO_2 rate 88.
4.3.3a : " " " : DIPA-CO_2 rate 90.

4.4.1a : Agitated Vessel : CHA-CO_2 93.
4.4.3a : " " : DIPA-CO_2 2- v 3-phase 95.
4.4.3b : " " : DIPA-CO_2,
Downflow Disc v Upflow Propeller 96.

4.5.1a : A v Q_G : Ring Sparger, Discs 99.
4.5.1b : A v N : " " , " 100.

4.5.2a : A v Q_G : Ring Sparger, Propellers 102.
4.5.2b : A v N : " " , " 103.

4.5.3a : A v Q_G : Single Tube, Propellers 105.
4.5.3b : A v N : " " , " 107.

4.5.4a : A v Fl, Downflow Disc and Propeller 109.
4.5.4b : log(A) v log(N) Ring Sparger 111.
4.5.4c : " v log(Q_G) " " 112.
4.5.4d : " v log(N) Single Tube Sparger 112.a
4.5.4e : " v log(Q_G) " " " 113.
4.5.4f : A v P, Disc Turbines 113.a
4.5.4g : " ", Propellers 114.
4.5.4h : log(A) v log(P), all impellers 114.a

GLOSSARY :

1. a : specific surface area (m^2)
2. A : active interfacial area per unit volume (m^2/m^3)
3. A.C. : alternating current
4. B_o : bulk concentration of B (mol/l)
5. C_{Ai} : interfacial concentration of A (mol/l)
6. CHA : cyclohexylamine
7. CMC : carboxymethylcellulose
8. d_S : diameter of solid particles (m)
9. D : stirrer diameter (m)
10. D_A : diffusivity of A (m^2/s)
11. D_R : reactor vessel diameter (m)
12. DEA : diethanolamine
13. DIPA : di isopropanolamine
14. E : extension of spring (cm)
15. E_a : activation energy of a reaction (Joules)
16. F : force on spring (N)
17. Fl : Gas Flow number (= G/ND^3) (-)
18. Fr : Froude number (= DN^2/g) (-)
19. G : volumetric gas flowrate (l/min)
20. H_A : height of A-component peak on chart recorder
21. Ha : Hatta number
22. i : interface
23. IPA : isopropyl alcohol
24. $k_{m,n}$: m-,n-th order reaction rate constant
25. k_2 : pseudo second order reaction rate constant
26. K_G : gas phase mass transfer coefficient
27. K_L : liquid phase mass transfer coefficient
28. L : length of spring (cm)
29. M : mass of solids (g)
30. M_A : molarity of a solution of A (mol/l)
31. M(A) : " " " " " " "
32. MEA : monoethanolamine
33. N : stirrer speed (rpm)
34. N_A : molar flux of A (mol/l/s)
35. Ne : Newton or Power number (= $P/\rho_L N^3 D^5$) (-)

GLOSSARY : (contd.)

36. N_{JS} : stirrer speed to just suspend the solids (rpm)
37. p_A : partial pressure of A (-)
38. P : power input to air motor (Watts)
39. P_G : power for an aerated system (Watts)
40. P_O : power for an unaerated system (Watts)
41. PTFE : polytetrafluoroethylene
42. Q_G : gas flowrate per unit volume of reactor (vvm)
43. r : radius of motor-spring attachment (m)
44. R : Gas constant (= 8.314 Joule/K/mol)
45. R_A : rate of absorption of A (mol/s)
46. Re : Reynolds number of stirrer (= $\rho_L D^2 N/\eta$) (-)
47. S : active gas-liquid interfacial area (cm^2)
48. t : time of an experimental run (mins or s)
49. T : temperature (^oC, K)
50. T : torque on the stirrer shaft (Nm)
51. u : superficial gas velocity (m/s per m^2)
52. u_B : relative velocity between solid and gas (m/s)
53. V(A) : volume of a solution of A (cm^3)
54. We : Weber number (= $\rho_S d_S u_B^2/\sigma$) (-)
55. X : proportion of solids (wt.%)

56. δ : bubble diameter (m)
57. δ_{sm} : sauter mean diameter of a dispersed gas phase
58. η : viscosity (kg/ms)
59. ν : kinematic viscosity (m^2/s)
60. π : 3.14...
61. ρ_L : density of liquid (kg/m^3)
62. ρ_S : " " " solid "
63. σ : surface tension (N/m)
64. τ : shear stress (kg/ms^2)
65. ϕ : volumetric gas holdup
66. ω : angular speed of rotation of stirrer

1. INTRODUCTION :

Three phase or 'slurry' reactors (consisting of a continuous liquid phase in which a gas is dispersed and solids are suspended) fall into four main categories :

(i) Stirred tanks : mixing by mechanical agitation.

(ii) Bubble columns : gas introduced at the base sets up convection currents in the liquid.

(iii) Jet-loop reactors : fluid is circulated in the vessel around a set of baffles.

(iv) Fluidised beds : mixing via an upward flow of gas and/or liquid through a column of solids.

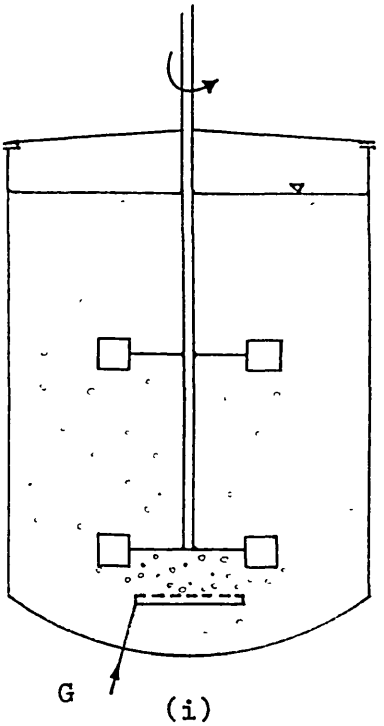
(see Fig.1.)

This project deals with the stirred tank, by far the most common type of mixer. Such slurry reactors have several advantages over other, more conventional types of fixed bed reactor :

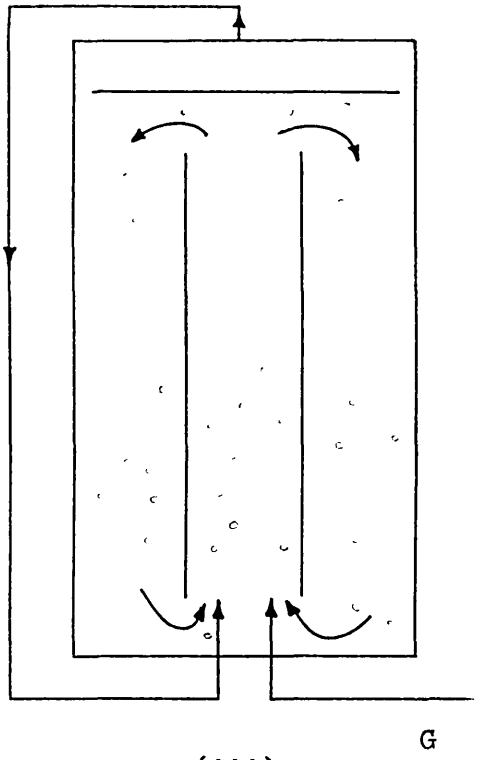
- intimate mixing of the reactants,
- rapid heat transfer, enabling isothermal conditions,
- uniform and hence more effective use of the catalyst,
- faster reactions achieved in smaller volumes,
- the possibility of continuous catalyst regeneration,
- a reduced risk of blockage by solids c.f. fixed beds,
- ease of switching from batch or semi-batch to continuous operation.

It is for these reasons that slurry reactors are being increasingly used in a range of processes including :

- hydrogenation (mainly oils and, more recently, coal)
- oxidation

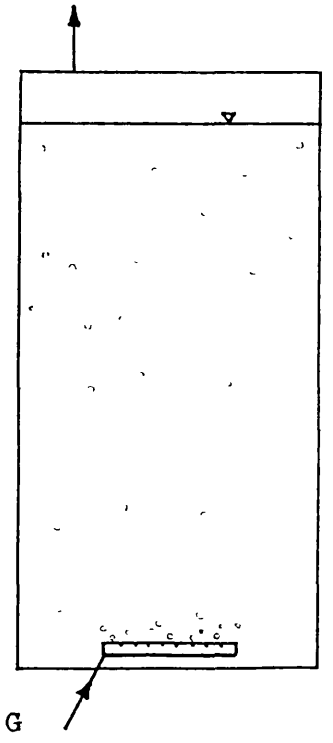


(i)

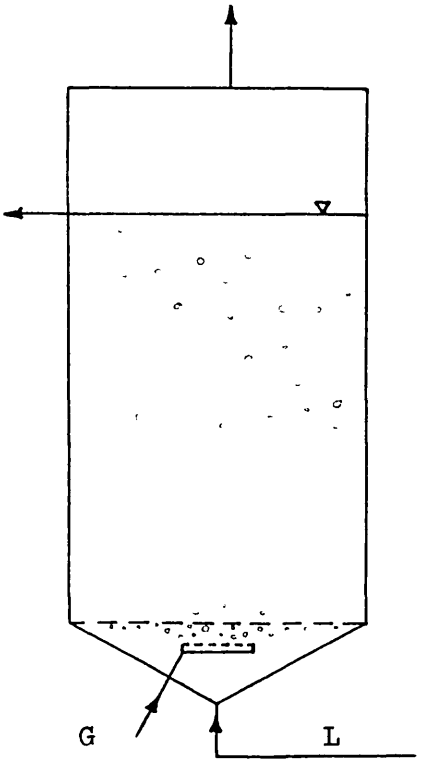


(iii)

Fig.1



(ii)



(iv)

- polymerisation
- halogenation
- fermentation
- waste water treatment and purification.

Note that the solid phase may be a catalyst, e.g. nickel in the hydrogenation of vegetable oils; a reactant, as in coal liquefaction; or a product, as in the oxidation of p-xylene.

It is from the last of these reactions, carried out in a stirred tank, that the present project originated. For this reason, certain limitations were placed upon the reactor design : the comparative height of the vessel necessitated the use of two impellers mounted on a single shaft (quite common in industrial processes), the upper one being a four blade open turbine (to re-disperse gas). For the lower impeller (suspending solids as well as dispersing gas) four designs were tested : up- and downflow, pitched blade disc turbines and propellers.

In earlier work on the project (16), gas (air) was supplied by a single tube sparger (the danger of product formation within the gas inlet precluded the use of, say, a sintered plate). Further experiments have now been carried out with a ring sparger, for comparative purposes.

Within these geometric constraints, the purpose of the study has been to examine, measure and (as far as possible) optimise the variables affecting the operation of such a vessel, bearing in mind three main aims, namely :

- good dispersion of the gas throughput,
- complete suspension of the solids,
- low power consumption.

2. LITERATURE SURVEY (THEORY) :

2.1 Mass Transfer Rates :

In any chemical process, the main objective is to maximise the rate of product formation under the most economic conditions. Thus in a slurry reactor, the rate of mass transfer is of overriding importance and, as Hofmann (15) points out, though little or no information is available for mass transfer in the gas phase ($K_G a$), fortunately the gas phase resistance is usually negligible with respect to that of the liquid phase.

For scale-up of, or comparison between slurry reactors, it is thus the value of $K_L a$ that is of interest and above all, the value of 'a' (the specific interfacial area) since the variation in K_L (the liquid phase mass transfer coefficient) is not generally very large. Also to be desired is a knowledge of the gas hold-up ($\emptyset$) and the distributions of bubble size (δ) and residence time (τ).

Methods of measuring these variables may be divided into two broad categories :

(i) physical

(ii) chemical

2.1.1 Physical Methods :

(see Charpentier & Morsi : 14.a)

These include photography, electrical resistivity, optical transmittivity, laser light scattering (applying the Lambert-Beer law) and light de-polarisation. Though the last three have the advantage of not interfering with the system being observed, they are all unsuitable in the present case because they cannot distinguish between scattering due to solid particles and that due to gas bubbles (and are also only effective over fairly short path lengths, i.e. for small vessels).

An electrical resistivity probe might provide useful data except that it must inevitably have some

influence on the system under examination, particularly since it would have to be robust enough to withstand the impact of any solid particles present and is also apparently unreliable for the measurement of bubbles less than about 0.5 mm in diameter (: Pohorecki 7.b) (which could account for a significant proportion of the gas-liquid interfacial area).

Although photography suffers from none of the aforementioned problems, it does have several disadvantages : It is inevitably time-consuming and tends to register only those bubbles that are in close proximity to the wall of the vessel. Since only small bubbles tend to congregate in the near wall region, unrepresentatively large values of interfacial area ensue : this explains, at least in part, why results using physical and chemical methods for the same apparatus can vary considerably (see Kürten & Zehner 1.c, Charpentier 14.a). Neither is the alternative of inserting light and photographic probes very satisfactory (for the same reasons as for the resistivity probe). Nevertheless, photography is one of the few methods able to provide a measure of the bubble size distribution.

Therefore, whilst use of physical methods to obtain overall values of interfacial area is not to be recommended, they are necessary for hold-up and bubble size distribution measurements and can be useful in pointing out local effects in a reactor, e.g. a chemical method may show that one reactor design is better than another (in that it produces a larger interfacial area) but only a physical method can show why, or in which region of a vessel, the difference between the two arises.

2.1.2 Chemical Methods :

Methods of this type give a direct measure of active surface area (S), i.e. bubbles depleted of reacting gas are not included, as opposed to physical techniques : this offers a further reason for the discrepancy between results using chemical and physical means. For example, a physical method

might suggest that an increase in stirrer speed has increased the interfacial area, whereas a chemical method may point out that the active area has hardly changed (i.e. that only an increase in residence time of largely depleted bubbles has been achieved : clearly a wasted effort).

Several chemical reactions have been used in the past, among them :

- absorption of oxygen into sodium dithionate (Sharma 2.e)
- absorption of carbon dioxide into sodium hydroxide (or other alkali) or into a sodium carbonate-bicarbonate buffer solution.
- absorption of oxygen into sodium sulphite solution :

$$2Na_2SO_{3(aq)} + O_{2(g)} \dashrightarrow 2Na_2SO_{4(aq)}$$

(Danckwerts 5.b)

For a review of these and other methods, see Sharma & Danckwerts (15.a)

Although both of the last two reactions above have been widely used and are well documented, it was shown by Mersman (13.b), that the sulphite method is more widely applicable and since, additionally, air (oxygen) was more conveniently available, the latter was selected and used successfully in earlier work on this project (16).

2.2.1 The Sulphite Method :

(see Danckwerts 5.a, 5.b)

To obtain a realstic value for gas-liquid area, it is necessary that :

- the reaction is fast enough to take place at or near the interface ($Ha \geq 3$),
- it is slow enough that there is no significant depletion of sulphite (or change of pH) near the surface of the liquid,

- the concentration of oxygen in the bulk of the liquid is approximately zero,
- there is no great depletion of oxygen in a gas bubble.

These conditions have been found to be satisfied when the sulphite concentration is in the range 0.5 to 0.8 M (by Reith 10.). The reaction is then of second order with respect to oxygen and zero order for sodium sulphite. (Onken and Schalk : 1.a, have since shown the possible range of sulphite concentrations to be wider : 0.2 to 0.8 M). The rate constant (k_2) is, therefore, dependent upon catalyst concentration, temperature and pH : Though the heat generated by the reaction has caused some problems due to the impracticality of temperature control on the apparatus used here, it can be monitored and taken into account, whilst the other two variables can be controlled fairly easily.

Thus the rate of absorption is :

$R_A = N_A S$ = Molar flux x Interfacial area

N_A for an irreversible m-,n-th order reaction (pseudo m-th order regime) is :

$$N_A = (2 \times k_{mn} \times D_A (C^*_{Ai})^{m+1} \times (B_o)^n / (m + 1))^{0.5} \quad \text{I}$$

where D_A = diffusivity of A (oxygen)

C^*_{Ai} = interfacial concentration of A (O_2)

and B_o = bulk concentration of B (sulphite)

With $m = 2$ and $n = 0$ (for $0.2 < B_o < 0.8$) :

$$\therefore N_A = (\tfrac{2}{3} \times k_2 \times D_A \times (C^*_{Ai})^3 \times (B_o)^0)^{0.5}$$

$$= (C^*_{Ai})^{1.5} (2k_2 D_A / 3)^{0.5} \quad \text{II}$$

(Danckwerts 5.a)

and $\therefore S = R_A/N_A = R_A/((C^*_{Ai})^{1.5}(2k_2D_A/3)^{0.5})$ III

C^*_{Ai} can be estimated from the partial pressure of A (oxygen) and Henry's law (for constants, see 11.) and diffusion coefficients are given in literature or may be calculated using the Wilke-Chang equation or a suitable equivalent.

Thus, having measured R_A experimentally, the only unknown is k_2. The sulphite method has been used extensively in the past and some values for k_2 are available (Linek : 2.b and 2.c, even gives an equation relating it to catalyst concentration, pH etc.) but as Danckwerts points out, k_2 is very sensitive to impurities in the sulphite solution. It is therefore advisable to obtain values for the actual sulphite used by measuring the rate of reaction across a known, constant gas-liquid area (see section 3.2).

2.2.2 Carbon Dioxide - Amine Method :

For the study of two- and three-phase mixing tanks, the sulphite method has one serious drawback in that it requires the use of an aqueous liquid phase (whereas many industrial processes that make use of this type of reactor involve organic liquids). The main difficulty stems from the consequent necessity to use hydrophilic (and inert) solid particles : the lightest available being glass or sand ($\rho_S/\rho_L \sim 2.6$) whilst the ratio of densities between solid and liquid in an organic system is generally only slightly greater than one.

One of the conclusions drawn from the initial work on this project was, therefore, that an organic reaction equivalent or similar to the sulphite-air system would provide a wider range of parameters (ρ, ν etc.) and help to establish a better model of the hydrodynamic conditions within a typical stirred tank reactor.

Some studies have been carried out (for gas-liquid systems) over the last few years with this in mind

and Charpentier and Morsi (14.a) provide a useful review of the work so far. The most commonly used method would appear to be the CO_2-cyclohexylamine (CHA) reaction. It has been shown to be of first order with respect to CO_2, second order w.r.t. CHA (: Alvarez-Fuster 2.d), and that the gas phase resistance is negligible :

$$CO_2 + 2RNH \longrightarrow RNCOO^- + RNH_2^+$$

However, it has also been pointed out by Alvarez-Fuster that the rate of reaction is sufficiently fast that for efficient systems (such as a long packed column or well-agitated reactor) 'the conditions of a rapid chemical reaction might not be respected everywhere in the contactor' (14.a).

Other amine-CO_2 reactions have been put forward as possible alternatives, including mono- and di-ethanolamines :

MEA-CO_2 : 2^{nd} order (1 CO_2, 1 MEA)

DEA-CO_2 : 3^{rd} order (1 CO_2, 2 DEA)

(Both in aqueous solution) (2.d and 17)

For each amine, the rate of reaction had first to be measured across a known interfacial area for given conditions of CO_2 partial pressure and type of solvent (as had previously been done with the sulphite reaction) using a cell constructed for the purpose (see section 3.2).

2.3 Gas Flowrate, Gas Sparger :

Clearly, in order to achieve as high a rate of reaction as possible, a large interfacial area is required and hence a thorough dispersion of the gas phase (3.d), (bubble formation mechanisms : 1.h). It has already been indicated though (section 2.1.2), that making bubbles of gas too small and increasing their residence time by too much, would represent a waste of energy : the gas becoming depleted of

reactant (oxygen for the sulphite method, carbon dioxide with the amine reaction) and power being expended in the dispersion of inert gas.

However, the earlier work on this project demonstrated that this is much less of a danger than at first expected. Indeed, using a single tube sparger, any increase in stirrer speed improved the active interfacial area and the only operating problem seemed to be to avoid flooding the impellers at higher gas rates (accompanied by a rapid fall in gas-liquid surface area).

A considerable amount of work has been done in the past (for two phase systems) to ascertain the best means of introducing gas into the vessel. For example, it has been shown that the sparger is better placed beneath, rather than adjacent to, the lower of the two impellers. Further, there is reportedly (for a given ratio of impeller to tank diameter) an optimum depth of inlet below the turbines : Nagata (6.a).

Bearing all these results in mind, it was decided to focus attention on the use of a better gas sparger. Sintered plates, though they provide a very high degree of pre-dispersion of the gas, do have disadvantages, particularly for slurry reactors, where the danger of blockage by solids is high, especially if the particles are forming as a product of the reaction. (Buchholz et al (1.j) have studied gas distribution and mass transfer rates for sintered and perforated plates in (two phase) bubble columns and stirred vessels).

It was felt that a ring sparger (section 3.1) was rather less likely to suffer from blockage problems, at the same time dispersing incoming gas much better than a single tube (thereby increasing interfacial area and reducing the risk of flooding). Note : Smith et al (22) have found the diameter of the sparger to be of little importance unless it is greater than the diameter of the impeller, in which case power consumption is larger and gas hold-up is smaller.

The gas flowrates used in this work are quite high c.f. the experimental work of many others but they are comparable to flowrates commonly encountered in industrial size equipment (19.b). Consequently, on the laboratory scale, the power required to pump gas is of similar magnitude to the impeller power consumption (see Appendix 3.1.1). However, in scaling up to full-size (i.e. increasing the diameter by about 10 to 50 times) the two components of energy needed will increase divergently : Gas sparging power is proportional to volumetric flowrate x height and therefore needs to be increased as D^3H, i.e. $P_{gas} \propto D^4$ (if D/H is constant); whereas impeller power is proportional to D^5 (: for turbulent flow, $Ne = P/\rho N^3D^5$ = constant) i.e. in full-scale, the power to pump gas will only be a few per cent or less of the total energy requirement. So although gas compression power requirement is not negligible on a small scale, it is the impeller power that is decisive in practice. On a larger scale, the potential savings in gas sparging power are orders of magnitude smaller than the possible benefits of optimising the stirrer design and operating conditions.

2.4 Power Input, Stirrer Speed :

(see Herringe : 3.a)

The power consumption of stirred, gas-liquid systems has been the subject of considerable study, particularly by Smith and co-workers (2.f, 22, 23, 24.b) who have used photographic techniques for Rushton disc turbines to help analyse the effect of gas sparging. Smith et al (and others) have made a number of observations which help to explain the complex behaviour that is encountered and these are discussed below and in the following sections :

The power consumption of an aerated system has been found to be controlled entirely by the formation of gas-filled cavities behind stirrer blades, on the size and shape of these cavities and the resulting drag reduction effect they have (22).

Roll vortices form behind the blades of a stirrer and these tend to entrain gas (even large bubbles some distance from an impeller). At very low stirrer speeds ($\lesssim$ 0.4 m/s : 2.f) the cavities are unstable and gas is swept away or coalesces and escapes. At low to high speeds (N), stable cavities are formed with only excess gas escaping after being dispersed as small bubbles at the turbulent tip of a cavity (i.e. this is the mechanism by which larger gas-liquid areas are generated : gas from larger bubbles is entrained and re-emerges in smaller bubbles).

The size and shape of the cavity is dependent on gas supply and impeller speed but three main types have been identified :

(i) At low gas rates (G), the air occupies the trailing vortex core behind the blade : capture and dispersion of gas bubbles is highly efficient but there is little effect on the power consumption since only the vortex core is filled with air and the drag on the blade is barely reduced.

(ii) At intermediate gas rates, the vortex cavities enlarge and fasten on to the horizontal edge of a blade : although dispersion of bubbles still takes place via a trailing vortex, there is now some hydrodynamic smoothing of the blades and the drag is reduced to about 80 % of its unaerated value.

(iii) At slightly higher gas rates, there is a sudden transition (at Fl : $G/ND^3 \sim 0.03$) where alternate blades become totally blanketed by large cavities (note : these have been found to be stable in position if the number of blades is even but unstable if odd). This gives a sudden reduction in drag and drop in power consumption. However, part of the radial outflow from the turbine is now blocked, the trailing vortex is eliminated and the distribution of gas is poorer.

Further increases in gas flow result in the gradual formation of progressively larger cavities

behind each blade (although they still tend to alternate in size) until a maximum is reached. The gas rate can then still be increased considerably before the impeller stops pumping i.e. is flooded and any more gas passes through undisturbed. (22, 23, 24.b)

By this stage, the power (P_G) to maintain a constant speed (N) is about a third to a half of the unaerated value (P_0). The relationship between (P_G/P_0) and Fl is further complicated by the effects of recirculation and speed :

At stirrer speeds above about 1.0 m/s ($\sim$ 300 rpm for our apparatus) recirculation of gas occurs below the impeller and both above and below it at about 2.5 m/s or more. This results in shorter residence times of gas in a cavity (hence large bubbles are broken up more rapidly) i.e. the effective flowrate past the impeller is higher at higher speeds resulting in greater streamlining and a more rapid drop in gassed power. The magnitudes of such recirculation effects have been estimated (23) and this allows the plots of (P_G/P_0) vs Fl to be reduced to one curve, independent of N : but only until the formation of large cavities.- Since the size and maximum size of large cavities (and therefore the drag reduction effect) are functions of speed, once this type of cavity forms, the power curves diverge for different speeds : G/ND^3 is not therefore an entirely satisfactory correlating variable (especially at the higher gas rates to be considered here).

2.5 Stirrer Configuration :

As well as noting the instability of cavities with odd numbered blades, Smith et al (22) have observed that the greater the number of blades, the greater the number of cavities and therefore the higher the gas handling capacity i.e. lower susceptibility to flooding. Although more blades need more power, they give more radial flow and better liquid mixing, so that smaller but multibladed impellers are more effective than larger ones with fewer blades operating at the same speed and power.

Nagata (6.a,b) discusses many of the possible stirrer designs but comes to two fundamental conclusions, namely that :

- some form of disc turbine is better than, for example, a paddle arrangement which would allow a sizeable proportion of the gas to pass straight up through the vessel around the stirrer shaft without making significant contact with the liquid phase (especially at higher gas flowrates and lower stirrer speeds).
- for slurry (three phase) vessels, two stirrers are recommended : the lower one primarily to suspend the solids whilst the upper one serves mainly to disperse gas bubbles.

The four alternatives considered here all incorporate two (co-axial) impellers, all with four, equally spaced blades.

The upper impeller is always a disc turbine (with vertical blades) its purpose being to re-disperse gas on the way up through the tank (the comparatively large height to diameter ratio of the vessel makes the presence of such a second impeller advisable).

In the first part of this project, the two lower impellers employed were both pitched blade disc turbines, the difference between the two being the direction of the slant,- 'forward' (45^{o}) or 'back' (135^{o}) providing a downflow and upflow respectively.

Chapman et al (18), having carried out exhaustive studies using angled blade impellers (as well as some work on disc turbines and propellers) state that :

(i) the more blades on an impeller, and

(ii) the larger the blades, the better the gas dispersion and solids suspension for a given power input.

(iii) Whilst downflow stirrers are better for both gas dispersion and solids suspension at zero and low gas rates, they suffer from 'instabilities' due to their countercurrent effect on the upward flow induced by the sparger and that, therefore :

(iv) upflow arrangements are more stable and are more efficient at high gas rates.

(v) Disc turbines are thought to be the most versatile for three phase operations, though the point is made that the 'best' two phase impeller need not be the ideal three phase one.

This study has not looked at how the size or number of blades affects the mixing process, though clearly there will be limits to the benefits gained by increasing either of them (e.g. a stirrer only slightly smaller than the tank diameter would surely inhibit solids suspension).

However, some work has been carried out to compare up- and downflow stirrers in an air-water-sand system (16.) and the downflow design was found to be better under all conditions (particularly for solids suspension) though it should be re-emphasised that this was for pitched blade disc turbines (not angled paddle blades as mostly used in 18).

It has now been decided to try comparable up- and downflow propellers to see if the resulting decrease in energy requirement could be achieved without adversely affecting the solids suspension and gas distribution performance. (For completeness, the two propellers were to be tested with the single tube gas sparger in addition to experiments using all four stirrer designs with the 'new' ring sparger).

2.6 Solids :

In a slurry reactor, the nature of the solids, the part they play in the reaction, will vary from one process to another : reactant, catalyst or product. Whatever the case, it is generally desirable to keep the solid phase suspended, if not evenly dispersed. For catalyst or reactant particles, the reasons for this are plain; for solids produced as a result of the reaction it may be important to simply prevent agglomeration at the base of the vessel and to attain a more or less uniform product size.

At this stage it is necessary to define what exactly is meant by suspension. Nienow (19.a) describes three possible criteria :

(i) Just completely suspended (at stirrer speed N_{JS}),- the most commonly used condition, occurring when no particles are observed to remain at the bottom of the vessel for more than 1 to 2 seconds, at which stage all of the particles should be available for the reaction.

(ii) Homogeneous suspension (at N_H) : cannot really be applied to multi-impeller vessels such as the one used here since (particularly for heavy particles)

homogeneity is almost impossible to achieve (and difficult both to assess and observe in a highly turbulent slurry).

(iii) Interface height (at N_{SH}) : the agitator speed at which solids are seen to reach 90.% of the liquid level. Though easily measured, this is not a satisfactory criterion when considering light and/or small particles which will fulfil the condition even whilst a substantial proportion of the solids remains undisturbed.

This study has therefore used (i), the N_{JS} measurement.

Clearly, particle size and density (relative to the fluid) play an important part in determining the suspension characteristics. Having carried out experiments for an air-water-sand system (with only limited success : complete suspension could only be achieved by the downflow turbine at high rotor speeds and low proportions of solids) it was hoped to obtain data for more buoyant particles by using organic liquids and solids (see sections 3.1, 3.1.2) and trying both the disc turbines and the propellers.

Some correlations for the power or stirrer speed required to attain complete suspension have been put forward (see Wiedmann et al : 1.e, Herringe : 3.a, Chapman et al : 18 and Nienow : 19.a) but they all need to be treated with caution : the complexity of three phase flow makes it extremely difficult to produce a reasonable model and the wide variety of vessel, stirrer and gas sparger designs tends to add to the confusion : Nienow gives a number of examples :

- the 'Bourne bottom' : an up-turned cusp-shaped base around the stirrer shaft that discourages particles from settling out, perhaps used in conjunction with
- a draught tube around the impeller that also aids the convective flow around the tank.

- On the other hand, the presence of a sparge pipe creates a dead zone in which particles tend to accumulate.

Note : the effect of gas flowrate on suspension is dealt with in detail in sections 4.2.1 to 4.2.5 inclusive, but essentially the presence of gas cavities (see section 2.4) diminishes the pumping capacity and hence inhibits the mechanisms thought to be responsible for solids suspension, namely : drag and turbulence.

Therefore, it remains only to predict the effect that the solids will have (if any) on the gas-liquid area . The change from two to three phases has been observed to decrease the interfacial area in some cases :

Lee et al (24.d) carried out experiments with aqueous suspensions of small glass and orlon beads at concentrations up to 50. % by volume. They noted substantial reductions in both the gas hold-up (by up to $\sim$ 30. %) and the mass transfer rate (as much as 60. %) accompanied by a rise in Sauter mean bubble diameter from 0.7 to 3.2 mm. They also found that the power consumption rose proportionally with increases in density due to the presence of solids. (For fully developed turbulence, this is to be expected : $P/\rho(N^3D^5)$ = constant).

The orlon particles, being 7 μm in size (i.e. less than the liquid film thickness in which resistance to mass transfer is concentrated) were thought to affect the diffusivity. The somewhat larger glass beads were still small c.f. the gas bubbles and were regarded as blocking direct access to the bubble surface as well as reducing the effective area of contact between gas and liquid. The larger bubble size and diminished hold-up were ascribed to enhanced viscosity and non-Newtonian behaviour in the case of small particles and the damping out of turbulent eddies by larger solids (decreasing the break-up of bubbles and increasing coalescence).

However, given sufficient momentum, particles would be expected to penetrate gas bubbles and break them up - increasing their surface area and assisting the progress of the reaction. This was certainly found to be true for an air-water-sand slurry in the initial part of this project (16) where the introduction of sand (200 to 1000 μm) increased interfacial by about 30. % on average.

This apparent discrepancy has been explained by Kürten and Zehner (1.d) who have made theoretical calculations to show that such secondary dispersion of bubbles will occur, provided that the momentum of the particles is sufficiently high. Equilibrium between the inertial forces of a particle and the surface tension forces of a bubble is given by :

$$(\pi/6)(\rho_s/2)d_s^3 u_b^2 = \sigma(\pi/4)d_s^2$$

$$\therefore We_{critical} = (\rho_s d_s u_b^2/\sigma) = 3. \qquad \text{IV}$$

ρ_s, d_s : density, diameter of solids

u_b : relative velocity between solid particle and gas bubble

σ : surface tension

We : Weber number

If We is greater than about three, an increase in surface area due to bubble disruption is predicted and the opposite for We less than three (i.e. low momentum solids).

2.7 Liquid Viscosity :

This variable is of interest in its influence on both energy requirement and interfacial area.

For an aqueous system, carboxy methyl cellulose (CMC) was tried (16). It can be manufactured to various specifications of viscosity, enabling measurements over a broad range of viscosities above that of water and requiring only a concentration of 1. wt.% or less. CMC has also been shown by Onken and Schalk (1.a) to have no adverse effect on the sulphite reaction : though the kinetics are altered, i.e. the diffusivity and rate constant are quite different (c.f. water and sulphite alone) the overall rate of absorption of oxygen remains very much the same (down by about 5.%). However, it was found (and confirmed by Höcker et al : 1.f) that CMC solutions exhibit pseudo-plastic behaviour (i.e. that viscosity decreases with speed of agitation - especially in the regions immediately surrounding the stirrer). So whilst the power consumption is in fact lowered by the addition of CMC, as the decrease in viscosity is localised (in most of the tank it is much greater than that of water) the interfacial areas were significantly reduced (see 16).

Previously, glycerol has been used as an additive but fairly large proportions of it are required to have much effect on the viscosity (1.a). However, of considerably greater importance is the fact that addition of glycerol (5.%) reduces the rate of reaction (by a factor of 25). This means that the criterion for a fast reaction ($Ha > 3$) is no longer satisfied and the sulphite method becomes invalid for determining the gas-liquid area. (The reduction in rate has been attributed to the formation of a complex between glycerol and the cobalt catalyst, inhibiting the oxidation of the sulphite ion).

Therefore, as regards viscosity, an organic reaction (in place of the sulphite method) offers a further benefit in the possible use of solvents of various viscosities.

Smith et al (22) observed that other properties such as surface tension and dissolved ionic solutes, although changing the bubble size distribution throughout the vessel (and therefore the interfacial area) did not alter the shape of the cavities around the impeller and had little effect on the power requirements.

However, they found the viscosity of the liquid affected the shape of the cavities for $\eta \gtrsim 0.02$ kg/ms and that such cavities could, under certain circumstances, remain stable even if the gas supply was turned off : as long as the buoyancy of a cavity is not too large (Fr : $D^2N/g \gtrsim 0.02$) but the inertial forces are not so great that gas is dispersed from the tip of a cavity ($Re < 500\text{-}1000$).

3. EXPERIMENTAL :

3.1 Agitated Vessel : Description :

(see Fig.3.1a)

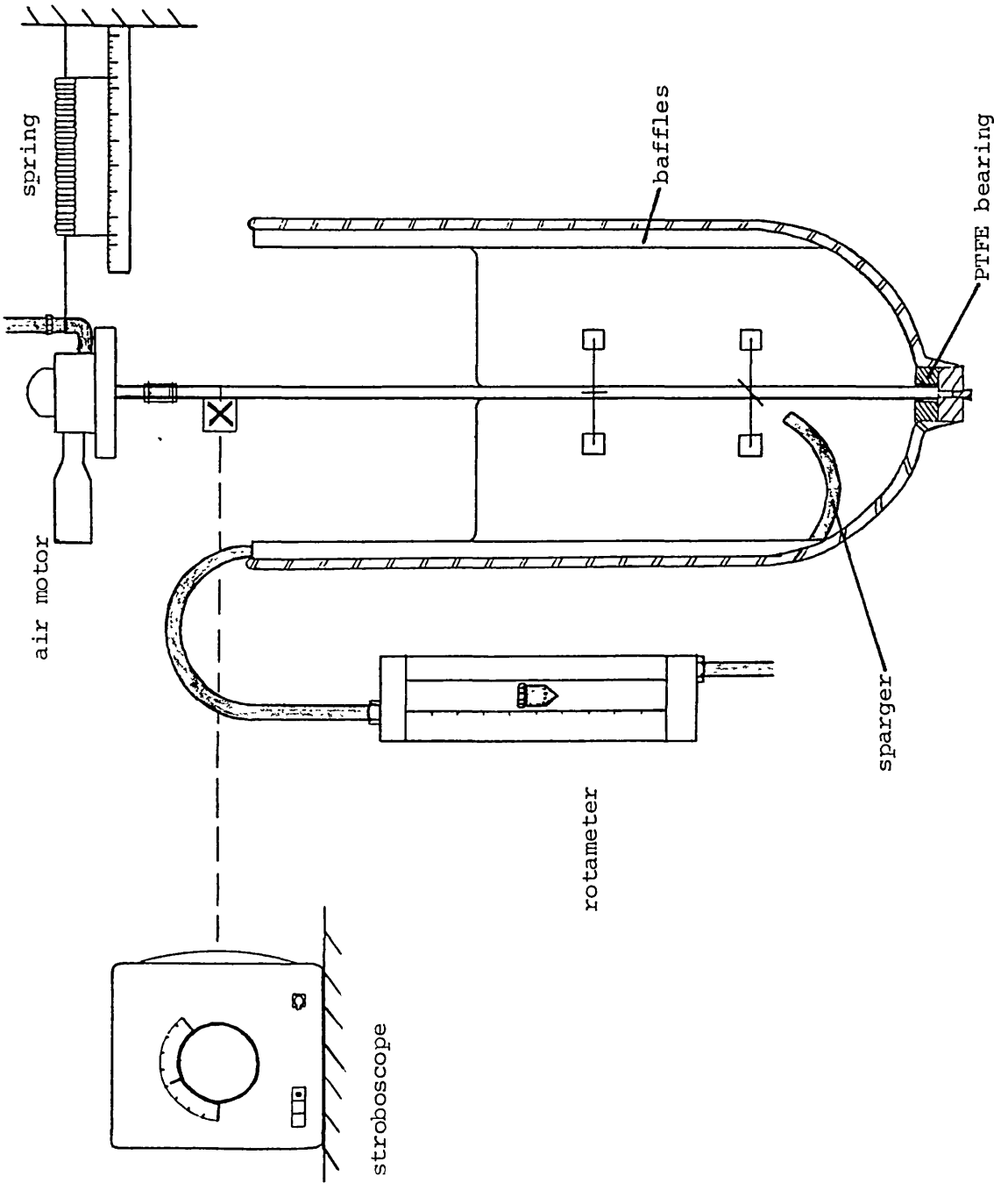
The cylindrical glass vessel (with a dished end) is of overall height 38. cm and diameter 16. cm and thus has a maximum capacity of about 7. litres. Four, equally-spaced, vertical baffles (width 1. cm) are positioned at the vessel walls to prevent vortex formation. The gas sparger is fixed alongside one of the baffles so as to minimise the sparger's effect on flow around the tank. The stirrer is mounted on a PTFE bearing, beneath which is the drainage port. The impeller is driven by a compressed air motor which sits on a frictionless bearing but is restrained by a calibrated spring so that the power consumption can be calculated.

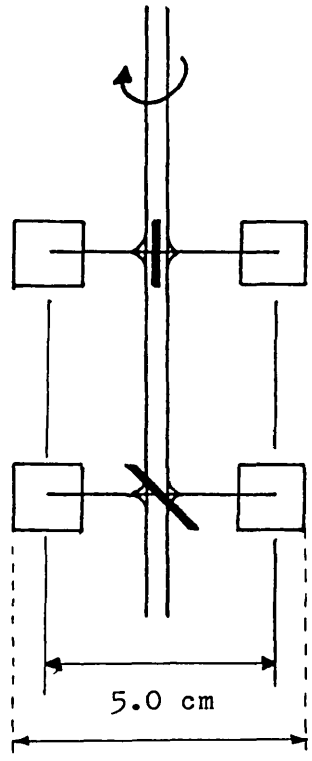
All of the metal parts are made of stainless steel since copper, as well as cobalt, catalyses the oxygen-sulphite reaction, and the organic amines used tend to be corrosive.

As mentioned in the introduction and section 2.5, four stirrer configurations were to be tested. All of them have two, 4-blade impellers mounted on one shaft, one directly above the other, 7. cm apart, with the lower disc 8. cm from the base of the tank. In all cases, the upper impeller is the same : a disc turbine (radius 2.5 cm) with four, vertical, equally-spaced, 2.25 cm^2 blades. The four lower impeller designs are : an upflow propeller, an upflow pitched blade disc turbine, a downflow propeller and a downflow pitched blade disc turbine. The discs are of the same design as the upper turbine except that the blades are angled, at 45° for upflow and 135° for downflow (i.e. leading edge uppermost). Similarly, the two propellers are also of radius 2.5 cm (angled at about 25° and 155°). (see Fig.3.1b)

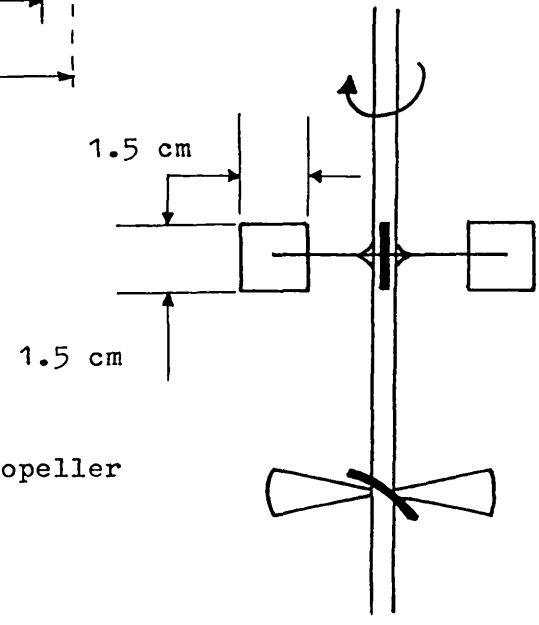
A sparger introducing air radially, adjacent to the lower impeller has already been shown to be unsatisfactory (16) : too much gas was allowed to escape upwards undispersed.

Fig.3.1a : AGITATED VESSEL





Downflow Disc Turbine



Downflow Propeller

Fig.3.1b

Data for a single tube, sparging gas to a point just beneath the lower impeller, have previously been obtained for the disc turbines (using the sulphite method) but no measurements had yet been made for the two propellers. It was also hoped to further improve the performance of the reactor by trying a ring sparger (with twelve, equally-spaced, 1. mm holes on a 5. cm pitch circle diameter) for better initial gas distribution. Narrow stainless steel tubing (3. mm outside diameter, 1. mm bore) was used to reduce the likelihood of solids suspension being impeded by the ring.

3.1.1 Experimental Procedure :

The gas flowrate is varied between about 6. and 30. litres per min. for the single tube sparger and from 6. to 25. l/min with the ring sparger.

The speed of the impeller is monitored by directing a stroboscope at a label attached to the top of the stirrer shaft. The power consumption is calculated by measuring the torque on the air motor by noting the extension of a (previously calibrated) spring which is tied to the motor and to a fixed point on the frame of the apparatus. The spring is recalibrated periodically. (See Appendix A 3.1.1 for power calculations).

Four litres of liquid are used in all experiments so that the base of the tank, the two impellers and the liquid level are all approximately equidistant.

3.1.2 The Sulphite Method :

350. g of anhydrous sodium sulphite is dissolved in 4. litres of distilled water to give an $\sim$ 0.7 Molar solution. The pH is reduced (from about 10.5) to 8.5 by the addition of a few ml of 1. M sulphuric acid. The gas rate and stirrer speed are adjusted to their desired values and only then is the catalyst added (1. g of cobalt acetate in 10. ml of water : 9.3×10^{-4} M). An initial sample is taken and

subsequent ones obtained at regular intervals (usually every 10 mins.) with the temperature being noted on each occasion.

Unfortunately, the construction of the apparatus inhibits any attempt at temperature regulation. Consequently, though the reaction is sufficiently slow and mildly exothermic that the temperature rise is generally small, on warmer days the initial temperature is inevitably well above 20°C (the point at which the rate is usually determined) and so allowances for this had to be made (see Appendix A 3.1.2). Note : the heat of mixing of anhydrous sodium sulphite with water raises the temperature of the vessel contents by about 2°C above room temperature.

Though the pH can be adjusted (and is measured at the end of each experiment) it has been found to be unnecessary since the pH remains well within the range 8.0 to 8.5, even under the faster reacting conditions (see Appendix A 3.3.1 for the analysis and calculations for the sulphite method, as well as section 3.3.1).

3.1.3 Amine-Carbon Dioxide Method :

(see section 3.4 : safety)

For the organic systems, three changes (c.f. air-sulphite) were made :

- for reasons of safety, the whole apparatus was moved to a fume cupboard (the stroboscope was directed through a side window outside the cupboard);
- a CO_2 line (from a cylinder) was passed through its own rotameter and then mixed in the desired proportion with the air supply to the sparger;
- for the three phase experiments, 3. mm spherical polythene beads were used.

Three different amines were tried in the attempt to find a suitable organic equivalent to the (aqueous) sulphite method : cyclohexylamine, diethanolamine and di isopropanolamine. Each was reacted in turn with CO_2 (at a partial pressure of 0.1) in a solution of 70.% xylene, 20.%

propanol (10.% amine : 4 litres in all). Toluene had been used by Charpentier (14.a) as the principal component of the liquid phase but it was decided to use xylene, which is similar but somewhat safer (and costs the same). Propanol is added to keep the carbamate product of the amine-CO_2 reaction in solution. Although 10.% of it should be sufficient, the evaporation rate in the reactor is likely to be quite large (especially at high gas rates and stirrer speeds) and a propanol:amine ratio of 1:2 was chosen which also keeps the overall liquid density at $\sim$0.86 (i.e. that of pure xylene). However the viscosity of the solution is increased.

3.1.4 Aims :

(i) Physical Measurements :

Power consumption was to be measured across the range of gas flowrates (6. to 25. l/min) and stirrer speeds (250 to $\sim$650 rpm) for the various impeller designs (propellers and disc turbines, upflow and downflow) using the ring sparger and trying water and xylene in turn as the liquid phase. A brief comparison between power requirement for the ring sparger vs the single tube was made (any difference was expected to be small).

Three phase experiments were to be carried out for air-xylene with 3. mm polythene beads as the solid phase, investigating the ability of the four stirrers to achieve suspension at different gas rates.

(ii) Chemical Measurements :

(a) Sulphite Method : values of interfacial area (S) were to be found for all four impellers with the ring sparger at different gas flows and stirrer speeds. Having already measured S for the two disc turbines with a single tube sparger, it was decided, for completeness, to obtain similar data for the propellers.

(b) Amine-CO_2 Method : since the method was largely untried, the main aim was to establish which (if any) of the amines tested is suitable for the determination of gas-liquid

area and, if so, to carry out experiments similar to (a) overleaf.

3.2 Quiescent Interface Cell : Description :

(see Fig.3.2a)

The cell is enclosed by a cylindrical, glass water-jacket of internal diameter 7.1 cm. Glass draught tubes (radius 2.5 cm) are mounted inside on three adjustable steel pins, one tube fixed to either of the two end plates. Four tie rods hold the water-jacket in place between the plates which are made of steel with a layer of PTFE attached to provide a seal during operation.

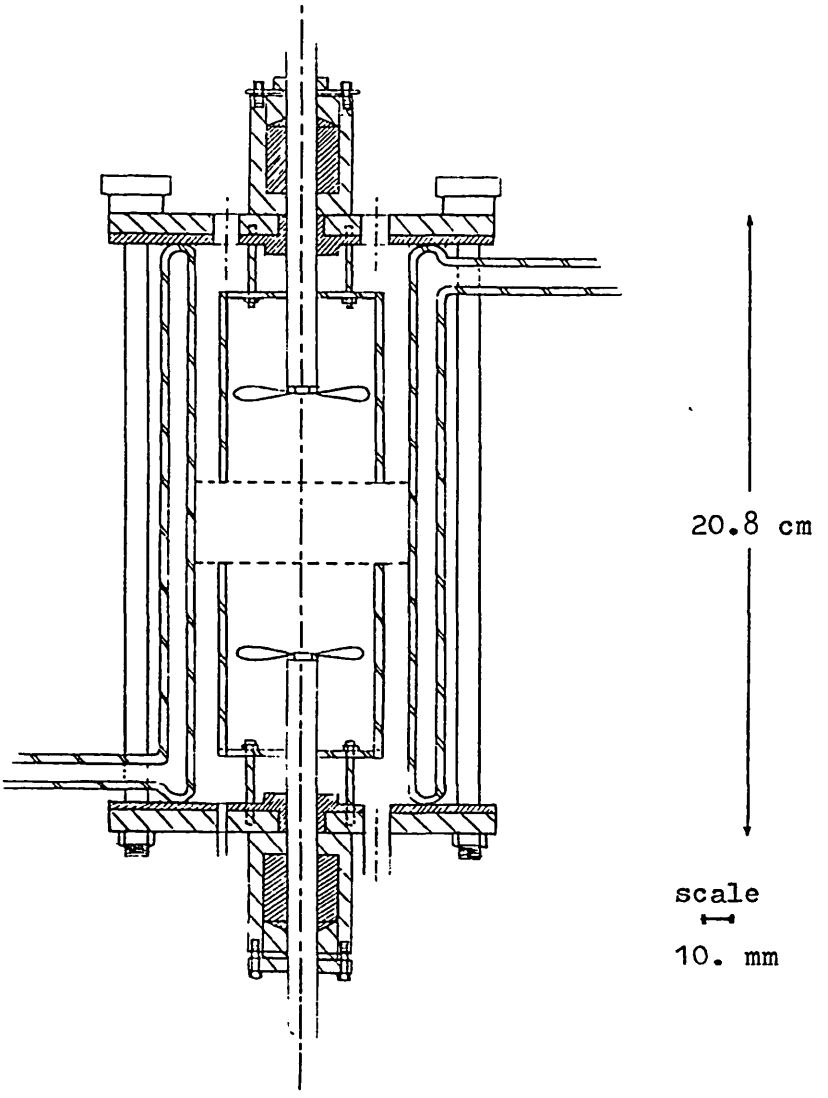
Two, triple-bladed impellers circulate fluid through the centre of the cell and the annulus between the jacket and the draught tubes (air or air and CO_2 in the top half and sulphite or amine solutions in the bottom). Wire gauze discs are held over the draught tubes, downstream of the impellers, in order to smooth out primary eddies and hence maintain a quiescent, constant gas-liquid interface. A fresh supply of gas is supplied to the top of the cell through one of two holes in the upper end plate, whilst the lower plate has a tapped capillary for sample removal and a larger hole for drainage.

The stirrers are independently powered by 250 volt A.C. motors at 400 to 600 rpm. Although feedback speed regulators were not available for the two motors, it is considered that the volume of the cell is small enough and the stirrer speeds are sufficiently high that the cell is in effect perfectly well-mixed and that the exact speed of rotation of the impellers is of no great consequence.

3.2.1 Experimental Procedure :

The empty cell is assembled and the tie rods tightened to seal in the liquid phase which is poured in through the top. The impellers are set in motion and the gas flow is turned on, samples being taken periodically (typically

Fig.3.2a : QUIESCENT INTERFACE CELL



every 5 to 10 mins). Water is continuously circulated through the jacket to keep the cell contents at a steady temperature.

When taking samples, a certain amount of liquid is run off before collecting the sample itself, to drain the liquid in the capillary that is not representative of the bulk of the cell. Since the liquid level must lie between the two wire mesh discs (to maintain a quiescent surface) the possible length of an experimental run is limited (to about 90 mins) by the amount of liquid removed in samples, as well as the danger of the motors overheating (though these have not proved to be serious problems).

3.2.2 Aims :

Measurements of the rate of reaction for the sulphite method have already been carried out (16) and since the supplier of the sulphite is the same as before, it was not thought worthwhile to repeat the experiments.

However, no rate information was available for the organic systems being used, so tests were to be performed on CHA, DEA and DIPA in turn (in solutions of xylene and propanol) each being contacted with 10.% CO_2 in air.

3.3 Analysis of Samples :

(preparation of solutions and analysis calculations are given in Appendices A 3.3.1 and A 3.3.2)

3.3.1 Sulphite Method : Analysis :

A series of titrations is required : firstly, the sulphite ions present in the (1. ml) sample are oxidised by the addition of a known excess of iodine solution (20. ml, $\sim$0.05 M) :

$$SO_3^{2-} + I_2 + H_2O \longrightarrow SO_4^{2-} + 2I^- + 2H^+$$

This mixture is then titrated with sodium

thiosulphate (: $Na_2S_2O_3$, $\sim$ 0.15 M) using a starch solution indicator, reacting with the remaining iodine :

$$I_2 = 2S_2O_3^{2-}$$

Both thiosulphate and iodine solutions are standardised beforehand (and checked at the end of each experiment) : sodium thiosulphate titrated against 25. ml of acidified potassium iodate solution (0.0187 M, with crystals of potassium iodide added),

$$KIO_3 = 6S_2O_3^{2-}$$

then the iodine solution is titrated against the thiosulphate. (See 9).

Each sulphite sample is tested three times because occasionally, analysis gives an inconsistent reading for no apparent reason.

It is clear that this method, though quite accurate, is fairly laborious (and prevents the taking of samples more often than every 10 mins., otherwise they cannot be analysed immediately and are likely to deteriorate by further oxidation). However, there seems to be no satisfactory alternative : that suggested by Eremin and Kiseleva (8), namely ultra-violet absorption spectrophotometry, was tried without success (16).

3.3.2 Amine-Carbon Dioxide Method : Analysis :

Three methods of analysis have previously been tried :

(i) by titration with alcoholic, concentrated hydrochloric acid, but this requires standardisation using a known amount of the appropriate carbamate (for each amine) and these are not readily available;

(ii) by liberation of the CO_2 from the sample (again by using concentrated hydrochloric acid) and measuring the volume of gas released. However, since the

samples from the quiescent interface cell must be kept fairly small, the accuracy of such a method would be in doubt.

In neither case is the method well-tried or -documented and it was therefore decided to try :

(iii) chromatography. This has been used successfully and has the advantage that quantitative values are obtained for all four components present in the sample : CO_2 (which is driven off from the amine on injection into the chromatograph), propanol, xylene and the amine (registered in that order). Calibration is also much easier since the amine and CO_2 (as well as propanol and xylene) are readily acquired as pure components, just as their product (the carbamate) is not.

A thermal conductivity detector was used for the gas chromatograph (flame ionisation would not detect CO_2). The conditions (temperature, column packing, carrier gas etc.) for each amine are given in Appendix A 3.3.2 .

3.4 Safety :

The principal difficulty arising from the change to an organic system for the study of slurry reactors is that of safety.

The oxidation of sulphite presents few problems of this nature (: only the cobalt acetate catalyst, present in very small quantities, and the iodine used for titration purposes, needed to be handled with any particular care) and the apparatus could be operated in an open laboratory without taking special precautions.

Contrastingly, the organic chemicals used for the liquid phase are all potentially dangerous (as outlined in (20),(21) and Appendix A 3.4) and must be confined in some way to prevent the escape of vapours that are both highly flammable and toxic.

At first it was proposed that for the agitated vessel, a sealed lid would be made. However, this was

rejected because of several difficulties that would have to be overcome i.e.

- a good seal around the stirrer shaft would have been difficult to achieve and would, in any case, affect the power consumption, thus making future measurements incompatible with those obtained previously;
- further seals around the gas sparge pipe and some sort of sample port would be required;
- an outlet for the departing gas phase with a condenser and possibly a recycle would also be needed.

Rather than to attempt to solve all of these problems, it was decided to transfer the experiments to a fume cupboard (class C, though class B would probably be sufficient). This effectively dealt with the toxicity hazard, whilst to eliminate the only possible source of ignition, the stroboscope was mounted just outside the fume cupboard, sighted through a glass panel. (Note that a further advantage of using an air motor is its inherent safety).

The quiescent interface cell too, despite its much smaller capacity and greater degree of enclosure, was placed in a fume cupboard. The electric motors were sealed and all metallic surfaces (including the wire gauzes inside the cell) were earthed to the frame of the apparatus.

4. RESULTS :

4.1 Physical Measurements : Two Phase :

Power consumption was measured for a range of gas flowrates (introduced via a ring sparger) and stirrer speeds, using up- and downflow disc turbines and propellers for both air-water and air-xylene.
(see Appendix B)

4.1.1 Stirrer Speed vs Power :

(see Figs.4.1.1a,b,c,d)

Clearly, regardless of other conditions (gas rate, type of impeller etc.) each increase in stirrer speed requires a progressively greater increase in power input.

Equally apparent is the lowering of the energy requirement by the introduction of gas to the system : for a given stirrer speed, the change from Q_G = 0. to 2.0 vvm approximately halves the power consumption. Further increases in gas rate also lower the power input needed, though the effect diminishes (e.g. the energy saved from Q_G = 0. to 2.0 is more than from Q_G = 2.0 to 4.5, - see next section).

As expected, both of the propellers proved to be more energy efficient than either of the disc turbines. A more detailed comparison is made in sections 4.1.3 and 4.1.6 .

4.1.2 Gas Flowrate vs Power :

Figs.4.1.2a,b,c,d all show a drastic fall in power consumption (or increase in stirrer speed) when even small amounts of gas are introduced into an agitated, unaerated liquid phase. However, they also demonstrate that this improvement tails off quite sharply, especially at lower impeller speeds; so much so that at 250 rpm, the increase in gas flow from Q_G = 1.5 to 6.5 vvm brings about only an insignificant change in the energy used. The higher the

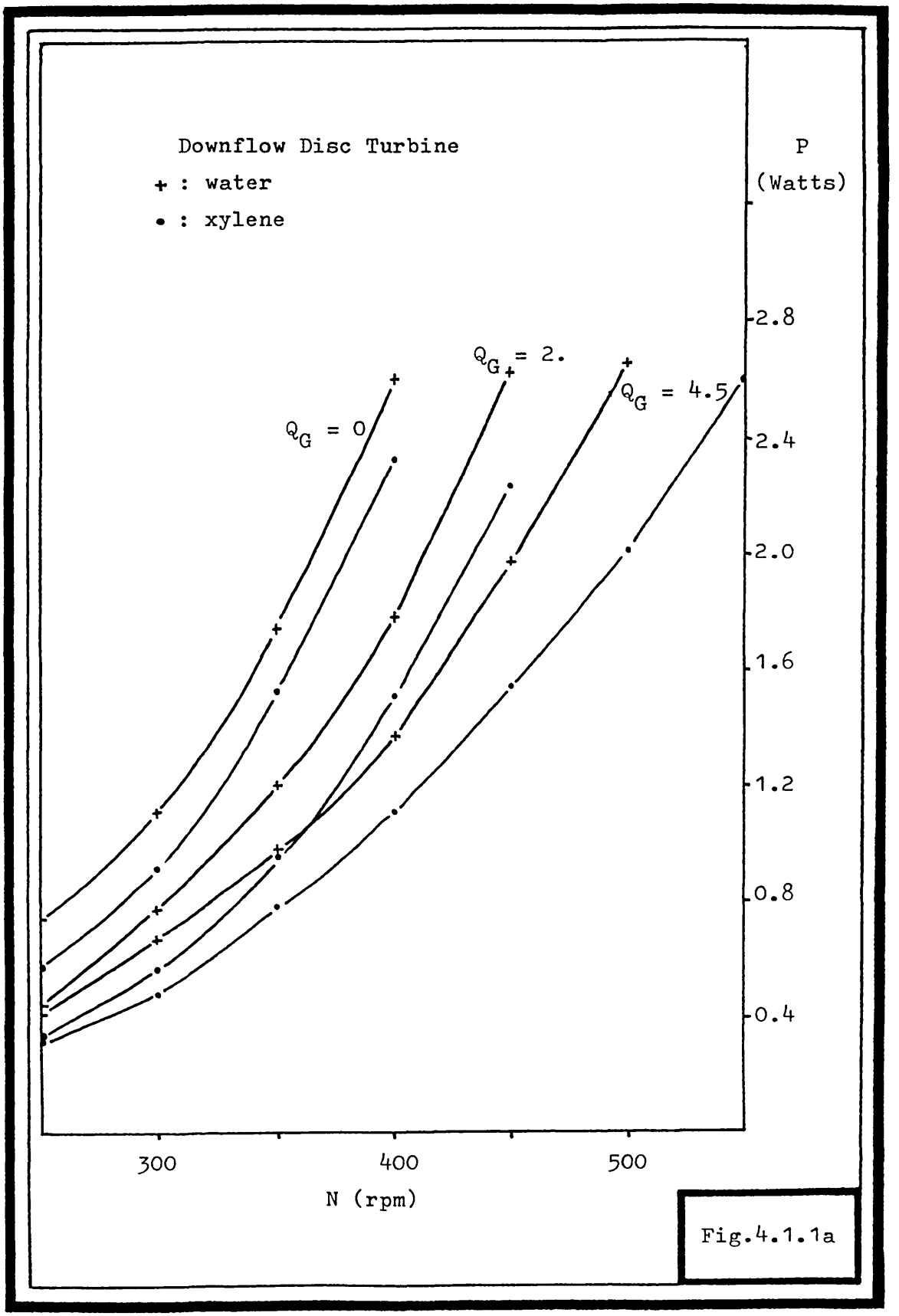

Downflow Disc Turbine
+ : water
• : xylene
P
(Watts)
2.8
2.4
2.0
1.6
1.2
0.8
0.4
Q_G = 0
Q_G = 2.
Q_G = 4.5
300
400
500
N (rpm)

Fig.4.1.1a

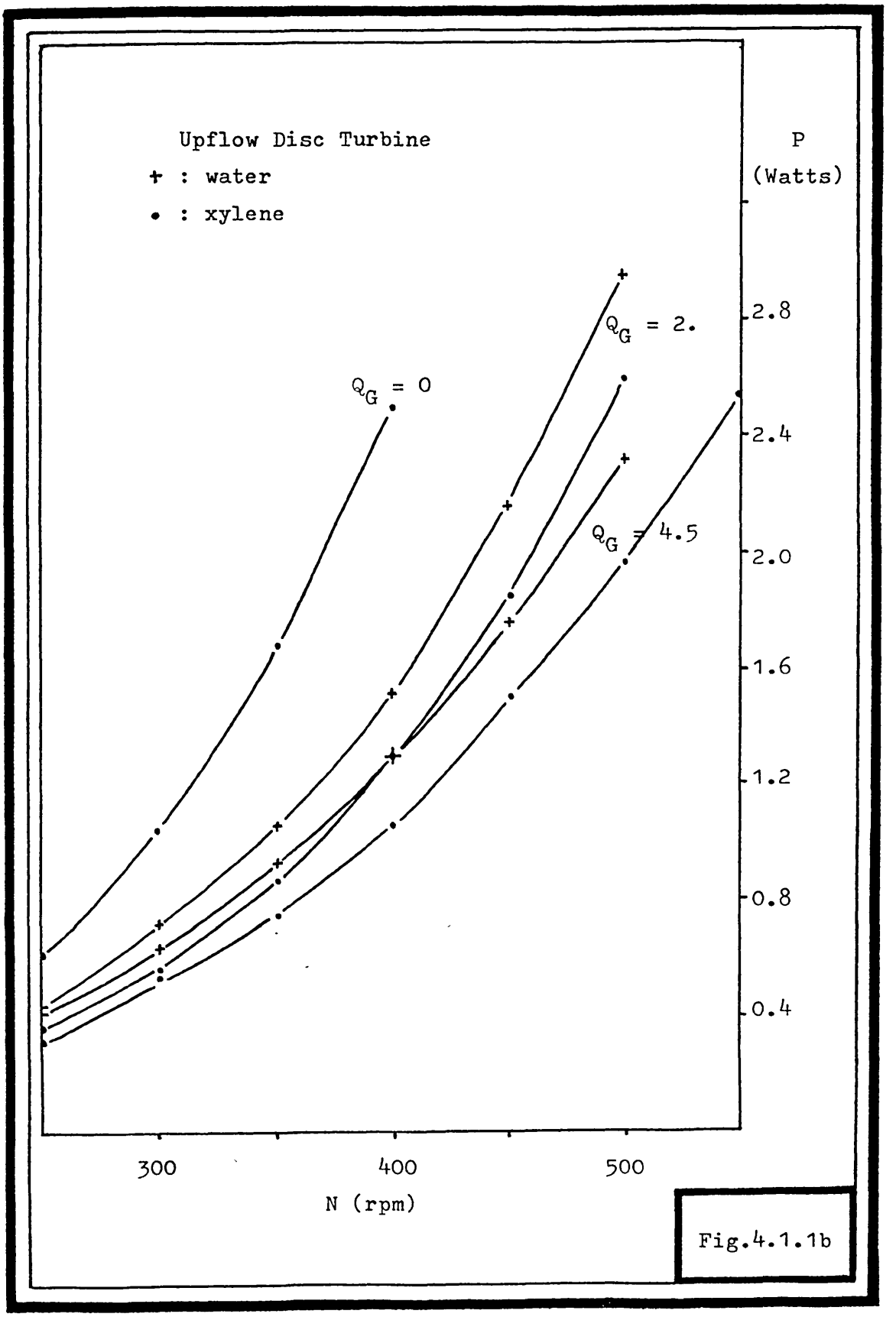

Upflow Disc Turbine
+ : water
• : xylene
P
(Watts)
Q_G = 0
Q_G = 2.
Q_G = 4.5
2.8
2.4
2.0
1.6
1.2
0.8
0.4
300
400
500
N (rpm)

Fig.4.1.1b

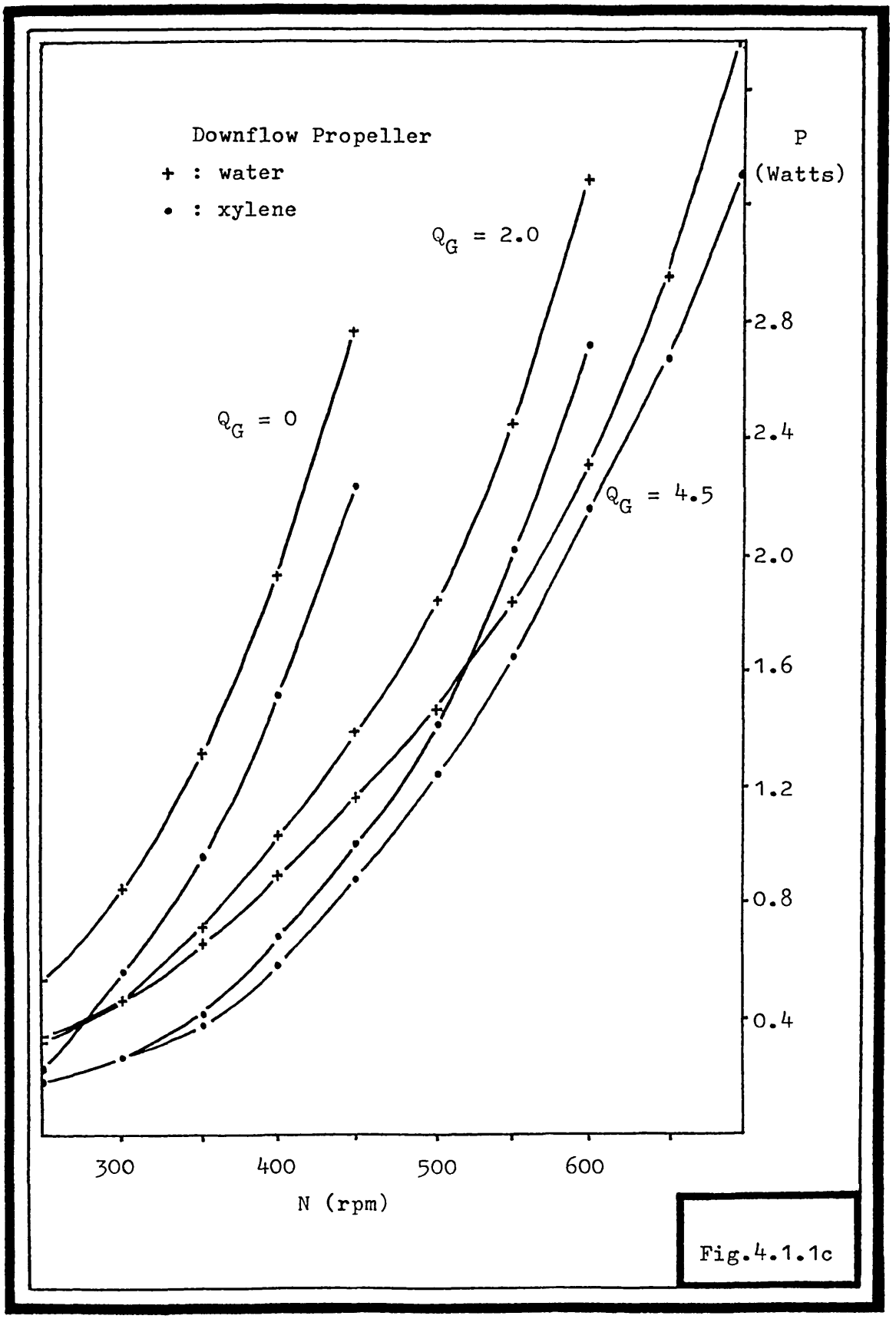

Downflow Propeller
+ : water
• : xylene
Q_G = 2.0
Q_G = 0
Q_G = 4.5
P
(Watts)
2.8
2.4
2.0
1.6
1.2
0.8
0.4
300
400
500
600
N (rpm)

Fig.4.1.1c

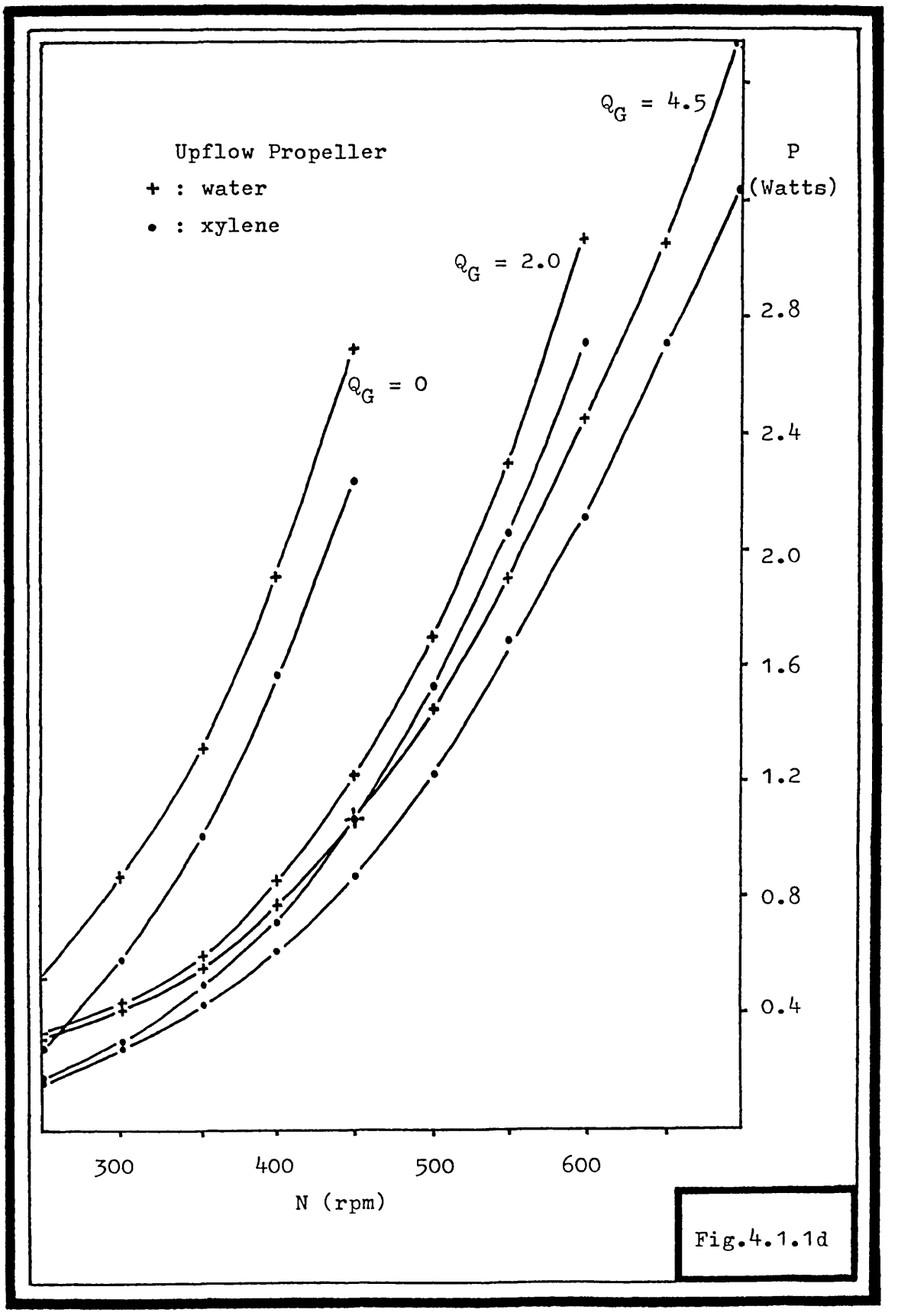

Upflow Propeller
+ : water
• : xylene
Q_G = 4.5
Q_G = 2.0
Q_G = 0
P
(Watts)
2.8
2.4
2.0
1.6
1.2
0.8
0.4
300
400
500
600
N (rpm)

Fig.4.1.1d

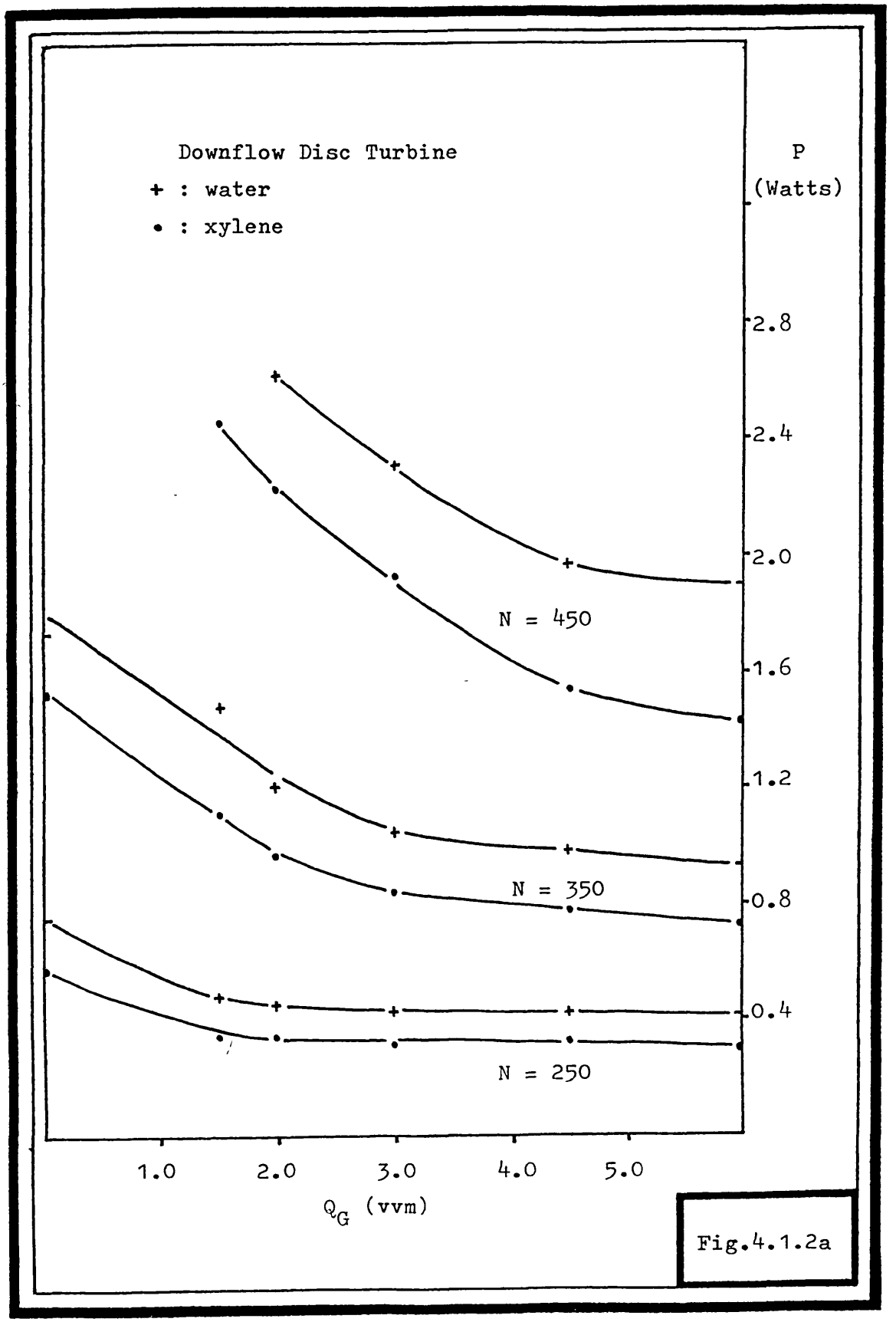

Downflow Disc Turbine
+ : water
• : xylene
P
(Watts)
2.8
2.4
2.0
1.6
1.2
0.8
0.4
N = 450
N = 350
N = 250
1.0
2.0
3.0
4.0
5.0
Q_G (vvm)

Fig.4.1.2a

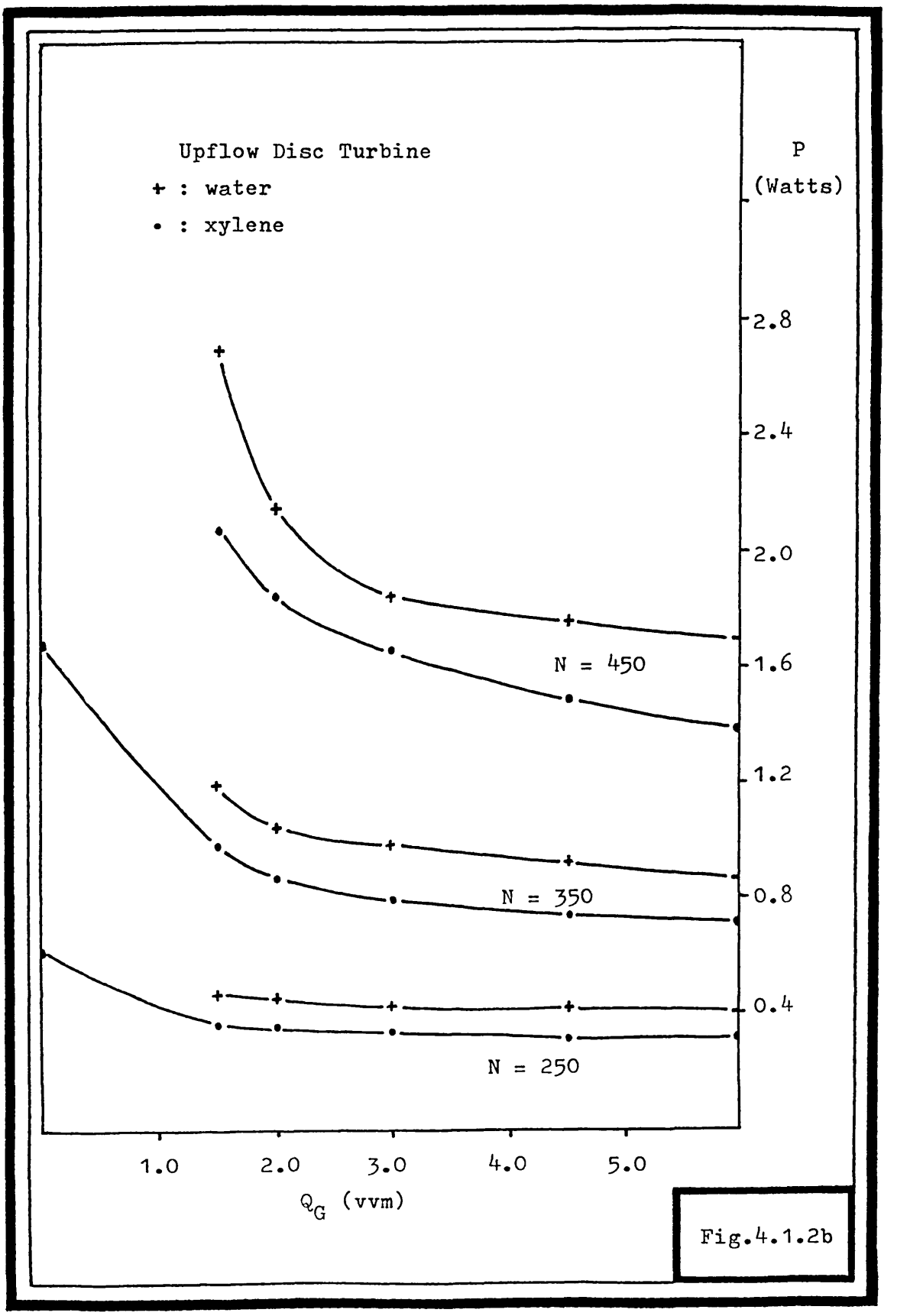

Upflow Disc Turbine
+ : water
• : xylene
P
(Watts)
2.8
2.4
2.0
1.6
1.2
0.8
0.4
N = 450
N = 350
N = 250
1.0
2.0
3.0
4.0
5.0
Q_G (vvm)

Fig.4.1.2b

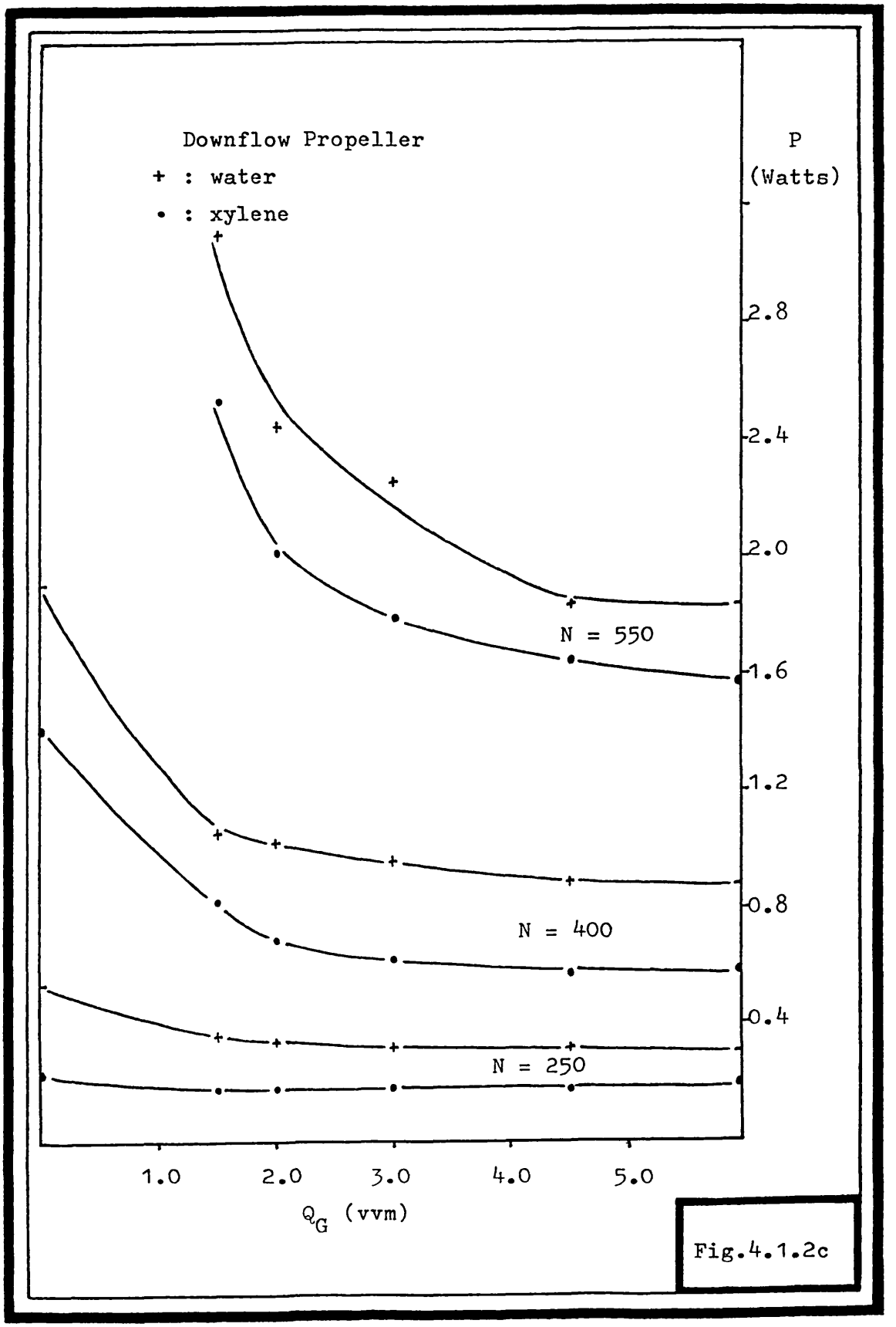

Downflow Propeller
+ : water
• : xylene
P
(Watts)
2.8
2.4
2.0
1.6
1.2
0.8
0.4
N = 550
N = 400
N = 250
1.0
2.0
3.0
4.0
5.0
Q_G (vvm)

Fig.4.1.2c

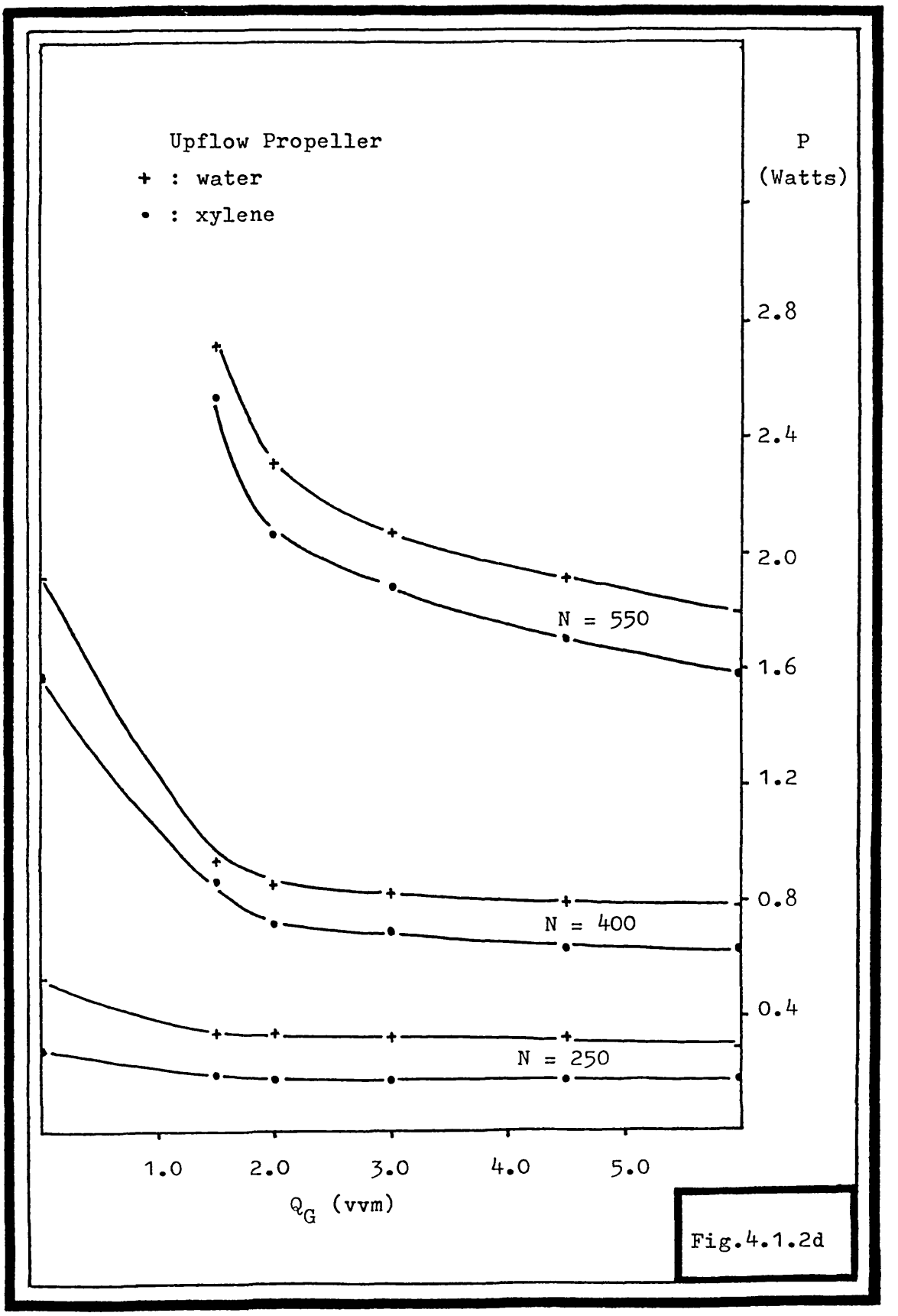

Upflow Propeller
+ : water
• : xylene
P
(Watts)
2.8
2.4
2.0
1.6
1.2
0.8
0.4
N = 550
N = 400
N = 250
1.0
2.0
3.0
4.0
5.0
Q_G (vvm)

Fig.4.1.2d

stirrer speed though, the more noticeable is the effect of changing the gas supply : Overall then, the results correspond to what the work of Smith et al would predict for fairly high gas flow numbers (see section 2.4). Presumably the points at which increasing the gassing rate ceases to lower the power requirement should equate with what Chapman et al (18.b) refer to as a 'just completely dispersed' gas phase, but neither of these conditions necessarily imply that gas-liquid interfacial areas have reached a peak or have even levelled off, as previous (16) and current results (section 4.5) show.

4.1.3 Stirrer Configuration :

The graphs depicted in the last two sections give ample proof that the propellers, as predicted, use much less energy than the disc turbines : for the same supply of power, the propellers can achieve a stirring rate 50 to 100 rpm faster than discs in the usual operating range (the difference being greater still at very high power inputs/ stirrer speeds and large gas flows). However, it should be remembered that this saving in energy would be of little value if the propellers were found to produce substantially lower interfacial areas or were unable to suspend solids.

It has been observed (18) that upflow impellers use somewhat less energy than downflow ones since they pump in the same direction as the flow of bubbles from the gas inlet, whereas downflow stirrers are 'countercurrent' in this respect. Results here do indeed show upflow impellers to consume a little less energy but only by a small amount and no 'flow instabilities', as mentioned by Chapman, have been seen for downflow systems. Of course, a possible reason for the only minor differences noted between up- and downflow in these experiments is the presence of the second, upper impeller (a flat blade disc turbine) which (in addition to its role in the secondary dispersion of gas) must account for a significant proportion of the power : about 50. % for the discs (and more for the propellers).

Again it must be stressed that simply because an upflow arrangement uses less energy, it need not be preferable : in fact previous experimental data gathered in the first stage of this project (16) implied the opposite, with the upflow disc turbine producing interfacial areas about 15.% smaller than the downflow disc, which was also better able to achieve a solids suspension (for air-water-sand). It remained to be seen if this was also the case with a ring sparger and for propellers (section 4.5).

4.1.4 Liquid Phase :

Experiments were performed using water and xylene in turn as the liquid phase. With a density of 860 kg/m^3 (and viscosity about 0.7×10^{-3} kg/ms), the organic liquid was naturally expected to use rather less energy than water under the same conditions of gas flowrate and stirrer speed and this is confirmed by Figs.4.1.1a,b,c,d and 4.1.2a,b,c,d. (The exact viscosity of the xylene is in doubt since it is a mixture of the three isomers in unknown proportions, each of whose viscosities is slightly different : 11). Apart from this power consumption gap, the corresponding water and xylene curves all follow similar if not approximately parallel paths.

It was not possible to ascertain whether bubble size distributions, and flow in the tank generally, were greatly affected by the change from water to xylene, though this does not seem probable. Certainly any difference was too small to be seen without the aid of photography or some other suitable method : unlike the results obtained beforehand (16), when carboxymethylcellulose (CMC : a pseudoplastic additive) was mixed in with an aqueous liquid phase, producing a fluid of fairly high viscosity (except in the region immediately around the impeller) and a tendency for large gas bubbles to form and quickly escape to the top of the tank (resulting in diminished gas-liquid interfacial areas).

4.1.5 Flow Patterns, Gas Distribution :

During normal operation, the only aspect distinguishing between the various stirrer designs is the somewhat poorer distribution of gas when using an upflow impeller, characterised by an absence (or at best a minor presence) of bubbles in the lower region of the vessel, below the gas sparger and the bottom impeller. As previously reported, this was reflected in :

(i) smaller interfacial areas for an upflow disc turbine c.f. a downflow disc (with a single tube gas sparger)

and (ii) shorter retention of gas bubbles by the upflow disc (seen when the gas supply is turned off).

The more thorough gas distribution achieved by a downward pumping stirrer has now also been observed for the propeller, though perhaps to a marginally lesser extent than the disc turbine.

The change to a ring gas sparger visibly improves the distribution of gas within the tank at low stirrer speeds, in comparison with a single tube inlet, but it is obviously necessary to obtain quantitative values (e.g. by using the sulphite method : section 4.5). At higher stirring rates, the difference might be expected to be smaller (the stronger the agitation, presumably the less important the means of gas introduction becomes) but under such turbulent conditions it is impossible to make valid visual assessments.

The overall flow circulation produced has already been described for the two disc turbines (16,18) including systems with two or more impellers on one shaft and the propellers produce patterns similar to their appropriate pitched-blade disc counterparts.

4.1.6 Correlation and Comparison of Results :

With the exceptions of the lower stirrer and the gas sparger designs, the geometry of the tank (i.e. tank diameter; size and number of baffles, impeller location etc.) has been kept constant. Thus for dimensional analysis of the vessel, the diameter of the impeller (D) may be used as the characteristic linear dimension and the series of dimensionless groups describing the geometry need not be considered here.

	D	ρ_L	G	N	P	g	η	
M	0	1	0	0	1	0	1	Gas-Liquid + physical
L	1	-3	3	0	2	1	-1	properties :
T	0	0	-1	-1	-3	-2	-1	σ, (ρ_G/ρ_L), (ν_G/ν_L)

Letting [L] = D, [M] = $\rho_L D^3$, [T] = 1/N
gives the dimensionless groups :

$$\pi_1 = G/ND^3 \ (= Fl) \qquad \pi_2 = P/(\rho_L N^3 D^5) \ (= Ne)$$

$$\pi_3 = g/DN^2 \ (= 1/Fr) \qquad \pi_4 = \eta/(\rho_L D^2 N) \ (= 1/Re)$$

So :

$$Ne = P/(\rho_L N^3 D^5) = f(Re, Fr, Fl, \text{Geometry, G-L properties})$$

For an unaerated system, this reduces to :

$$Ne = f(Re, Fr, \text{Vessel Geometry})$$

It has been observed for a liquid alone (3.a) that for $Re > 10^4$ (i.e. turbulent conditions) Ne is constant with respect to Re.

For water alone (i.e. G = 0) :

D = 0.05 m : propeller $\qquad \eta = 10^{-3}$ kg/ms

(0.065 : disc) $\qquad \rho_L = 10^3$ kg/m^3

$$\therefore Re = (N/60)(0.05)^2 \times 10^3/10^{-3} = 41.67N \text{ (for a propeller)}$$

$$= 70.42N \text{ for a disc)}$$

$\therefore$ At N = 250 rpm (the slowest speed used), $Re = 1.042 \times 10^4$ for a propeller, i.e. for all $N > 250$, $Re > 10^4$ for any of the impellers. In fact, since $Re \propto D^2$ and the power consumption is proportional to D^5, the energy used by the propeller will be overshadowed by the slightly larger diameter disc above it and therefore, the plot of Ne against N (or Re) : Fig.4.1.6a is based on D = 0.065 m for both types of stirrer considered.

The graph shows that although the Newton number does not vary a great deal over the range investigated, it only becomes constant at $Re \gtrsim 2.8$ to $3. \times 10^4$. Fig.4.1.6a also depicts the corresponding curves for a well-aerated system (Q_G = 4.5 vvm). The use of Newton and (especially) Reynolds numbers becomes somewhat dubious for a gas-liquid system since :

(i) the density varies according to gas holdup : a function of both gas rate and stirrer speed, and

(ii) the viscosity of the fluid is unknown.

Nevertheless, by basing Ne and Re on the liquid properties alone, the results are similar to those for an unaerated system, with Ne becoming constant for $Re \gtrsim 3. \times 10^4$.

This compares well with the work of Kuboi and Nienow (24.c), who state that Ne = constant (+/- 5. %) for $Re > 4. \times 10^4$. They also give values of these Newton numbers (in unaerated tanks) in the range (1.4 to 5. for single) and 3.7 to 7.5 for dual impellers : this fits in with the unaerated values obtained here : $\sim$ 7.5 for the downflow disc and about 5.5 for the upflow propeller. The corresponding Ne numbers at a high gas rate (Q_G = 4.5 vvm) are 4.0 and 2.1 respectively (though based on liquid properties).

Thus the relationship between Ne and Fl ($= G/ND^3$) : the Gas Flow number, is such that as Fl increases, Ne decreases, tending to some constant value. This 'constant' is however, in the range studied, a function of gas rate (but independent of stirrer speed for $Re \gtrsim 3. \times 10^4$). The dependence of Ne upon gas rate does diminish as Q_G rises and would presumably become negligible at very high gas flows

(much higher than any likely to be encountered in a stirred, slurry reactor).

Clearly, it would be useful to be able to relate the power consumption of a two phase (gas-liquid) system to that of the liquid alone but, as explained in section 2.4, the relationship between (P_G/P_O) and Fl is not a simple one, especially at the fairly high gas rates used here, under conditions where large cavities (dependent on N for their size) are almost certain to exist. (: This will occur when the buoyancy of gas bubbles is overcome by the centrifugal forces generated by the impeller. According to Kuboi and Nienow (24.c) and Smith et al (22), this takes place at Froude numbers in excess of 0.085 to 0.1, c.f. the lowest Fr here : $(250/60)^2 \times 0.05/10 = 0.087$ for the propellers, or 0.113 for the upper, flat blade disc).

The graphs in Figs.4.1.6f,g cover the range $0.05 \lesssim Fl \lesssim 0.36$ and $0.4 < (P_G/P_O) < 0.83$ and show a continual (though diminishing) improvement in the aerated power consumption at increasing Fl (Kuboi and Nienow have obtained broadly similar results (24.c), also for dual impellers but for different stirrer designs and they found a minimum in (P_G/P_O) at $Fl \sim 0.06$). Again, the dependence of cavity size on stirrer speed is apparent.

Kürten and Zehner (1.d) give an empirical equation (due to Michel and Miller) for a six (flat-) blade turbine :

$$P_G = \text{constant}(P_O ND^3/G^{0.56})^{0.45} \qquad \text{IV}$$

P_G : aerated system power

P_O : unaerated system power

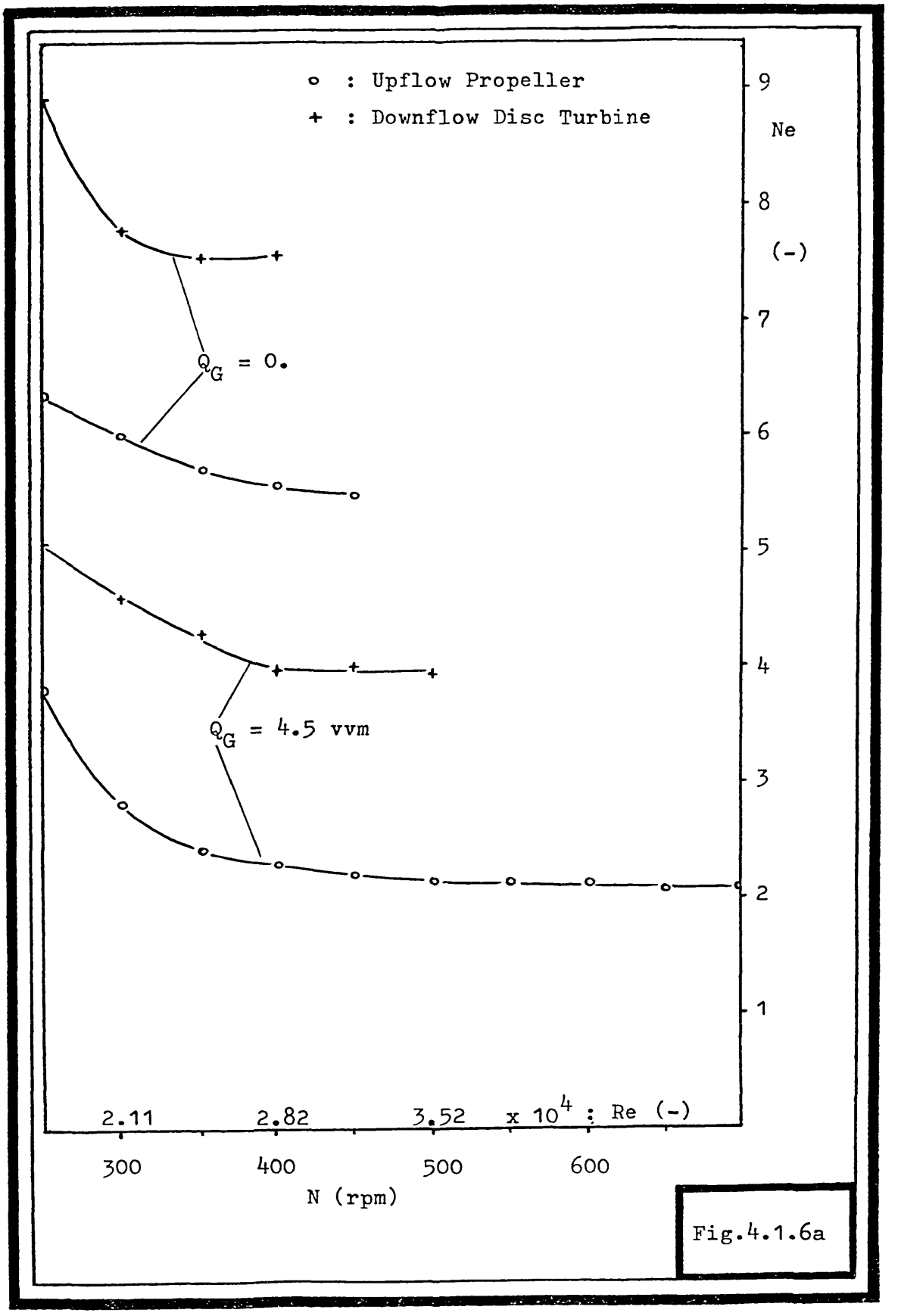

o : Upflow Propeller
+ : Downflow Disc Turbine
Q_G = 0.
Q_G = 4.5 vvm
Ne
(-)
9
8
7
6
5
4
3
2
1
2.11
2.82
3.52
x 10^4 : Re (-)
300
400
500
600
N (rpm)

Fig.4.1.6a

Fig.4.1.6b shows the results for the downflow disc turbine and that equation IV works fairly well, even though the stirrer geometry and operating range (G,N) are different. A log-log plot (of P_G against $P_0ND^3/G^{0.56}$) : Fig.4.1.6c, indicates that the exponent of $(P_0ND^3/G^{0.56})$ needs to be larger to fit the data obtained here : about 0.9 at low to intermediate gas rates, 0.7 at high gas flowrates.

Michel and Miller's results led them to try to correlate (P_G/P_0) and $ND^3/G^{0.56}$, but 'without success'. In their review article (2.e), Sharma et al recommend an equation proposed by Hughmark :

$$(P_G/P_0) = 0.1(NV_R/G)^{0.25}(gWV_R^{\frac{2}{3}}/N^2D^4)^{0.2} \qquad V$$

W : blade width

V_R : volume of reactor

i.e. $(P_G/P_0) \propto G^{-0.25}$ and

$\propto N^{-0.15}$ $(N^{0.25}/N^{0.4})$

- but they point out that it 'fails at extreme gas rates'.

Figs.4.1.6d,e show that the relationship between (P_G/P_0) and stirrer speed is irregular (especially at higher speeds) and is entirely different for the upflow propeller and the downflow disc turbine (: the former used the least energy to attain a given stirrer speed, the latter the most).

As expected, Figs.4.1.6f,g demonstrate that (P_G/P_0) decreases with increasing gas rate but again, no clear pattern emerges other than (i) at very low stirrer speeds the decrease in (P_G/P_0) is quite gradual, (ii) at higher stirrer speeds, (P_G/P_0) is almost independent of N except for very large gas throughputs.

It is apparent, therefore, that (like Michel and Miller) our results do not conform with Hughmark's equation (V) and that the ratio (P_G/P_0) does not follow any simple rules. The effect of stirrer design seems to be an important consideration. Thus neither would Nagata's (6) proposed

equation be of value :

$$\log(P_G/P_0) = -\text{const.}\left(\frac{D}{D_R}\right)^{4.38}\left(\frac{D^2N}{\nu}\right)^{0.115}\left(\frac{DN^2}{g}\right)^{1.96D/D_R}\left(\frac{G}{ND^3}\right)$$

VI Re Fr Fl

i.e.

$$\log(P_G/P_0) \propto {}^{(-)}G$$

and (for the disc turbine $D/D_R = 0.406$)

$$\log(P_G/P_0) \propto N^{-0.09} \quad (: N^{0.115} \times (N^2)^{1.96 \times 0.406} \times 1/N)$$

Note : As Nagata points out (6), power consumption is slightly less with a single tube sparger (16) than a ring, since impeller flooding occurs more readily with the former.

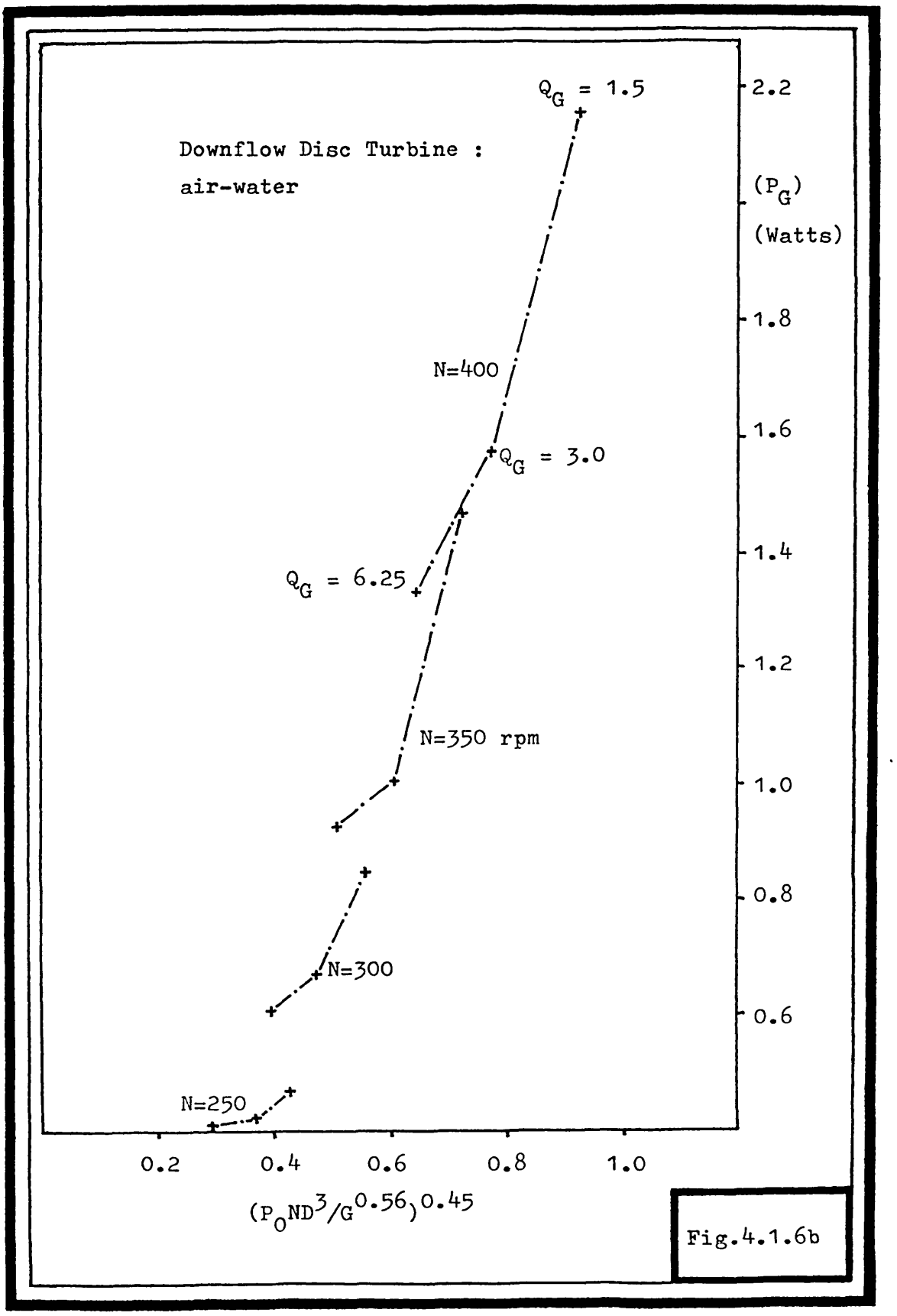

Downflow Disc Turbine :
air-water
Q_G = 1.5
Q_G = 3.0
Q_G = 6.25
N=400
N=350 rpm
N=300
N=250
(P_G)
(Watts)
2.2
1.8
1.6
1.4
1.2
1.0
0.8
0.6
0.2
0.4
0.6
0.8
1.0
$(P_0ND^3/G^{0.56})^{0.45}$

Fig.4.1.6b

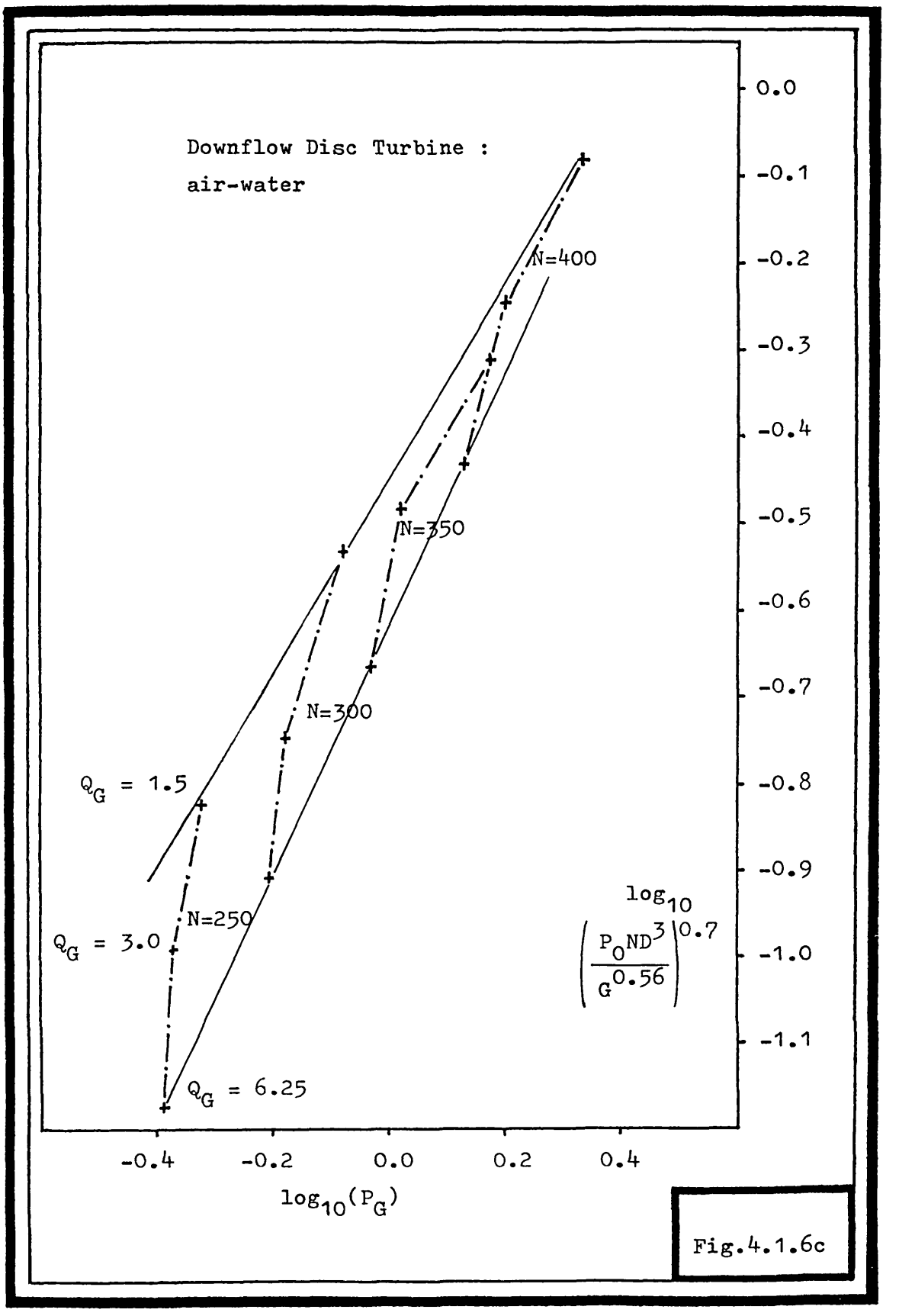

Downflow Disc Turbine :
air-water
N=400
N=350
N=300
N=250
Q_G = 1.5
Q_G = 3.0
Q_G = 6.25
0.0
-0.1
-0.2
-0.3
-0.4
-0.5
-0.6
-0.7
-0.8
-0.9
-1.0
-1.1
$\log_{10}\left(\frac{P_O N D^3}{G^{0.56}}\right)^{0.7}$
-0.4
-0.2
0.0
0.2
0.4
$\log_{10}(P_G)$

Fig.4.1.6c

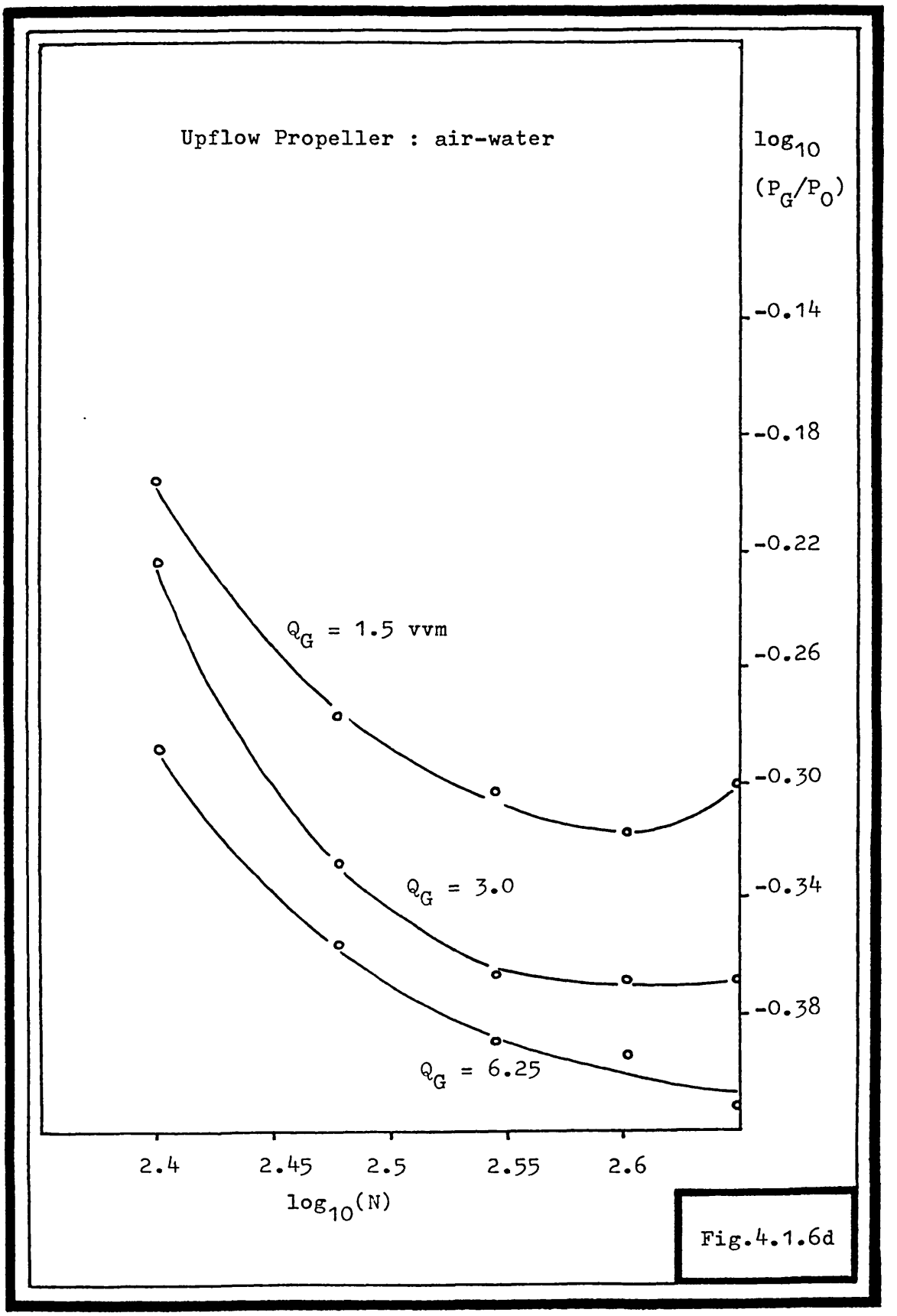

Upflow Propeller : air-water
log10 (PG/P0)
-0.14
-0.18
-0.22
-0.26
-0.30
-0.34
-0.38
QG = 1.5 vvm
QG = 3.0
QG = 6.25
2.4
2.45
2.5
2.55
2.6
log10(N)

Fig.4.1.6d

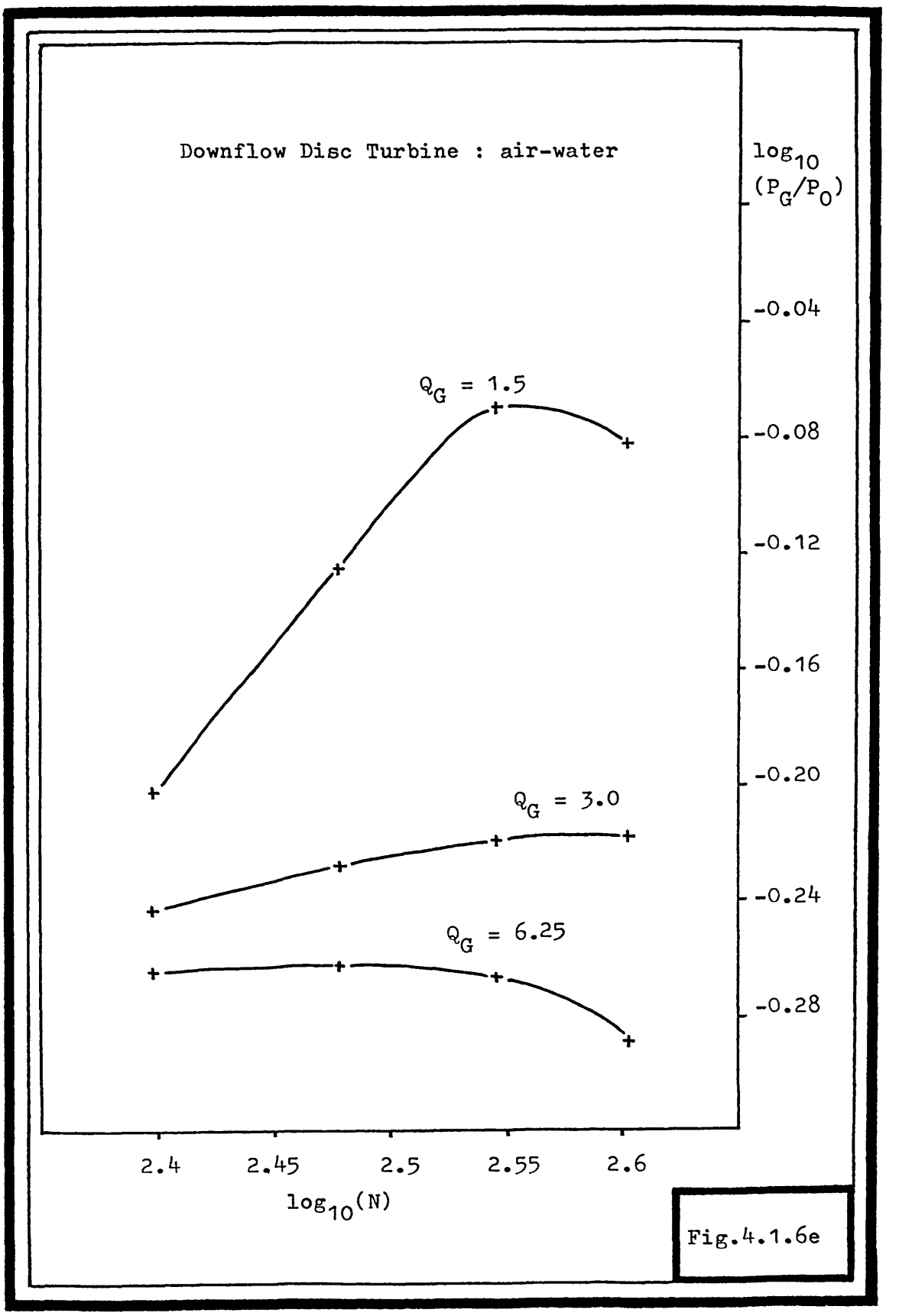

Downflow Disc Turbine : air-water
log10 (PG/P0)
-0.04
-0.08
-0.12
-0.16
-0.20
-0.24
-0.28
QG = 1.5
QG = 3.0
QG = 6.25
2.4
2.45
2.5
2.55
2.6
log10(N)

Fig.4.1.6e

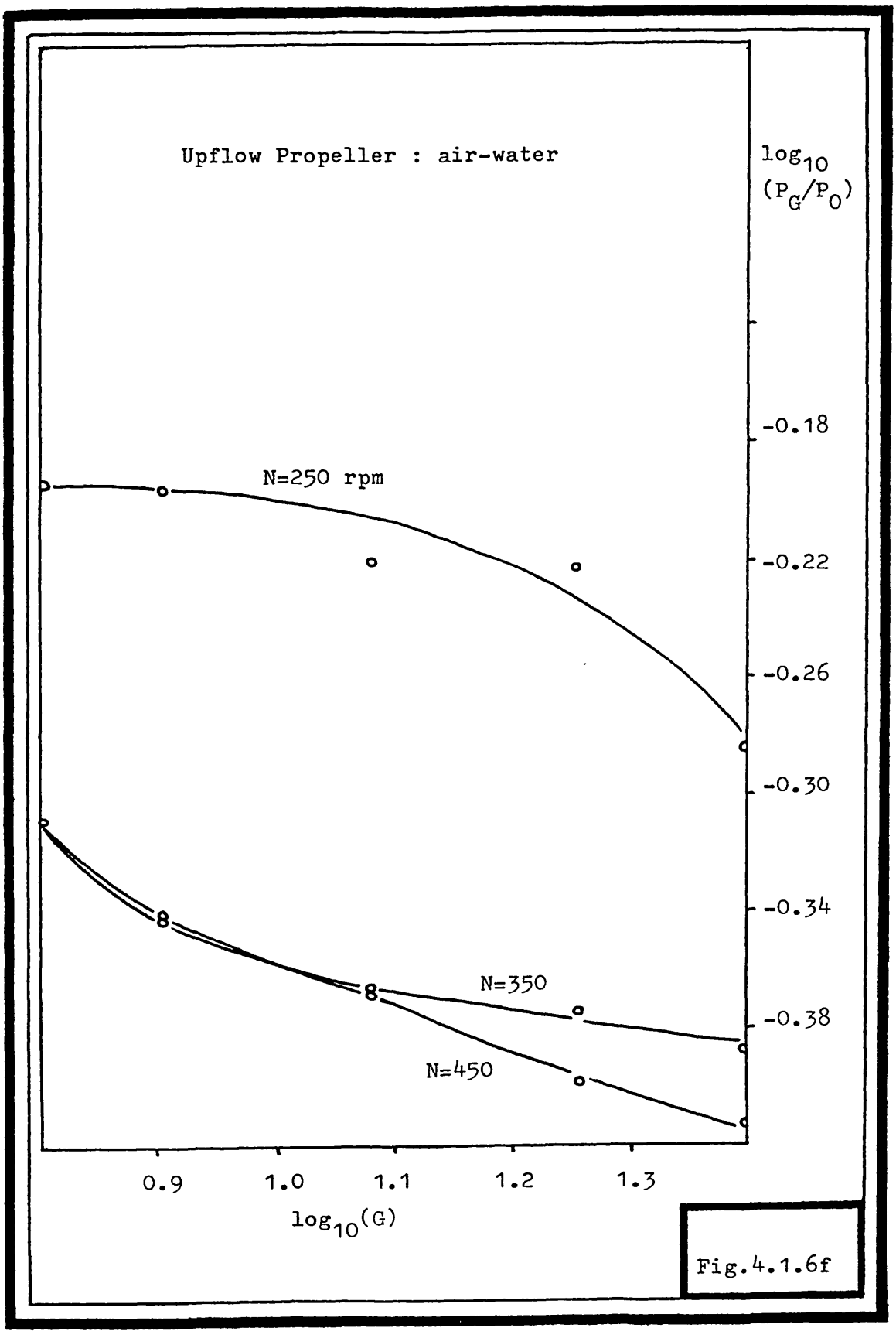

Upflow Propeller : air-water
log10 (PG/P0)
-0.18
-0.22
-0.26
-0.30
-0.34
-0.38
N=250 rpm
N=350
N=450
0.9
1.0
1.1
1.2
1.3
log10(G)

Fig.4.1.6f

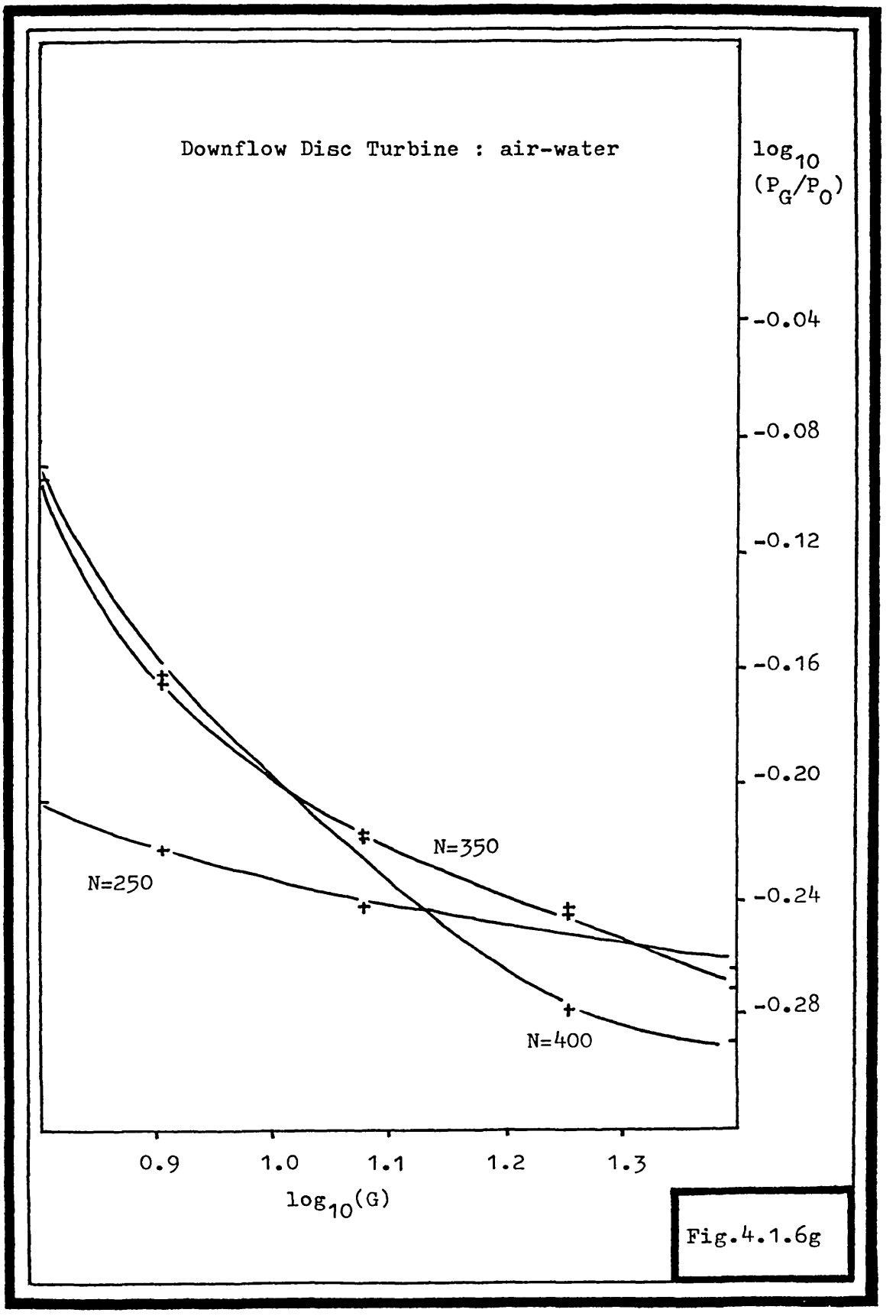

Downflow Disc Turbine : air-water
log10 (PG/P0)
-0.04
-0.08
-0.12
-0.16
-0.20
-0.24
-0.28
N=350
N=250
N=400
0.9
1.0
1.1
1.2
1.3
log10(G)

Fig.4.1.6g

4.2 Physical Measurements : Three Phase :

4.2.1 Solids Concentration vs Suspension :

The criteria for deciding when suspension has been achieved have already been described (section 2.6). For the 3. mm polythene beads used here, the 'just suspended' condition (at stirrer speed N_{JS}) was considered the most appropriate.

Figs.4.2.1a,b,c,d show that, for all of the stirrer configurations and gas flowrates tested, the speed of agitation required to achieve solids suspension grows with increasing solids concentration. However, there is also a marked tendency for this increase to level off when the proportion of solids is high, especially for the downflow impellers. The comparatively weak dependence of N_{JS} on the solids concentration (X) is consistent with Zwietering's equation (VII) and is examined further in section 4.2.5.

4.2.2 Gas Flowrate vs Suspension :

From Figs.4.2.2a,b,c,d it is apparent that, in all circumstances, the initial introduction of gas to an unaerated system has a profound effect on N_{JS} : As has been observed by various workers in the past (16,18,1.i) even a small amount of gas in the vessel makes suspension of the particles much more difficult. This can be explained in terms of the gas filled cavities forming around the impeller blades which inhibit the stirrer's pumping action and thus reduce the drag forces (associated with high liquid flows) and turbulent eddies, both of which are thought to be responsible for suspension of solids : $\therefore$ N_{JS} rises.

The results here also show that further increases in gas rate to an already aerated system do not have as drastic an effect on suspension as might have been anticipated. This could be because of the better dispersion of gas by the ring sparger. However, with the propellers in use (Figs.4.2.2c,d) an increase from a low to an intermediate

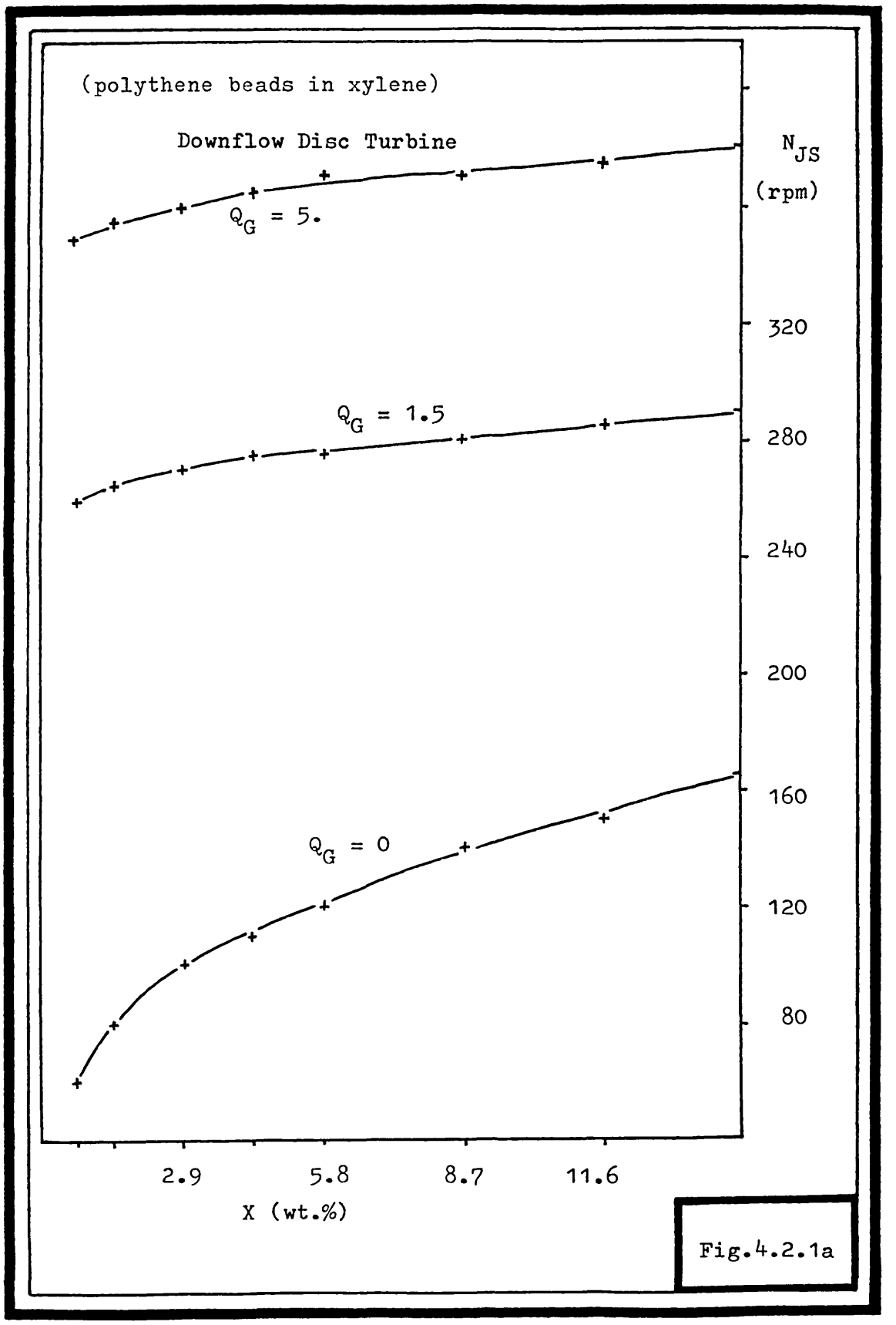

(polythene beads in xylene)
Downflow Disc Turbine
N_{JS} (rpm)
Q_G = 5.
Q_G = 1.5
Q_G = 0
320
280
240
200
160
120
80
2.9
5.8
8.7
11.6
X (wt.%)

Fig.4.2.1a

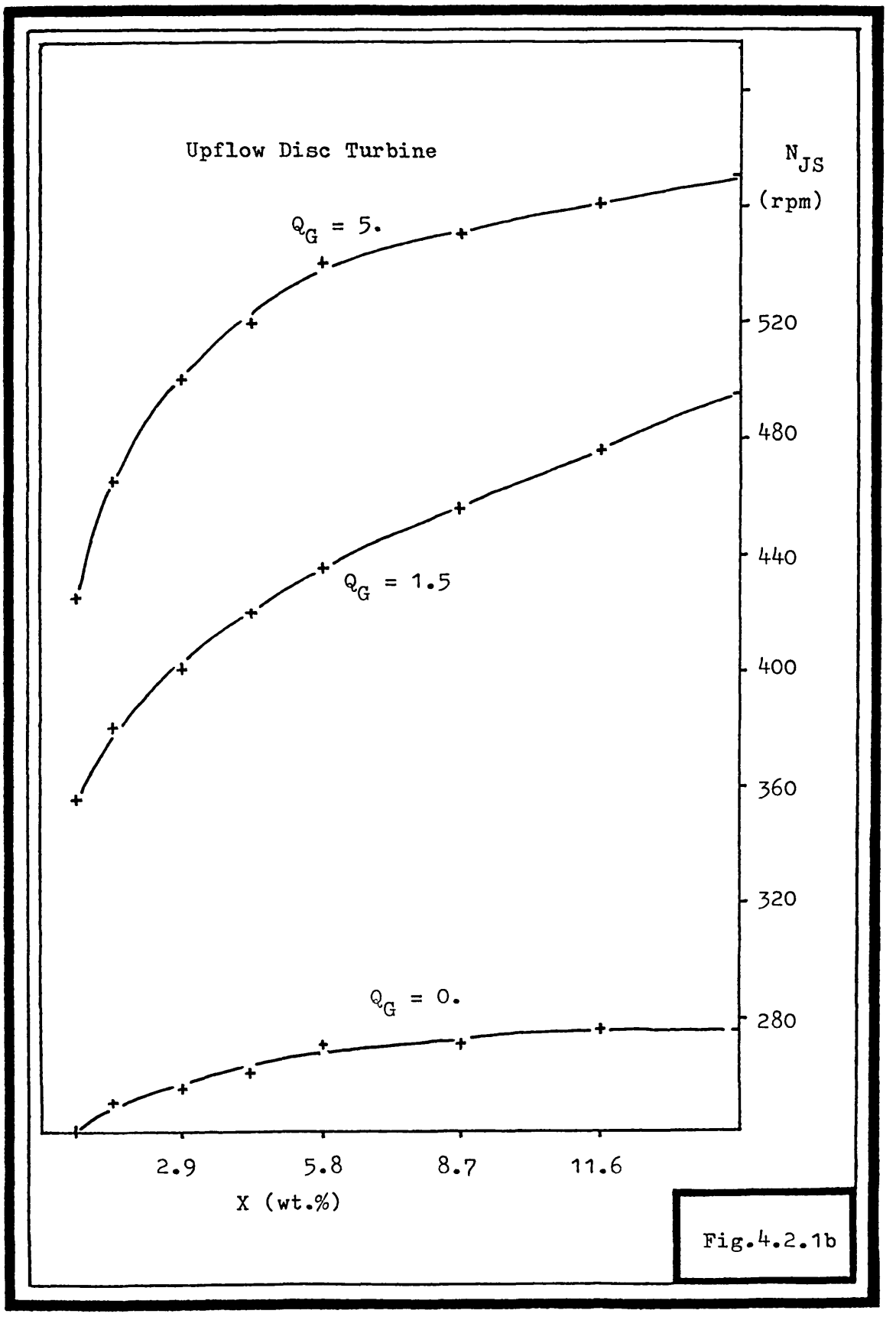

Upflow Disc Turbine
N_{JS}
(rpm)
Q_G = 5.
Q_G = 1.5
Q_G = 0.
520
480
440
400
360
320
280
2.9
5.8
8.7
11.6
X (wt.%)

Fig.4.2.1b

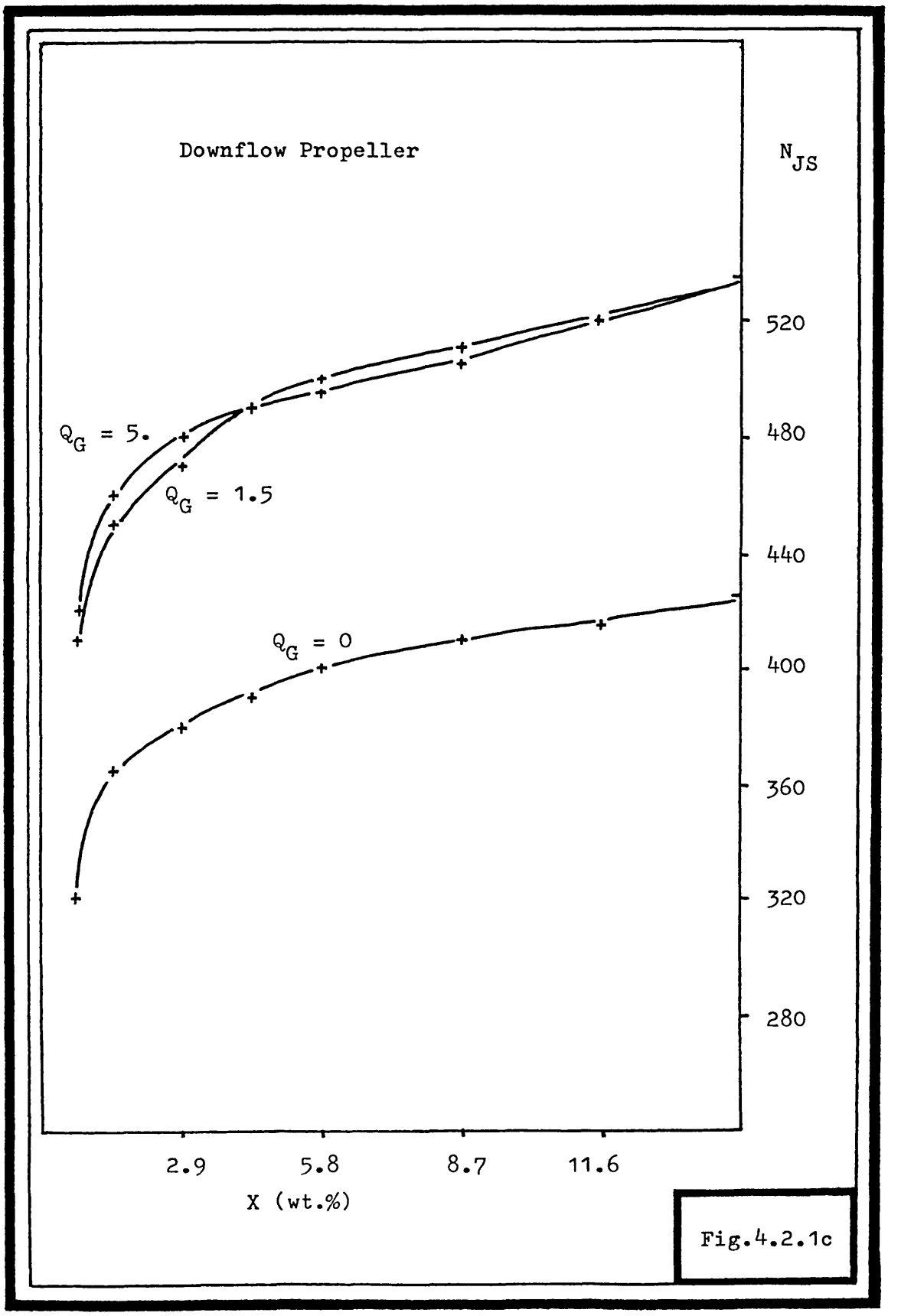

Downflow Propeller
N_{JS}
520
480
440
400
360
320
280
Q_G = 5.
Q_G = 1.5
Q_G = 0
2.9
5.8
8.7
11.6
X (wt.%)

Fig.4.2.1c

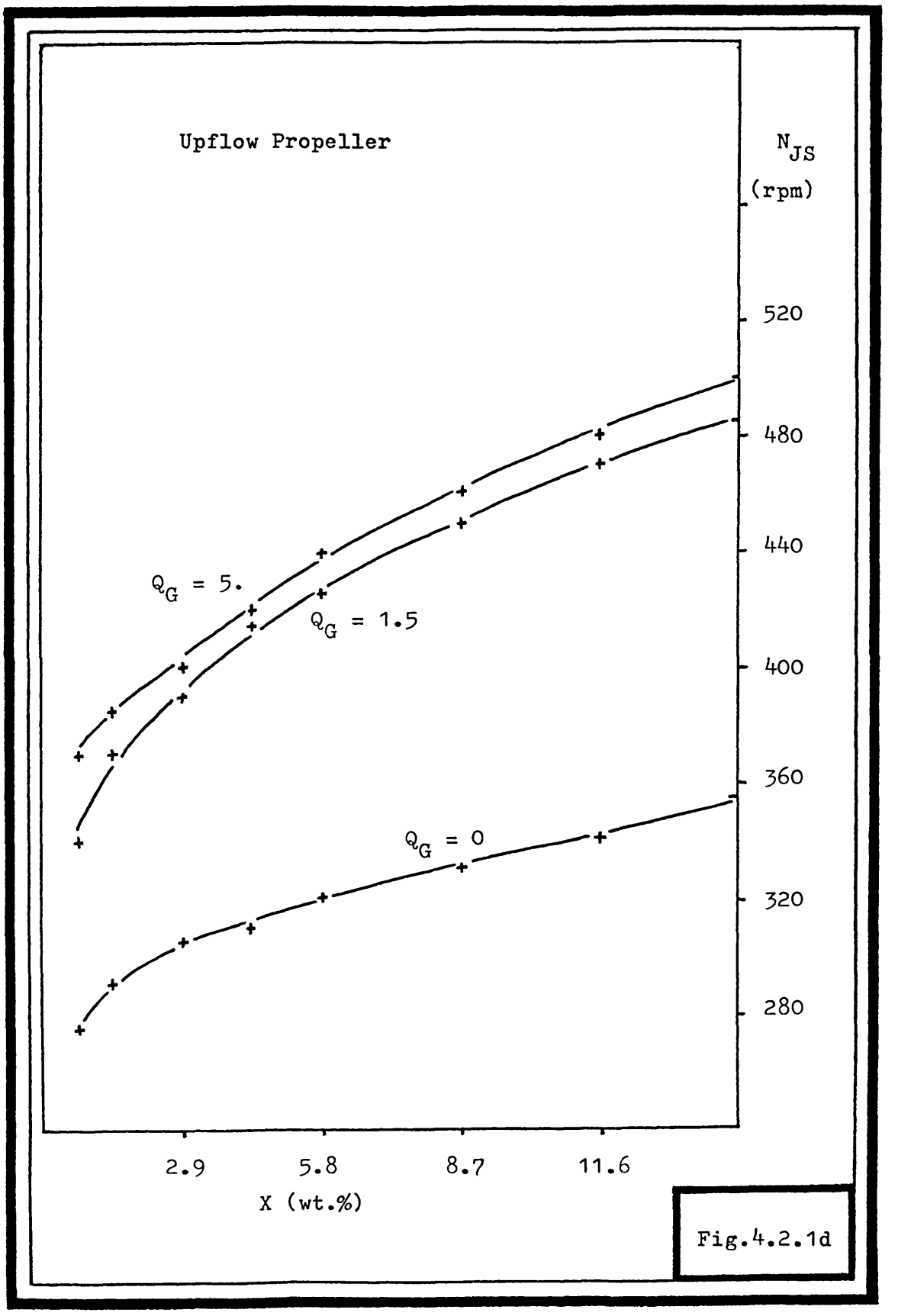

Upflow Propeller
N_{JS} (rpm)
520
480
440
400
360
320
280
Q_G = 5.
Q_G = 1.5
Q_G = 0
2.9
5.8
8.7
11.6
X (wt.%)

Fig.4.2.1d

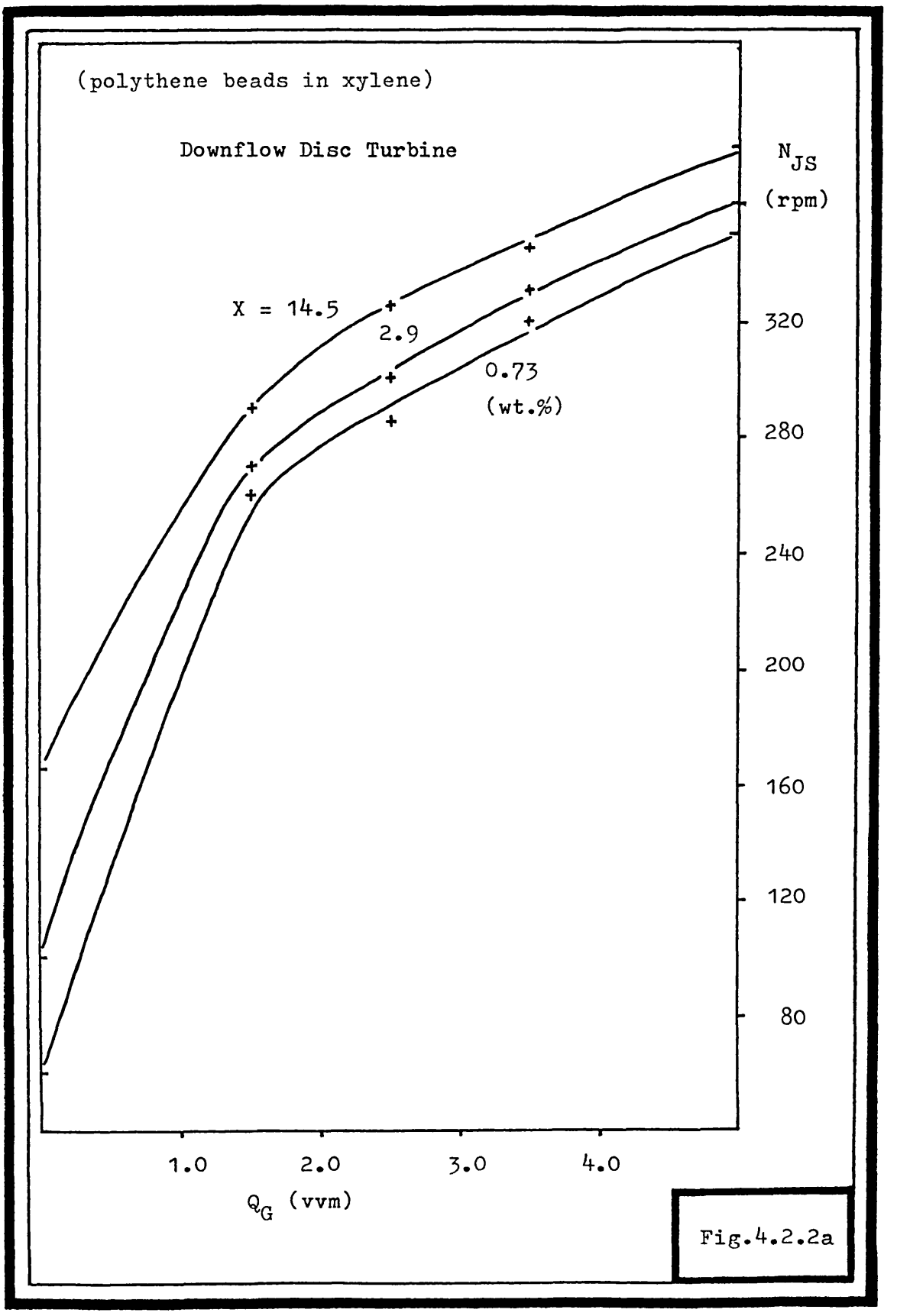

(polythene beads in xylene)
Downflow Disc Turbine
N_{JS} (rpm)
X = 14.5
2.9
0.73
(wt.%)
320
280
240
200
160
120
80
1.0
2.0
3.0
4.0
Q_G (vvm)

Fig.4.2.2a

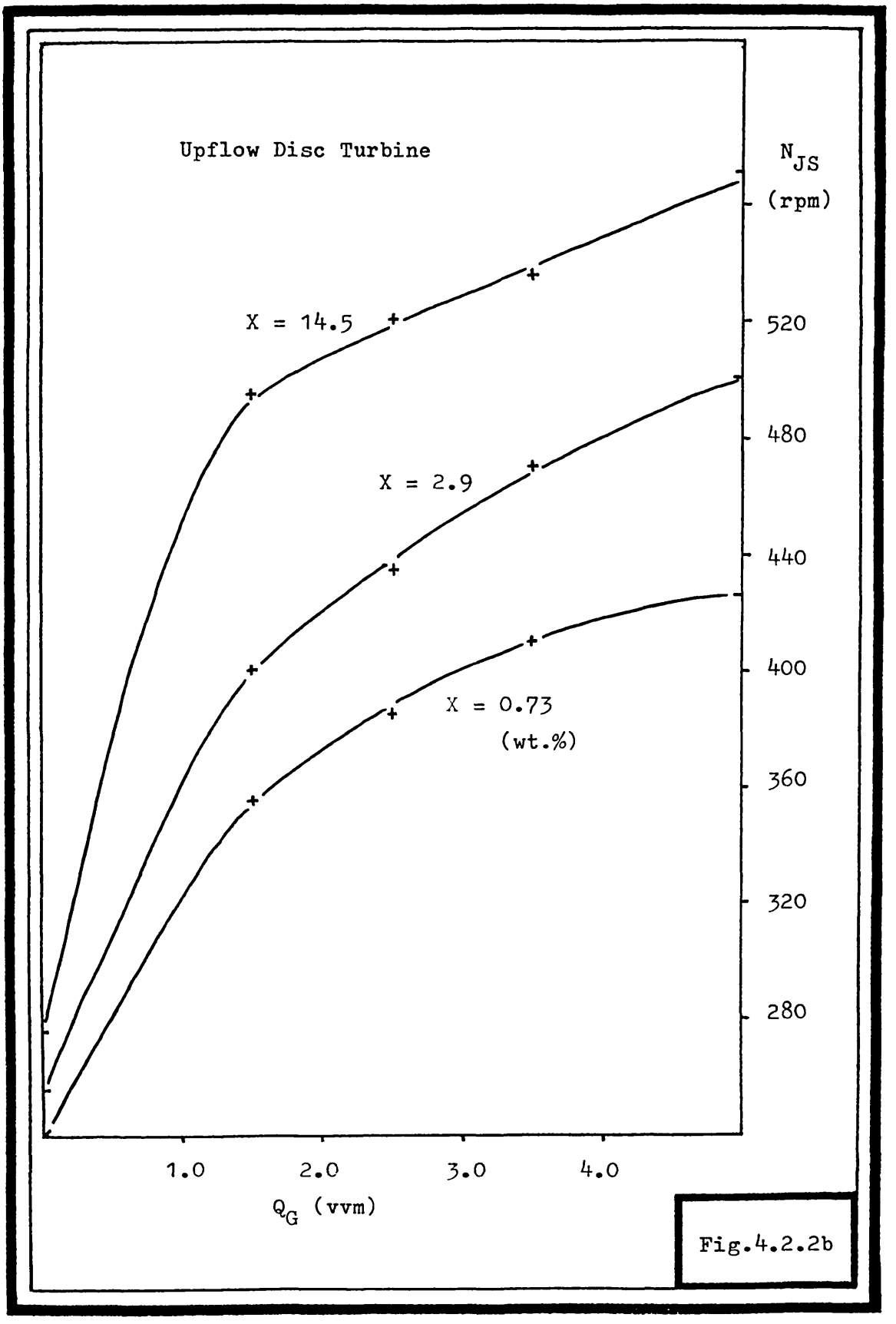

Upflow Disc Turbine
N_{JS} (rpm)
520
480
440
400
360
320
280
X = 14.5
X = 2.9
X = 0.73 (wt.%)
1.0
2.0
3.0
4.0
Q_G (vvm)

Fig.4.2.2b

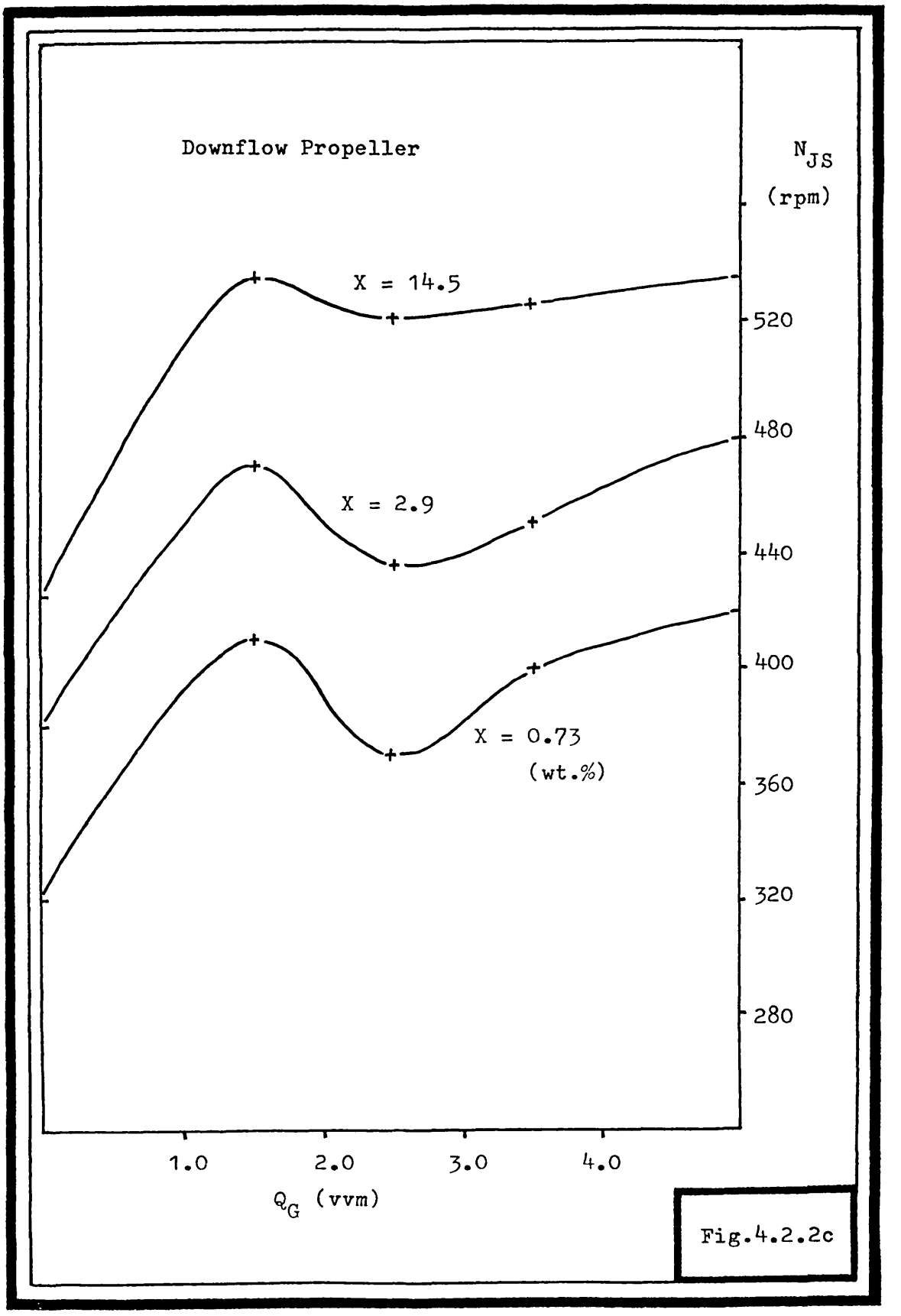

Downflow Propeller
N_{JS} (rpm)
X = 14.5
X = 2.9
X = 0.73 (wt.%)
520
480
440
400
360
320
280
1.0
2.0
3.0
4.0
Q_G (vvm)

Fig.4.2.2c

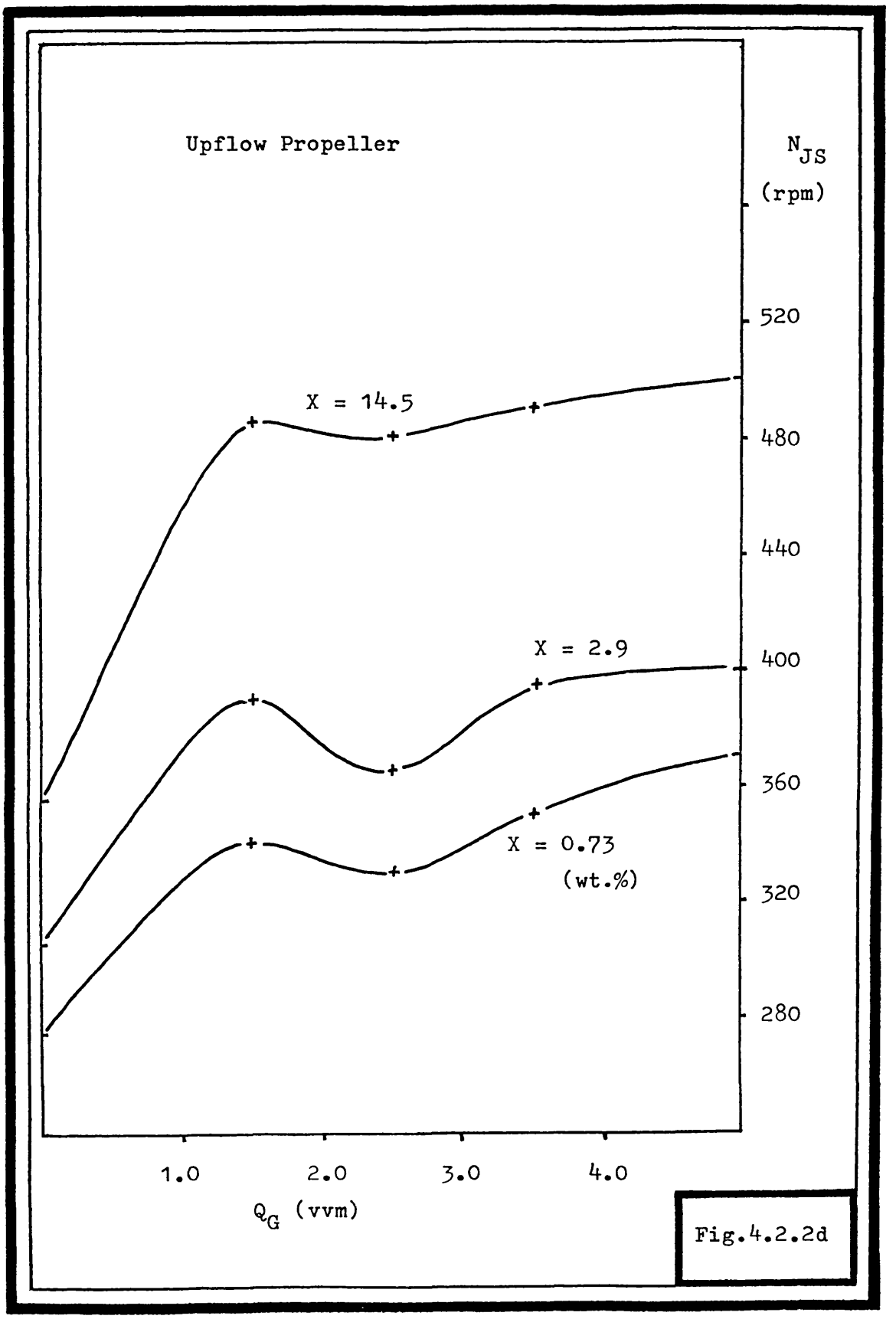

Upflow Propeller
N_{JS} (rpm)
520
480
440
400
360
320
280
X = 14.5
X = 2.9
X = 0.73 (wt.%)
1.0
2.0
3.0
4.0
Q_G (vvm)

Fig.4.2.2d

gas rate actually lowers the required suspension speed by a small but definite amount and at higher gas flows, N_{JS} starts to rise again but only slightly. This may be explained by the fact that, although the presence of gas reduces the buoyancy of the solids, a moderate flow of gas does set up quite strong convection currents which, for comparatively light solids, can play a significant part in their suspension. (This phenomenon has also been reported by Sharma et al : 2.e).

Certainly, no such effect was observed in earlier work for an air-water-sand system where the difference in density between solid and liquid phases ($\Delta\rho$) is approximately 1300 kg/m^3. For air-xylene-polythene though, $\Delta\rho$ is only about 100 kg/m^3 and at higher gas rates, some of the particles were suspended solely by the circulatory flow induced by the rising gas bubbles (i.e. without any mechanical agitation).

4.2.3 Stirrer Configuration :

The downflow disc turbine was seen to achieve solids suspension at lower stirrer speeds than any of the other impellers and it is preferable under most conditions (even allowing for the fact that it uses more energy to maintain a given stirrer speed than either of the propellers). Only at the highest gas rates does it become marginally less economical than the upflow propeller in terms of energy requirement.

The upflow disc is second-best at zero to low gas rates but is otherwise the poorest of the four designs considered. Both disc turbines share the feature that N_{JS} is strongly dependent on gas rate (: 2- to 6-fold increases in N_{JS} for Q_G = 0. to 5.0).

For the propellers on the other hand, the gas rate plays a much more minor role, with an increase in Q_G from 0. to 5.0 bringing about a 20.-30.% rise in N_{JS}. This could be explained by an extension of the argument applied to the dip in N_{JS} for the propellers (see Figs.4.2.2c,d) discussed in

the previous section : since an upflow propeller enhances the convection currents induced by the rapid upward passage of gas through the vessel (whilst a downflow propeller tends to nullify this effect) the upflow arrangement is better suited to achieving suspension of solids that are comparatively buoyant. (This implies that neither propeller would be very effective for the suspension of heavier solids).

Another possible reason for the difference between the two propellers is that particles striking or approaching an upflow propeller blade will be swept upwards, helping to maintain their suspension, the opposite being true for a downflow one. All this could explain the slightly better performance of the upflow propeller (c.f. the downflow propeller) even at zero gas rate. Note however, that just as the upflow propeller has performed more effectively as regards suspension, it will also tend to provide a poorer distribution of gas in the tank with a smaller interfacial area.

Unlike the propellers, both disc turbines prevent the predominance of gas-generated convection currents since they block the direct upward path of gas bubbles. It is suspected that, for the same reason, the upflow disc is so much worse at suspending solids : the disc gets in the way; with the downflow disc, solids are circulated upwards around the vessel walls, avoiding the turbine itself.

4.2.4 Comparison with Our Previous Results :

Some reference has already been made to past experiments using air-water-sand suspensions. Just as organic three phase systems usually contain solids that are only slightly more dense than the liquid phase, so inorganic reactors often have particles of quite high relative density and hence the characteristics of the suspensions are different.

The polythene particles used here were suspended fairly easily, even at substantial gas flowrates. Consequently, the 'suspension height' criterion (noting the stirrer speed at which particles reach 90.% of the liquid height in the

tank) was meaningless as a measure of whether or not suspension was achieved, because some particles always managed to satisfy the criterion well before the great majority of solids had been moved at all from the bottom of the vessel.

Taking homogeneity of the mixture as a guide might be useful if some satisfactory (and preferably simple) way of assessing its attainment could be devised, although the two-tiered impellers employed here make complete homogeneity improbable, even with fairly buoyant solids and at high stirrer speeds.

The 'just suspended' condition (described in section 2.6) was found to work well for the polythene beads.

With sand in water, total suspension was only achieved for low solids concentrations at low gas rates and high impeller speeds using the downflow disc turbine (the two propellers were not available then but it is not thought that they would have been much more successful than the poorly performing upflow disc : neither of them seems to generate sufficient turbulence). Note that better results would almost certainly have been obtained if the impeller clearance could have been reduced. Under no circumstances was anything approaching homogeneity observed, with by far the highest concentrations of sand present beneath the lower turbine. Again, the suspension height criterion proved to be of little value for the same reason as with the organic system.

The mass and size of an individual particle seems to be a comparatively minor factor in deciding how difficult it is to obtain a suspension : sand grains in the range 200-1000 μm gave similar results (all being very difficult to suspend) whilst the polythene beads (3. mm), despite being much larger and heavier, were considerably easier to suspend i.e. particle density relative to the liquid predominated. Particle shape has not been taken into account here but other studies have shown it not to be important unless the particles exhibit a tendency to interlock (18).

One further difference between the two sets of experiments carried out was that a single tube sparger was used initially (i.e. for air-water-sand) and the ring sparger was introduced later for the organic three phase experiments. Whether or not the different resulting degrees of gas dispersion have affected the results greatly seems questionable though, if anything, the ring sparger might be expected to have the more detrimental effect upon suspension because it takes up more space at the base of the tank than the single tube and is thus more likely to inhibit the motion of solids.

4.2.5 Correlation with Other Results :

It is generally accepted (2.e, 18) that the most reliable equation for predicting minimum suspension speed (for a solid-liquid system) is that of Zwietering :

$$N_{JS} = S\nu^{0.1} d_S^{0.2} (g\Delta\rho/\rho_L)^{0.45} X^{0.13} D^{-0.85} \qquad \text{VII}$$

$$\Delta\rho = \rho_S - \rho_L$$

S : a geometrical factor, is a function of impeller type, its diameter and its clearance above the base of the tank.

Other studies have found that the exponents associated with each term on the right hand side of equation VII differ and Chapman et al (18) give a summary of them :

exponents :

$0.10 < X < 0.22$ $\quad$ $0.17 < d_S < 0.5$

$0.43 < \Delta\rho < 0.5$ $\quad$ $-2.5 < D < -1.67$: depending on type of impeller

$0.1 < \nu < 0.2$

No comparably satisfactory equation for N_{JS} in a three phase (gas-liquid-solid) system exists though it seems likely that, with suitable modifications, Zwietering's equation (VII) might be used.

Fig.4.2.5a and Fig.4.2.5b show that, with the exception of the downflow disc turbine in an unaerated system,

$N_{JS} \propto X^c$ (or M^c) and the exponent : $0.04 < c < 0.13$

(for the downflow disc at $Q_G = 0.$, $c \sim 0.3$)

To take into account the effect of gas flowrate, Chapman et al plotted ΔN_{JS} (= $N_{JS}(G) - N_{JS}(G=0)$) against Q_G and found that :

$$\Delta N_{JS} = 0.94 \times Q_G \qquad \text{VIII}$$

(rps) (vvm)

From Fig.4.2.5c it can be seen that the relationship between ΔN_{JS} and Q_G is approximately linear for the two disc turbines over quite a broad range of gas flowrates. However, the slopes are all ~ 0.4 (c.f. 0.94) and if extrapolated back would not pass through the origin (as they must do since at $Q_G = 0.$, $\Delta N_{JS} = 0.$ by definition). Clearly, at lower gas rates, ΔN_{JS} must be more strongly dependent upon Q_G than it is in the range studied here ($1.5 < Q_G < 5.0$, and $Q_G = 0.$). This difference in operating conditions could explain why the results in this part of the project do not concur with those of Chapman ($0. < Q_G < 1.5$). A further reason is undoubtedly the very low relative density of the polythene beads used here : as has already been pointed out, for the propellers, an increase in gas rate, in a certain range, decreases N_{JS} slightly i.e. ΔN_{JS} falls with rising Q_G : this would not be observed other than for moderately large gas flows and, above all, light solids.

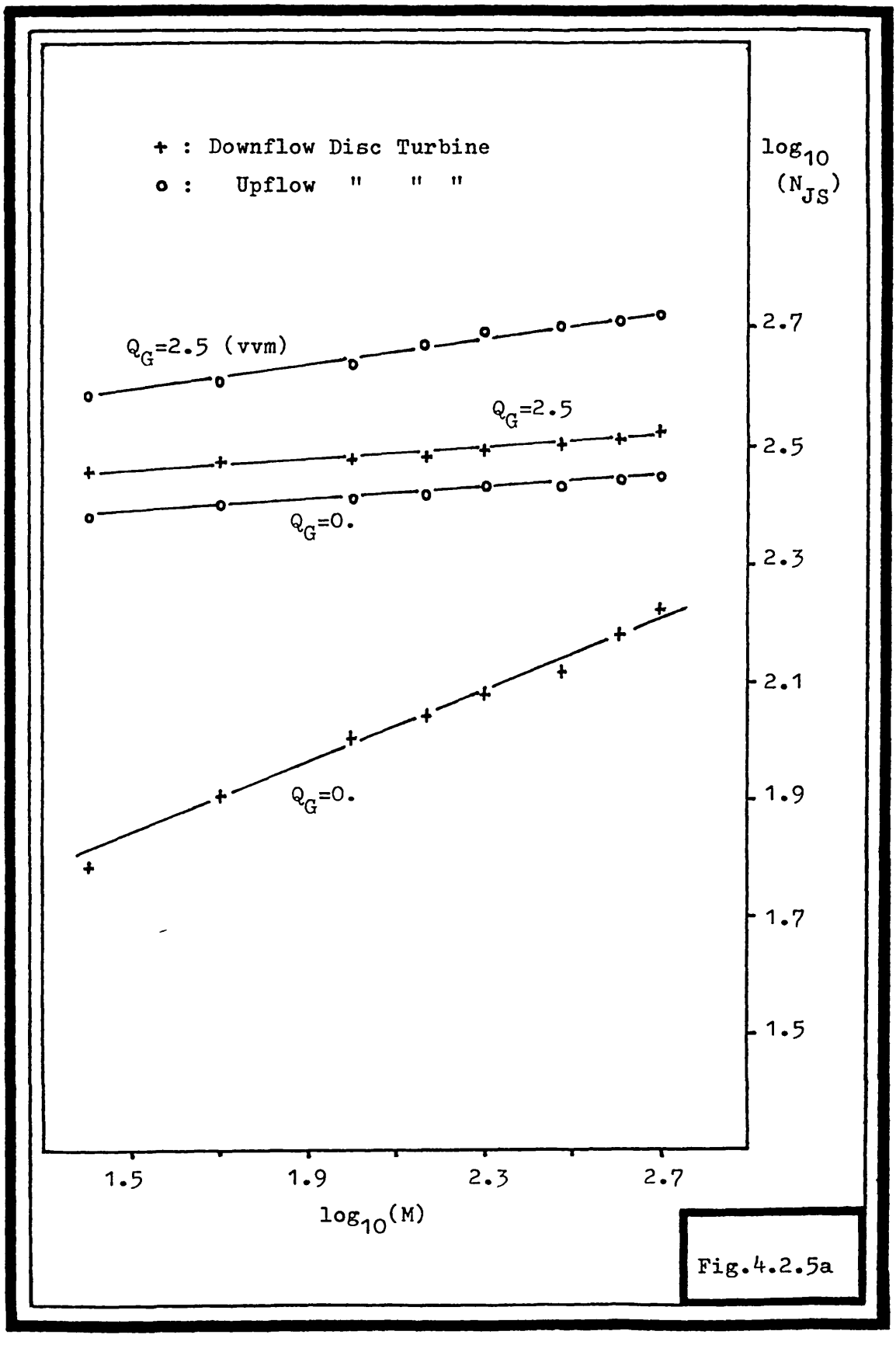

+ : Downflow Disc Turbine
o : Upflow " " "
$\log_{10}(N_{JS})$
Q_G=2.5 (vvm)
Q_G=2.5
Q_G=0.
Q_G=0.
2.7
2.5
2.3
2.1
1.9
1.7
1.5
1.5
1.9
2.3
2.7
$\log_{10}(M)$

Fig.4.2.5a

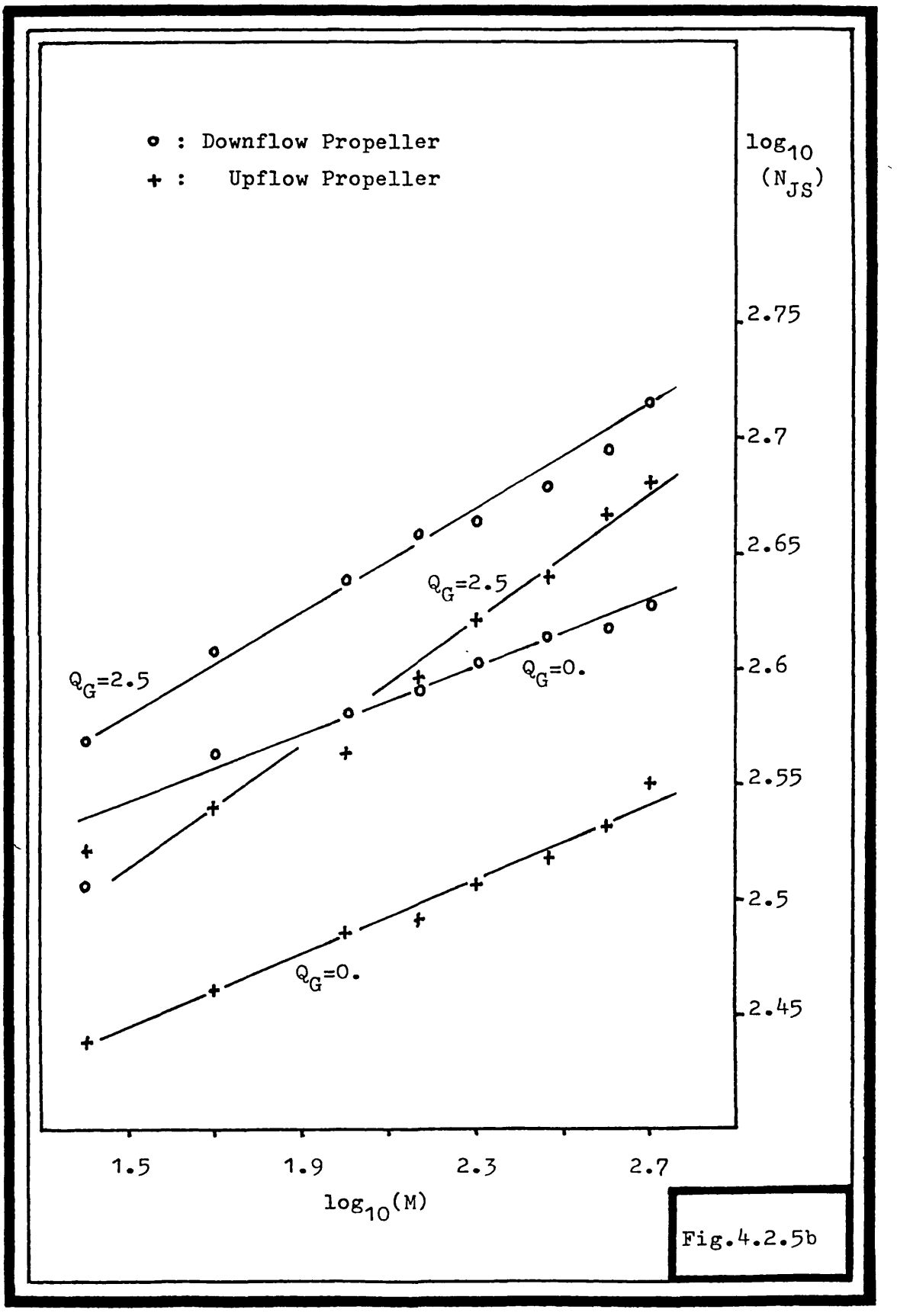

o : Downflow Propeller
+ : Upflow Propeller
log10 (NJS)
2.75
2.7
2.65
2.6
2.55
2.5
2.45
QG=2.5
QG=2.5
QG=0.
QG=0.
1.5
1.9
2.3
2.7
log10(M)

Fig.4.2.5b

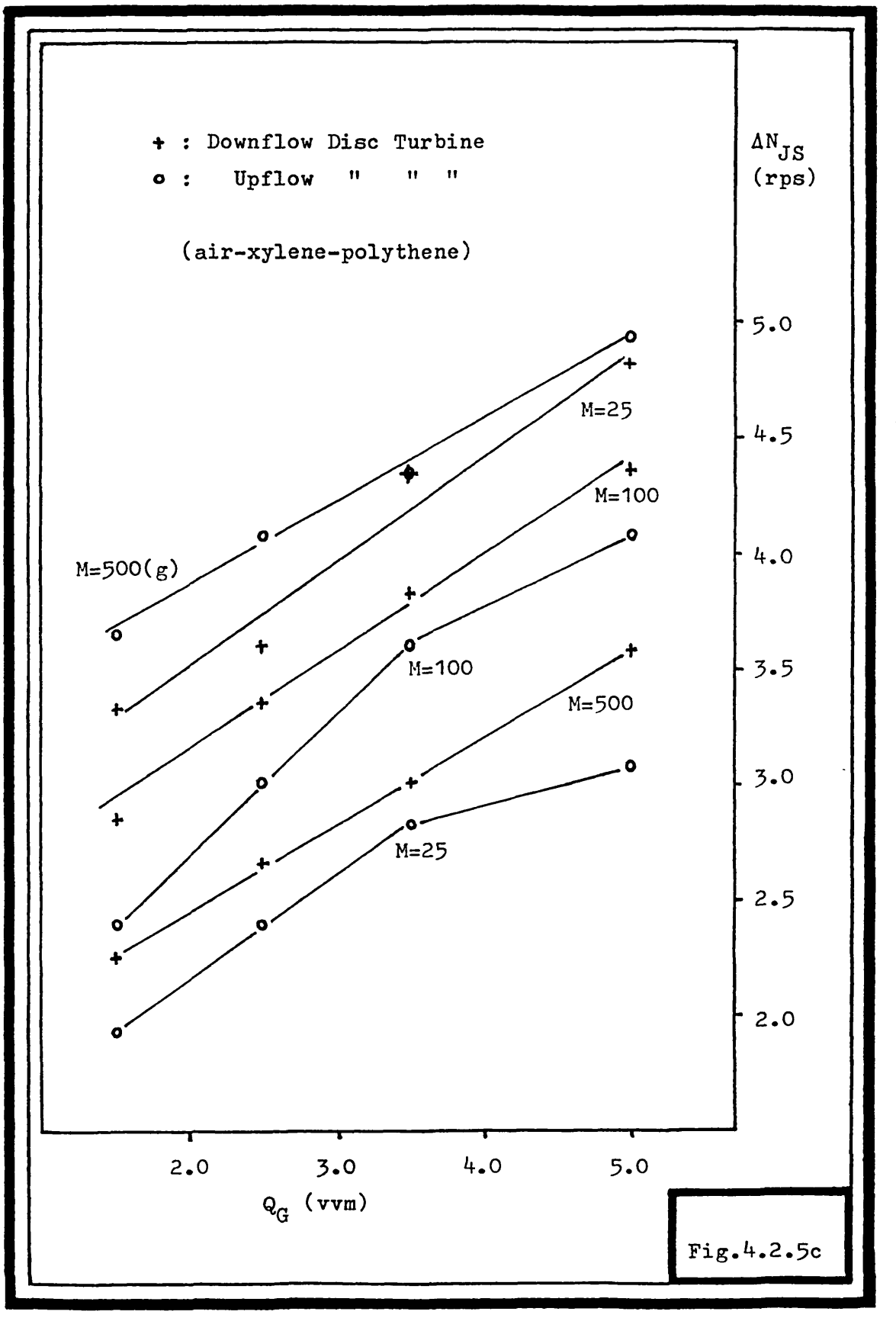

+ : Downflow Disc Turbine
o : Upflow " " "
(air-xylene-polythene)
ΔN_{JS} (rps)
5.0
4.5
4.0
3.5
3.0
2.5
2.0
M=25
M=100
M=500(g)
M=100
M=500
M=25
2.0
3.0
4.0
5.0
Q_G (vvm)

Fig.4.2.5c

4.3 Quiescent Interface Cell :

The cell, described in section 3.2, has been used to measure the rate of reaction of CO_2 with three different amines (as well as that of oxygen with sodium sulphite) across a known, constant interfacial area. With these results it was hoped to calculate values for the gas-liquid interfacial area by making similar measurements of the rate in the agitated tank.

4.3.1 Cyclohexylamine-Carbon Dioxide :

CHA has been used elsewhere to measure interfacial area but Charpentier (14.a) has suggested that for efficient reactors (e.g. well-agitated reactors or long packed columns) the criteria which make a chemical method valid, may not be satisfied throughout the vessel (due to depletion of the solute gas for example).

Fig.4.3.1a shows the results obtained for 10.% CHA in a solution of 70.% xylene and 20.% propanol (to keep the carbamate product in solution) reacting in the quiescent interface cell with a steady supply of CO_2 in air (20. l/min : 18. air, 2. CO_2). Unlike sulphite-oxygen, all of the amine-CO_2 reaction rates are dependent on the concentration of liquid phase reactant (though not very markedly so).

The initial rate of the CHA-CO_2 reaction is about :

$R_{CHA} = (0.45/25) = 1.8 \times 10^{-2}$ mol/l min (from Fig.4.3.1a)

$S = 39.6$ cm^2 $\therefore$ $N_{CHA} = 4.54 \times 10^{-4}$ mol/l min cm^2

This compares with 9.899×10^{-6} mol/l min cm^2 for sulphite-oxygen i.e. the CHA-CO_2 reaction is approximately fifty times as rapid as the sulphite one, implying that it would indeed be too fast for our purposes.

A further calculation shows that the amount of CO_2 absorbed is :

1.8×10^{-2} mol/l min of CHA in a volume of ~400. ml

$= 7.2 \times 10^{-3}$ mol/min of CHA in the cell

$= 2. \times 7.2 \times 10^{-3}$ mol/min of CO_2 (from the stoichiometry of the reaction)

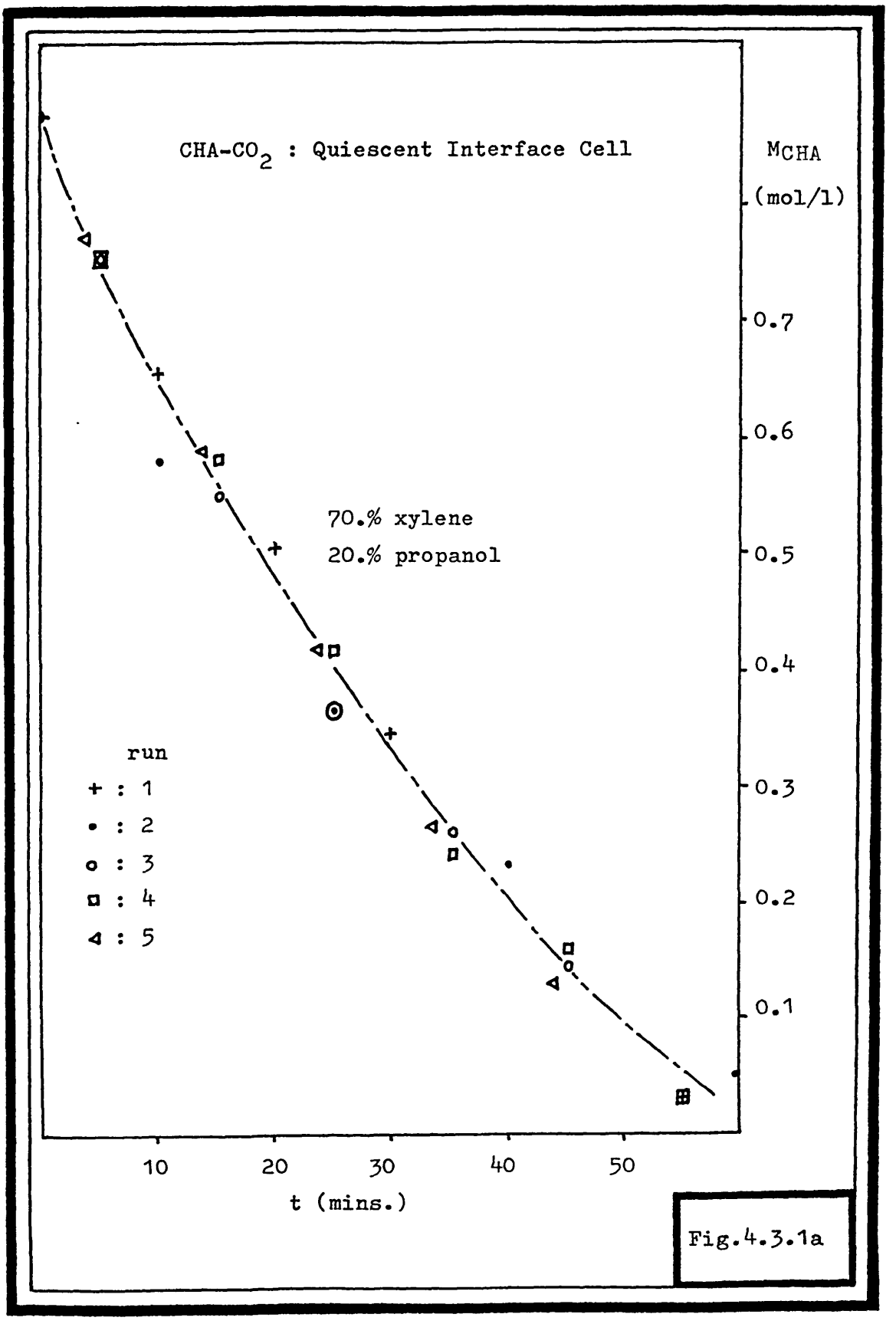

CHA-CO2 : Quiescent Interface Cell
MCHA
(mol/l)
0.7
0.6
0.5
0.4
0.3
0.2
0.1
70.% xylene
20.% propanol
run
+ : 1
• : 2
o : 3
□ : 4
◁ : 5
10
20
30
40
50
t (mins.)

Fig.4.3.1a

$= 1.44 \times 10^{-2}$ mol/min of CO_2

~ 0.35 litres of CO_2/min (1 mole $CO_2 \sim 24.$ litres)

(c.f. 2.0 l/min of CO_2 entering the cell)

- Again, the fairly high uptake of CO_2 suggested that severe depletion of gas bubbles would occur in the agitated vessel, invalidating the chemical method.

4.3.2 Diethanolamine-Carbon Dioxide :

The analysis of all three amines studied here was carried out by gas chromatography. For CHA, this did not pose any particular problems but both DEA and DIPA (see next section) are very viscous and have much higher boiling points than any of the other components to be analysed (see Appendix A 3.4). A new type of chromatographic column was available which is specifically intended for amine analysis but although it did produce good results as far as DEA (and DIPA) were concerned, the other components in the mixture : carbon dioxide, propanol and xylene, were flushed out so quickly that the propanol peak obscured any CO_2 trace present. However, 'Oronite' packing was used successfully, though the amines were rather slow to emerge ($\sim$ 20 mins.) and the peaks were small. A further problem with the DEA was the tendency for the amount of DEA present in an injected sample to decrease quite drastically with time, to the point at which peak height (even at large attenuation) was no longer proportional to concentration (and 'drift' and 'noise' meant that the area under the peak was hard to determine with any accuracy).

Consequently, the values of DEA concentration became progressively more unreliable with time (see Fig.4.3.2a).

To remedy this, experiments were performed without any xylene present i.e. 90.% propanol, 10.% DEA. In this way, the DEA peaks were much more consistent and the rate of reaction was also distinctly lower :

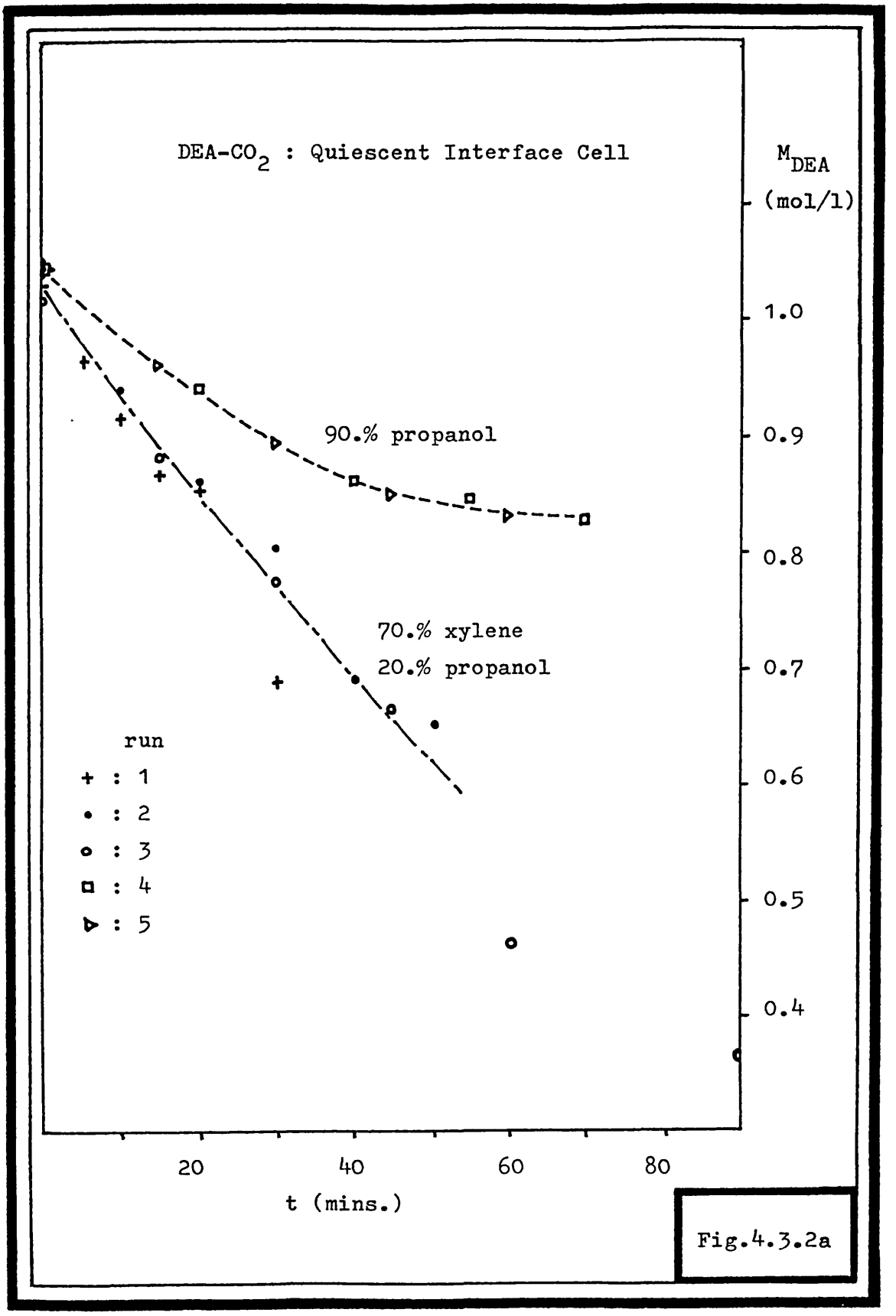

DEA-CO2 : Quiescent Interface Cell
M DEA (mol/l)
1.0
0.9
0.8
0.7
0.6
0.5
0.4
90.% propanol
70.% xylene
20.% propanol
run
+ : 1
• : 2
o : 3
□ : 4
▷ : 5
20
40
60
80
t (mins.)

Fig.4.3.2a

(i) DEA in xylene + propanol :

$N_{DEA} = (1.025-0.85)/(20.x39.6) = 2.21 \times 10^{-4}$ mol/l min cm^2

(ii) DEA in propanol :

$N_{DEA} = (1.044-0.94)/(20.x39.6) = 1.38 \times 10^{-4}$ mol/l min cm^2

One drawback of using DEA in just propanol however, is that after about an hour in the cell, crystals (presumably of carbamate) appeared in large quantities, choking the apparatus, so the possible running time of an experiment in the agitated vessel was expected to be short.

Both systems give somewhat slower reactions than CHA-CO_2 (as suggested by Charpentier : 14.a) though not by as much as had been hoped, probably still being too fast for the chemical method.

4.3.3 Di-isopropanolamine-Carbon Dioxide :

It was found that DIPA gave more consistent results (see Fig.4.3.3a) than DEA and the reaction rates are also slower :

(i) DIPA in xylene + propanol :

$N_{DIPA} = (0.75-0.6)/(52.5x39.6) = 7.22 \times 10^{-5}$ mol/l min cm^2

(ii) DIPA in propanol :

$N_{DIPA} = (0.75-0.7)/(42.x39.6) = 3.01 \times 10^{-5}$ mol/l min cm^2

Nevertheless, the rates are still greater than for the sulphite reaction but by less than a factor of 10 in both cases. So, even if depletion of CO_2 did occur in the agitated tank (so that the interfacial area could not be calculated) it was thought that qualitative comparisons between different systems should be possible.

One inherent disadvantage with all three of the organic chemical reactions used is that (especially for the agitated vessel) large amounts of waste are generated. To remedy this, the spent chemicals from CHA-CO_2 experiments

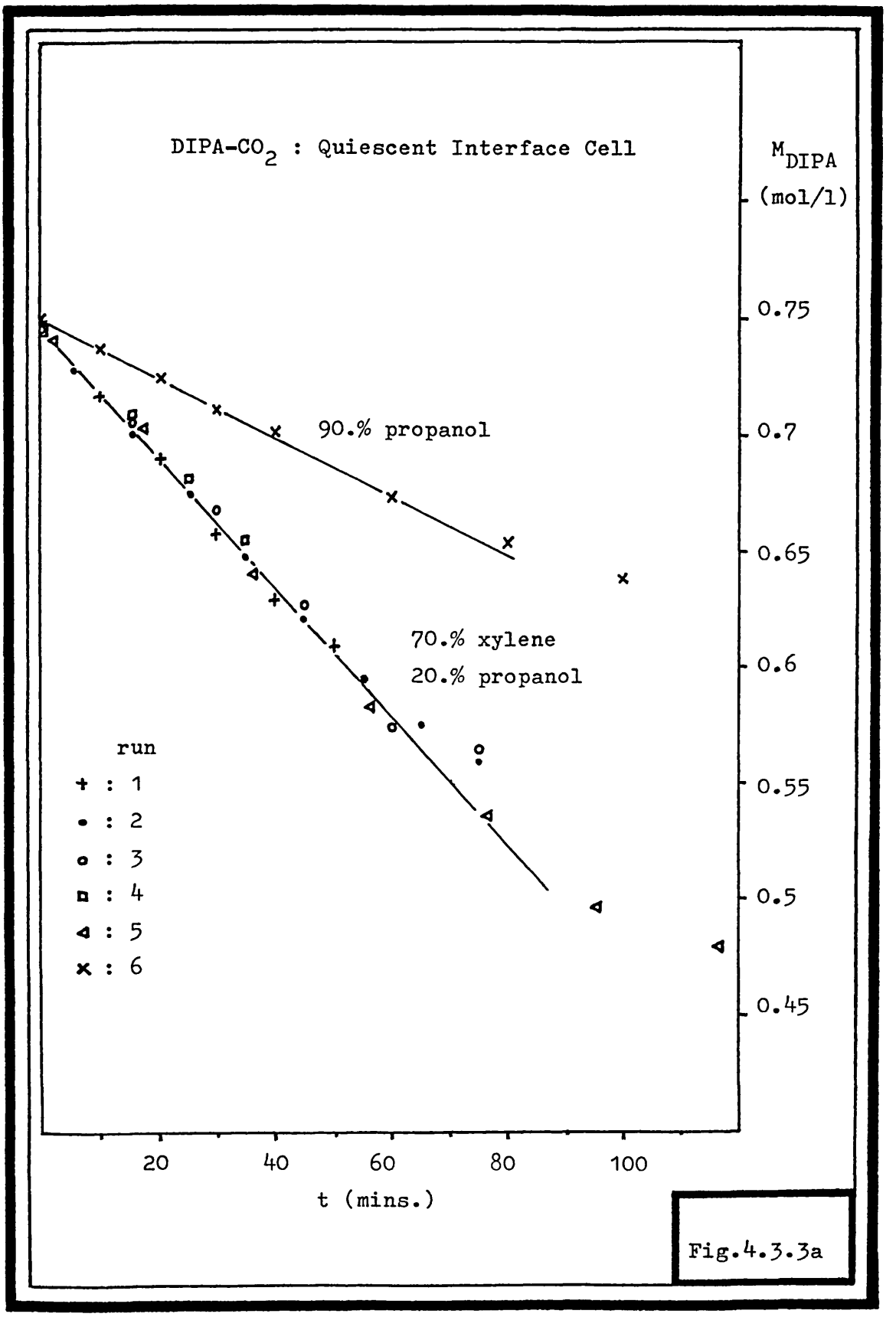

DIPA-CO2 : Quiescent Interface Cell
M DIPA (mol/l)
0.75
0.7
0.65
0.6
0.55
0.5
0.45
90.% propanol
70.% xylene
20.% propanol
run
+ : 1
• : 2
o : 3
□ : 4
◁ : 5
× : 6
20
40
60
80
100
t (mins.)

Fig.4.3.3a

were stored and separated in a batch distillation unit. The resulting products appeared to be pure according to samples tested by chromatography but it is suspected that the CHA tended to degrade into more volatile, but still chemically active, compounds that were not separable from the propanol : Propanol that had been distilled from waste was re-used in an experiment, giving a greatly increased rate of reaction for no apparent reason other than the possible presence of some impurities.

The larger-scale use of such organic reactions for a chemical method is, therefore, likely to prove expensive.

4.3.4 Sodium Sulphite-Oxygen :

The rate of this reaction has already been measured (16), using the same source of chemicals as in this work, so the quiescent interface cell experiments were not repeated but are summarised below :

$R_A = 3.92 \times 10^{-4}$ mol/l min $= 6.53 \times 10^{-6}$ mol/l s

$S = 39.6$ cm^2

$N_{Ai} = (C_{Ai})^{1.5}(2k_2D_A/3)^{0.5}$ II (p.23) Reith (10)

From (5.b) and (11), at 20°C : $D_A = 1.6 \times 10^{-5}$ cm^2/s

$C_{Ai} = 6.4 \times 10^{-7}$ mol/cm^3

$\therefore k_2 = (6.53\times10^{-6}/(39.6(6.4\times10^{-7})^{1.5}))^2\times1.5/(1.6\times10^{-5})$

$= 9.72 \times 10^9$ l/mol s

c.f. :

8.5×10^9 at pH 8.00

40.0×10^9 at pH 8.50 given by Danckwerts (5.b)

4.4 Agitated Cell : Organic Liquid Phase :

4.4.1 Cyclohexylamine-Carbon Dioxide :

Results for the agitated vessel using CHA confirmed that (as the quiescent cell measurements had indicated) the reaction of this amine with CO_2 was indeed too fast for interfacial area measurements to be made. A few experiments with the downflow disc turbine and the upflow propeller were carried out (these two, of the four possible, were chosen because they were expected to produce the most widely varying results). However, neither impeller design nor stirrer speed had any noticeable influence on the progress of the reaction. The rate was almost entirely dependent upon the amount of gas coming into the vessel, with as much as 90.% of the CO_2 entering, being absorbed. Clearly, gas bubbles leaving the vessel were virtually depleted of CO_2.

As Fig.4.4.1a shows, the rate of reaction was exactly doubled by a two-fold increase in the gas flow (even at a slightly lower stirring speed).

4.4.2 Diethanolamine-Carbon Dioxide :

One experiment was sufficient to show that, although the rate of CO_2 absorption may have been somewhat slower (than CHA-CO_2), the two major disadvantages observed whilst using the quiescent interface cell, persisted.

The liquid phase became cloudy and within half an hour, the tank was blocked by white, crystalline solids (barely soluble in propanol, soluble in water). Presumably as a result of this first difficulty, the amount of amine present in liquid samples rapidly declined to the stage that, on analysis, the chromatograph hardly registered a DEA peak at all (obviously making all but the first two or three samples very unreliable).

Note that this experiment was for a 70.% xylene, 20.% propanol, 10.% DEA mixture : though its rate of reaction was a little faster than for 90.% propanol, 10.% amine; the problem of crystal formation had not occurred. (see section 4.3.2)

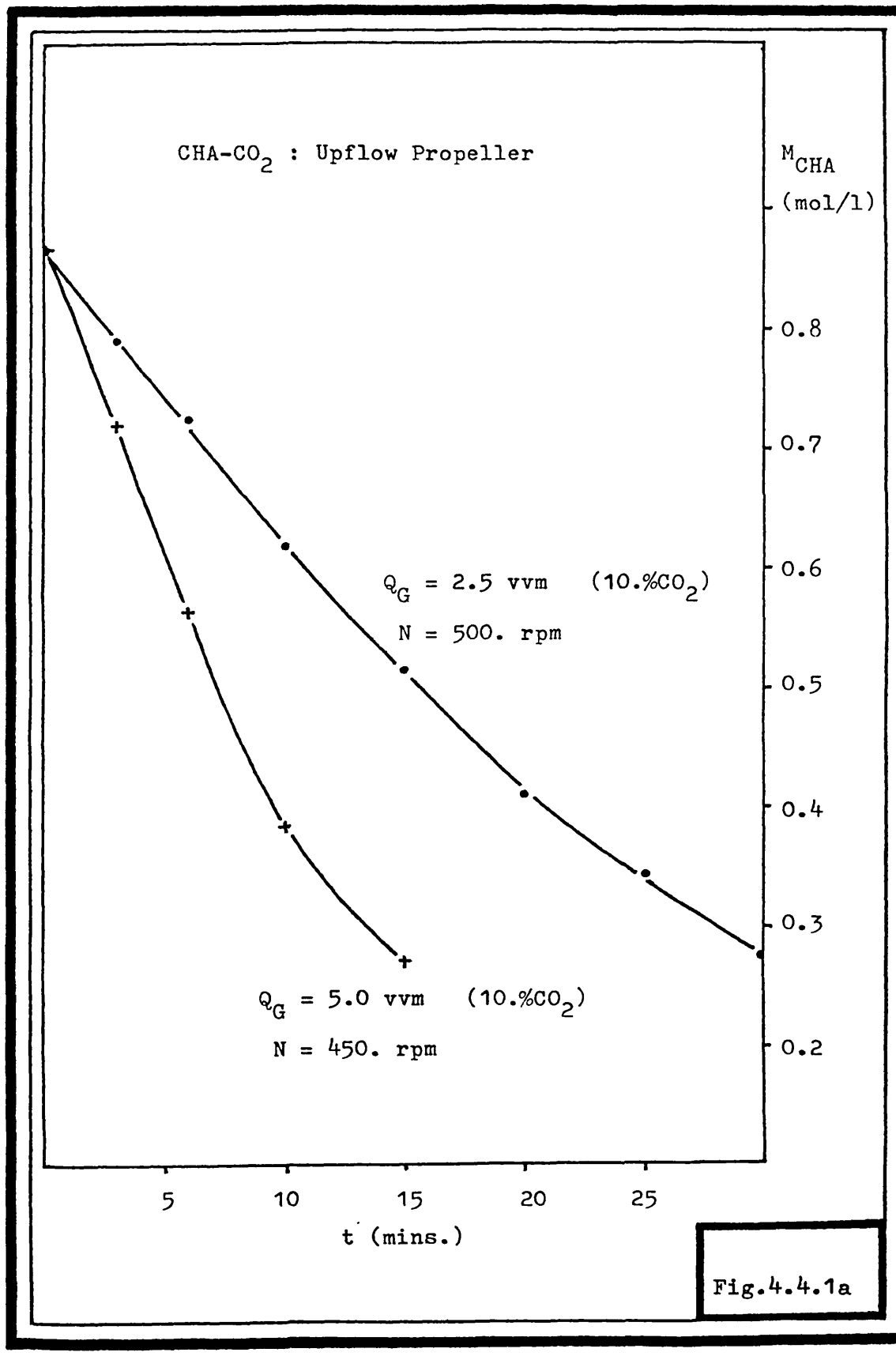

CHA-CO2 : Upflow Propeller
MCHA (mol/l)
0.8
0.7
0.6
0.5
0.4
0.3
0.2
QG = 2.5 vvm (10.%CO2)
N = 500. rpm
QG = 5.0 vvm (10.%CO2)
N = 450. rpm
5
10
15
20
25
t (mins.)

Fig.4.4.1a

4.4.3 Di-isopropanolamine-Carbon Dioxide :

With the slowest rate of reaction achieved for any of the amines tested (and with none of the operating difficulties encountered when using DEA) a 10.% solution of DIPA in propanol was expected to yield rather more useful results than the others.

Fig.4.4.3a compares a two phase system with a three phase one, using a downflow disc turbine at 350 rpm to see if the presence of 100 g (X = 2.9 wt.%) of polythene beads has any effect upon the gas-liquid area. As explained in section 2.6, such comparatively light particles, though large, were not expected to possess sufficient momentum to cause gas bubble disruption and an increase in interfacial area.

Conversely, neither does the graph show any significant difference between the two rate curves, indeed they coincide very well, implying that the solids have not decreased the contact area by reducing the degree of turbulence within the tank.

Note : the curves do diverge suddenly after 20. mins., with the three phase curve tailing off sharply but this is assumed to be due to faulty analysis (rather than a true reflection of the concentration-time profile) probably due to either :

(i) the decay of incorrectly sealed samples (it was not always possible to analyse all of the samples in one day);

or (ii) a change in the chromatographic column - the 'Oronite' packing deteriorated quite severely over the whole period of the amine-CO_2 experiments and occasional recalibration was necessary.

Fig.4.4.3b depicts the progress of the reaction for two stirrers : the downflow disc and the upflow propeller, and shows the former to give a greater rate of reaction at the same stirrer rate (though allowing for the disc turbine's greater power consumption, there might be

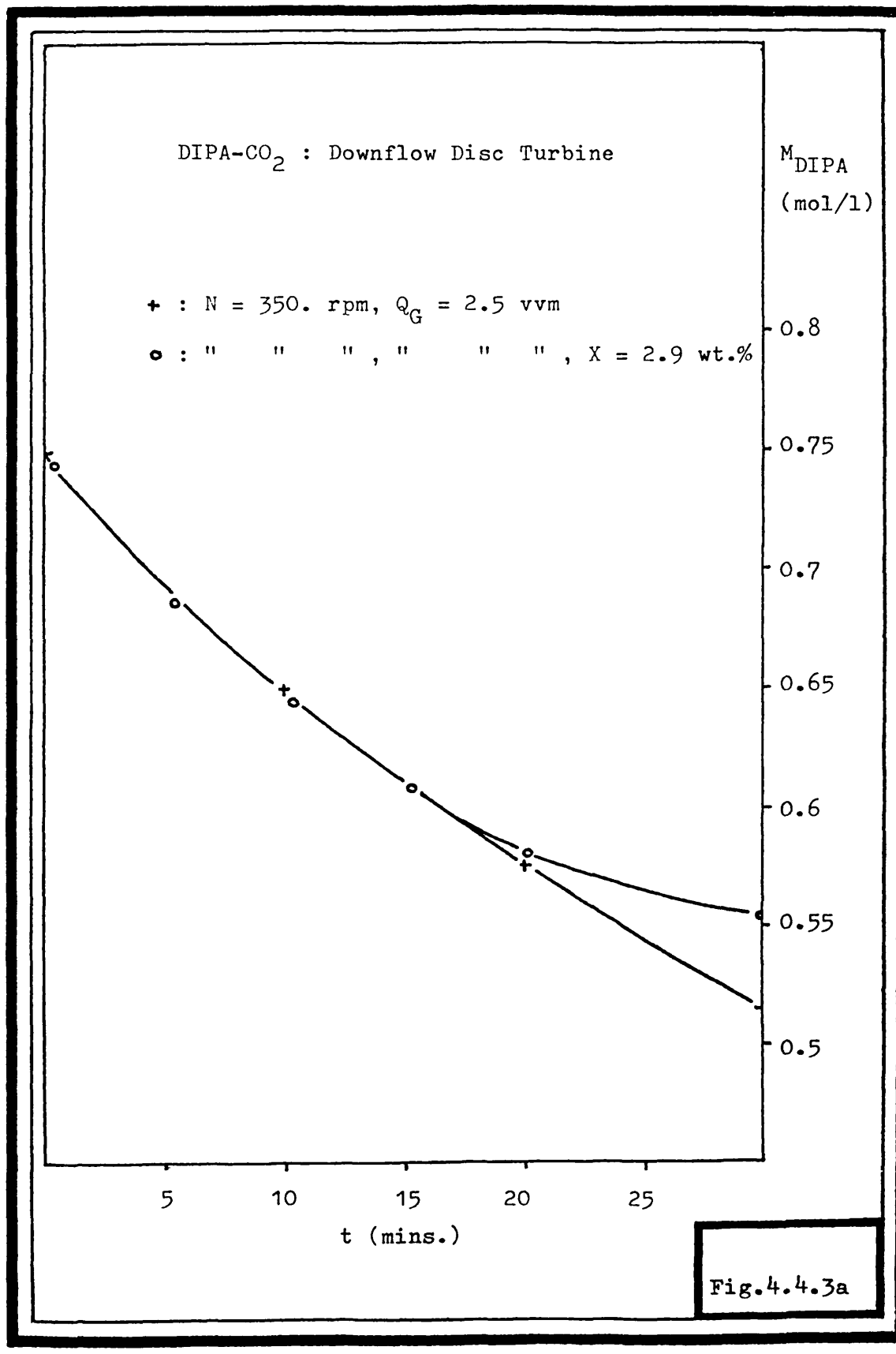

DIPA-CO2 : Downflow Disc Turbine
+ : N = 350. rpm, QG = 2.5 vvm
o : " " " , " " " , X = 2.9 wt.%
MDIPA (mol/l)
0.8
0.75
0.7
0.65
0.6
0.55
0.5
5
10
15
20
25
t (mins.)

Fig.4.4.3a

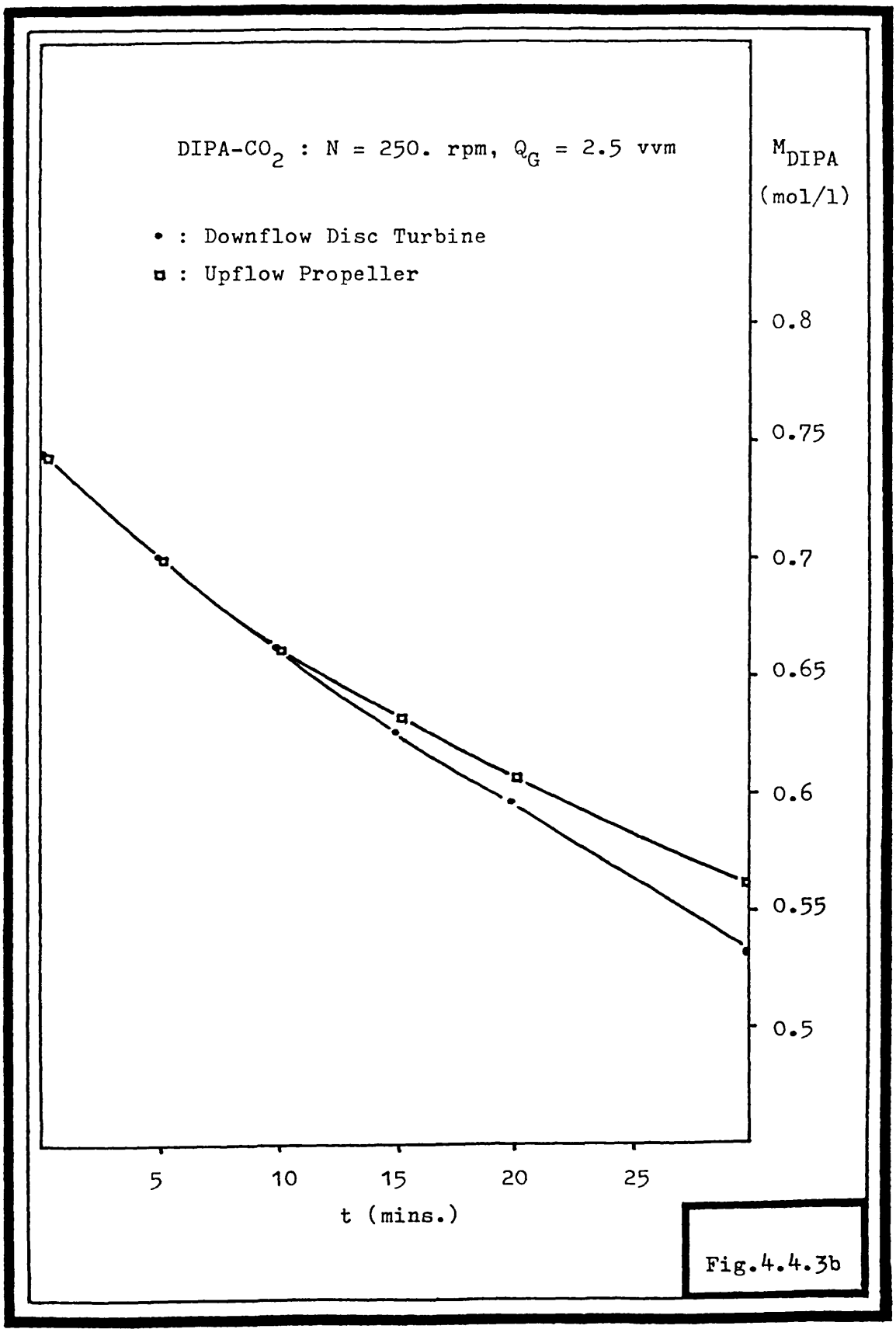

DIPA-CO2 : N = 250. rpm, QG = 2.5 vvm
• : Downflow Disc Turbine
▫ : Upflow Propeller
MDIPA (mol/l)
0.8
0.75
0.7
0.65
0.6
0.55
0.5
5
10
15
20
25
t (mins.)

Fig.4.4.3b

little to choose between them). Referring back to the previous figure, it can also be seen that, not surprisingly, the rate of amine reaction is less at the lower impeller speed (250. c.f. 350. rpm).

A rough calculation gives the typical rate of CO_2 absorption as about :

$$(0.75-0.55)/30. \times 2. \times 24. = 0.32 \text{ l/min}$$

(out of 1.0 l/min entering)

- so although some information can be obtained from such experiments, the partial pressure of solute gas is still considerably diminished, thus the interfacial area cannot be calculated and generally, the difference between two agitated systems must be fairly large before it can be reliably detected.

The substantial volumes of waste generated are also prohibitive.

4.5 Agitated Cell : Inorganic Liquid Phase :

Having failed to find a suitable organic reaction with which to measure gas-liquid areas, it was decided to revert to the sulphite method in order to obtain data for the ring sparger with all four impeller designs and the single tube sparger with the two propellers (to complement the results previously gained with the disc turbines and single tube gas inlet).

4.5.1 Ring Sparger, Disc Turbines :

Fig.4.5.1a shows the effect of gas rate on interfacial area (at constant stirrer speed). Perhaps the most important aspect was the change brought about by the introduction of a ring sparger. Whereas a maximum in surface area occurred with a single tube (16), the ring not only gave larger values of interfacial area (A) but there is little sign of A levelling off, let alone decreasing, at high gas rates.

Hence the relationship between gas flowrate and surface area is almost a linear one for both of the pitched blade disc turbines. The downflow curve is steeper i.e. it makes better use of increasing gas rates whilst the upflow line has quite a gentle slope (- A is a weaker function of gas flow). Rather surprisingly however, when Q_G is small, the interfacial area is lower for the downflow disc than the upflow one and only at intermediate and high gas rates does the downflow arrangement become preferable : there seemed to be no satisfactory explanation for this but a few further tests in this lower gas range merely confirmed the observation (and in any case, the discrepancy is too large to be due solely to experimental error).

Fig.4.5.1b depicts the strong dependence of interfacial area on turbine speed and, therefore, power input. Both up- and downflow curves rise quite sharply and follow a similar path, with the downflow arrangement becoming progressively more effective at higher rates of mixing. So, whilst there is little to choose between the two at low impeller speeds, the downflow stirrer gives a surface

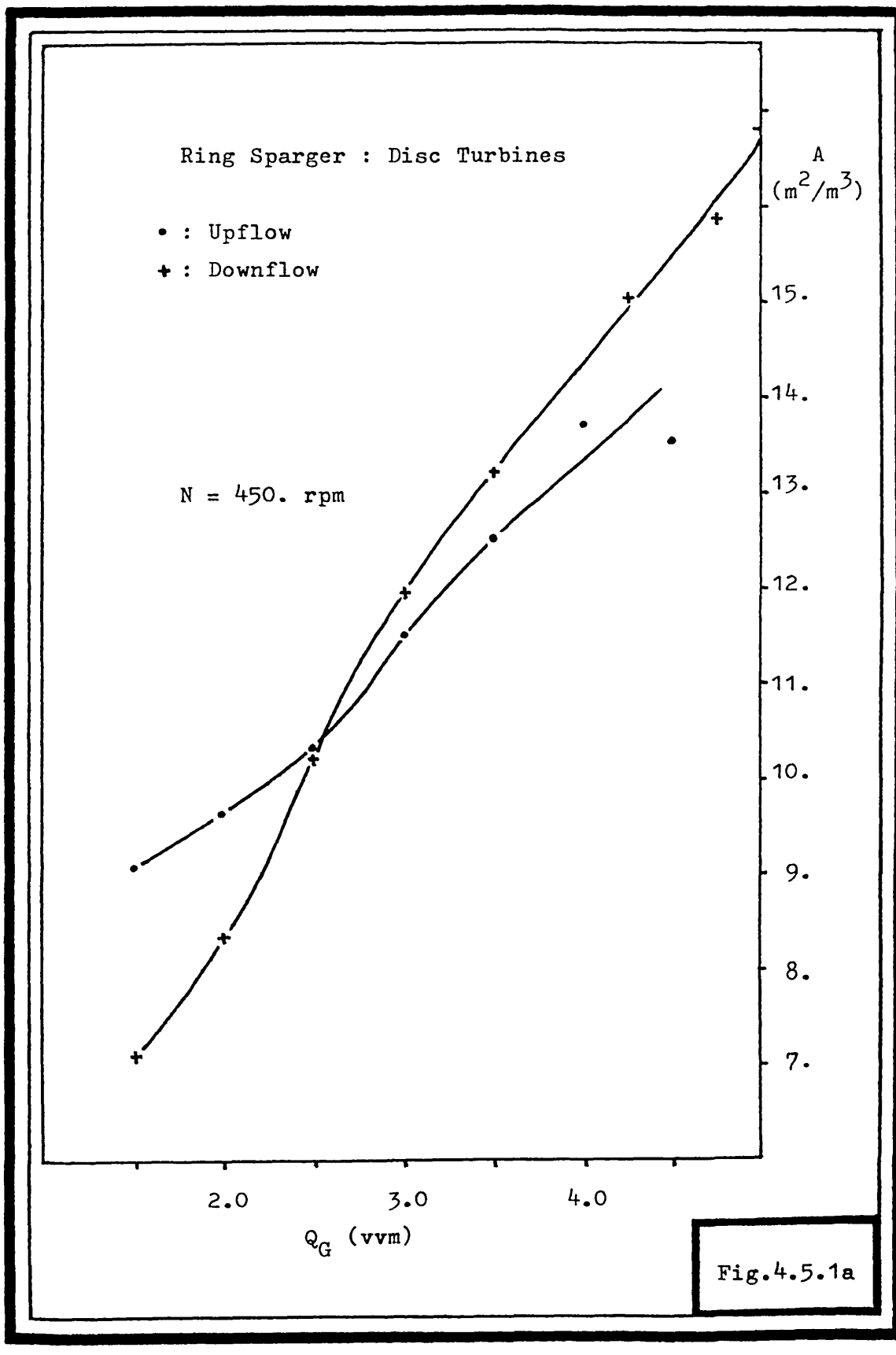

Ring Sparger : Disc Turbines
• : Upflow
+ : Downflow
N = 450. rpm
A
(m²/m³)
15.
14.
13.
12.
11.
10.
9.
8.
7.
2.0
3.0
4.0
Q_G (vvm)

Fig.4.5.1a

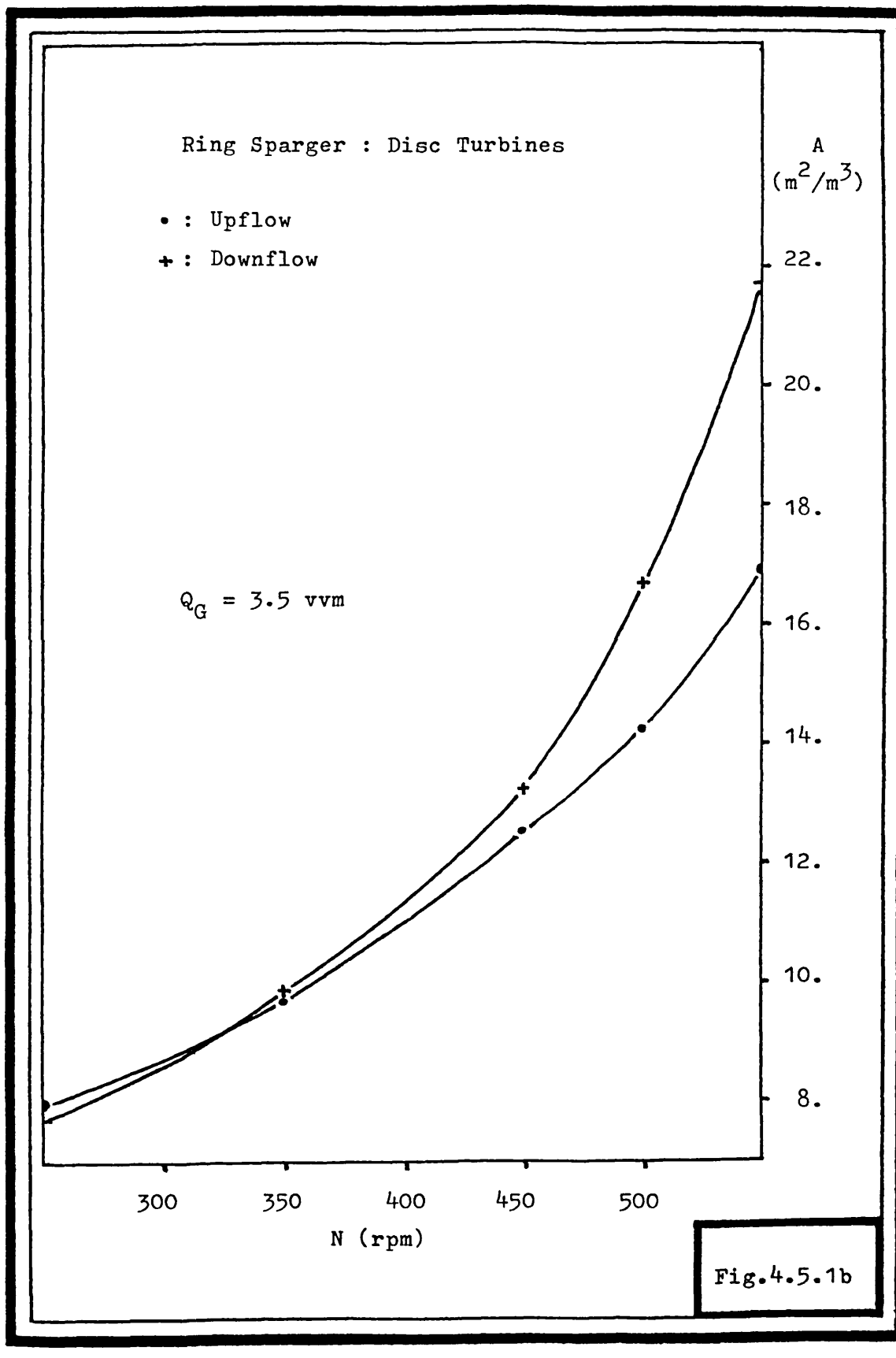

Ring Sparger : Disc Turbines
• : Upflow
+ : Downflow
Q_G = 3.5 vvm
A
(m^2/m^3)
22.
20.
18.
16.
14.
12.
10.
8.
300
350
400
450
500
N (rpm)

Fig.4.5.1b

area almost 30.% larger at 550. rpm.

The corresponding plot for the downflow disc with a single tube sparger (16) is slightly different : at lower stirrer speeds, the interfacial area is far smaller than with the ring sparger but, as the stirring rate rises, the improvement is more rapid until at ~550. rpm, it achieves a larger surface area than the upflow disc with ring sparger. Clearly, the higher the rate of agitation, the less important the type of gas sparger becomes and, presumably, at very high stirrer speeds, the difference in gas liquid area between ring sparger and single tube for the downflow turbine would eventually become negligible.

4.5.2 Ring Sparger, Propellers :

Similar experiments to those carried out with the disc turbines were also performed using the propellers :

The influence of gas flow on interfacial area for the downflow propeller (see Fig.4.5.2a) is like that seen for the disc turbines, the contact areas growing steadily with rising gas rates. However, the upflow propeller was the only one of the four impellers tested that failed to make good use of higher gas flowrates. Whilst its interfacial areas for small amounts of gas were only slightly below those of the downflow propeller, any increase from intermediate gas sparging rates upwards, brought minimal improvements in contact area.

Consequently, the downflow disc is (surprisingly) the poorest design at low gas rates with the other three yielding results quite close together. In the middle gas range, all four are very much alike but from then onwards, the two downflow stirrers are decidedly better. For both up- and downflow impellers in this upper half of the gas range, the angled blade discs give larger active surface areas than the corresponding propellers.

Fig.4.5.2b is unlike its counterpart of the previous section, in that the two curves of A vs N are approximately parallel, with the downflow propeller

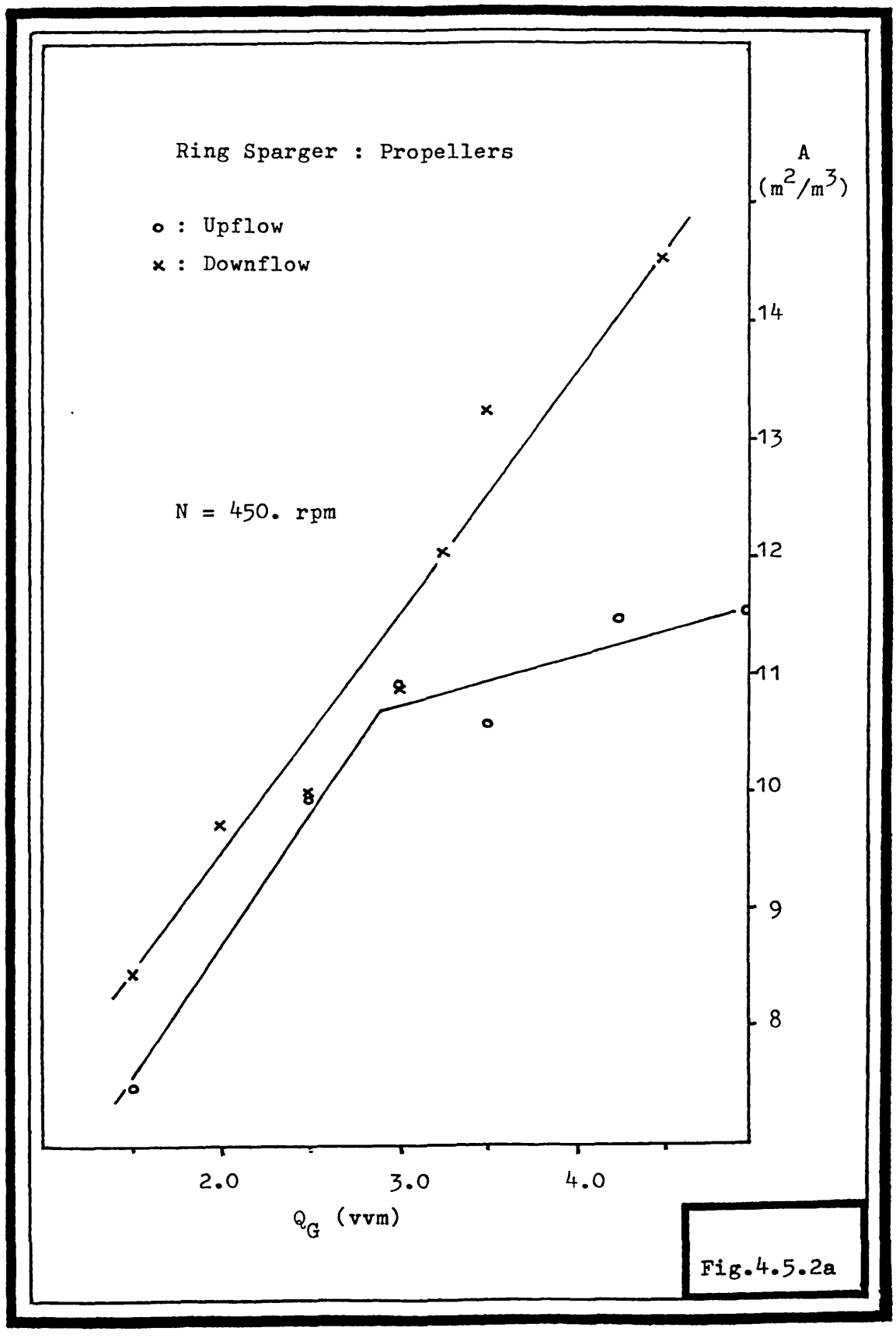

Ring Sparger : Propellers
o : Upflow
× : Downflow
N = 450. rpm
A
(m²/m³)
14
13
12
11
10
9
8
2.0
3.0
4.0
Q_G (vvm)

Fig.4.5.2a

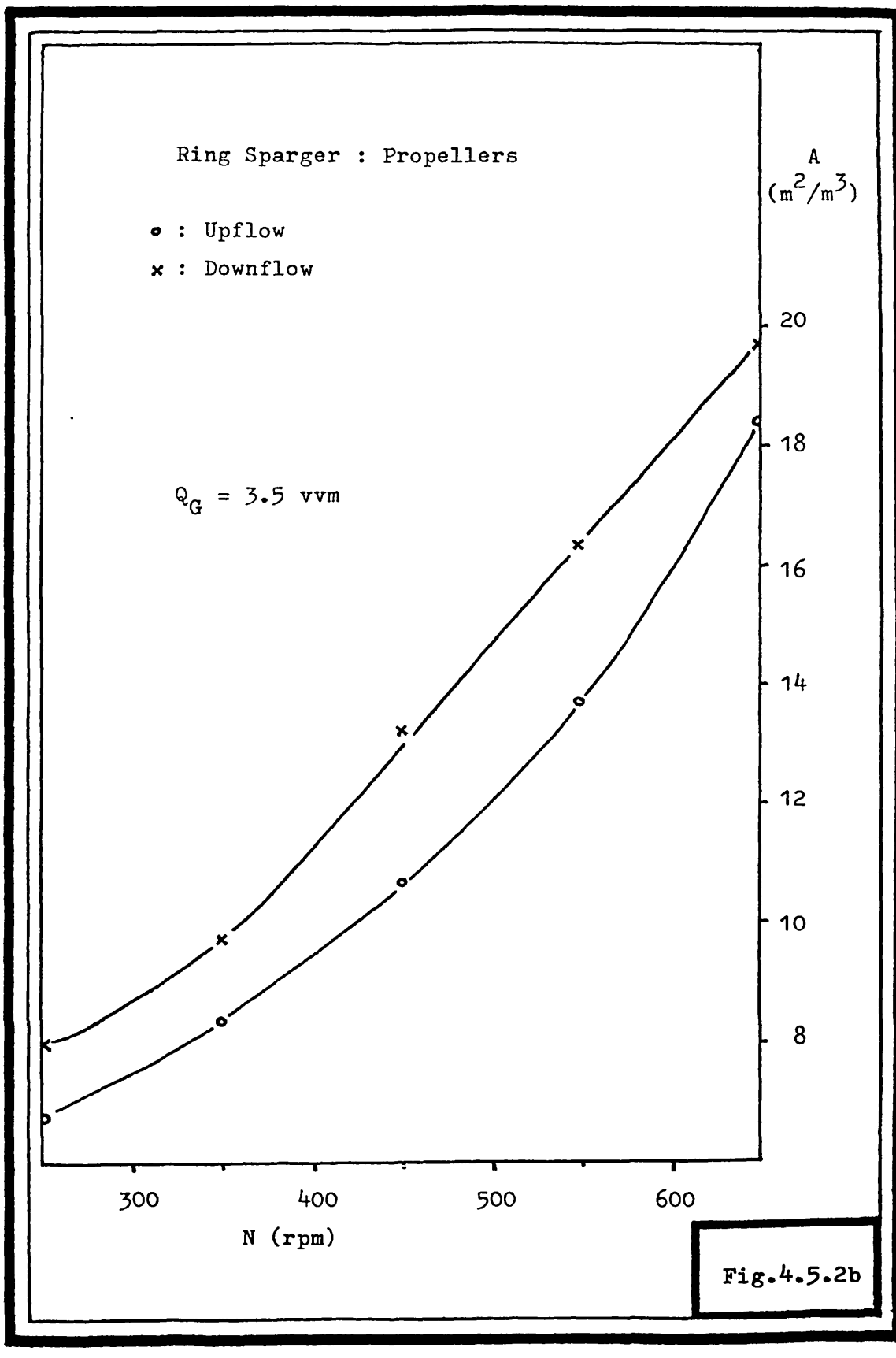

Ring Sparger : Propellers
o : Upflow
× : Downflow
Q_G = 3.5 vvm
A
(m^2/m^3)
20
18
16
14
12
10
8
300
400
500
600
N (rpm)

Fig.4.5.2b

producing a substantially greater interfacial area throughout. Indeed, at speeds up to about 450. rpm, it is never significantly worse than either of the disc turbines. Even above this stirring rate, although it begins to lag behind the downflow disc by an ever-increasing margin, allowing for its lower power requirement makes it just about as efficient as the downflow disc and far better than the upflow one.

On the other hand, the upflow propeller is definitely worse than the three alternatives, regardless of stirrer speed (and only about the same as the upflow disc when power consumption is taken into account).

4.5.3 Single Tube Sparger, Propellers :

Experiments for the disc turbines with a single tube sparger having been completed previously (16), it remained only to carry out similar tests using the two propellers.

(It should perhaps be borne in mind that most of the experiments reported in this section (and some of those in other sections) were performed at a time of high ambient temperatures and, since the agitated tank's temperature could not be controlled (see section 3.1.2) the results were calculated with allowances made for the ensuing higher rate of sulphite oxidation (Appendix A 3.1.2). This necessitated the use of tabulated literature values of oxygen solubility and diffusivity and rate constants as functions of temperature. Whilst there is no reason to doubt their accuracy, the temperature correction of the reaction rate does introduce a further possible source of error. Nevertheless, these results should still be reliable).

The results of gas flowrate against interfacial area (at N = 450 rpm : constant) are plotted on Fig.4.5.3a (including a line for the downflow propeller with ring sparger by way of a comparison). For all gas rates, the downflow propeller gives a larger surface area than the upflow one, though the difference between them is very small throughout. The slope of these A vs Q_G lines is, however, more gentle than that for the downflow propeller with ring

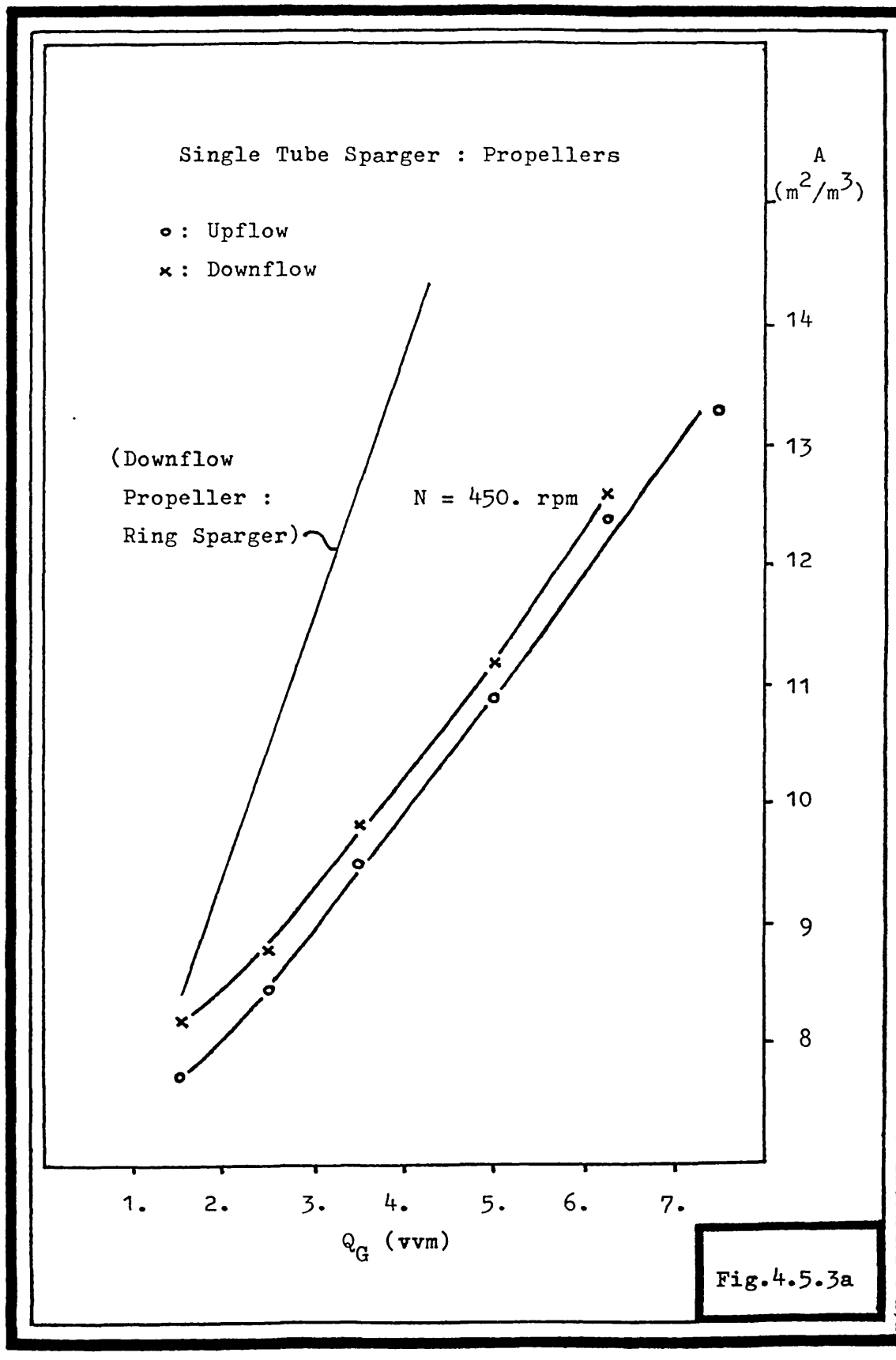

Single Tube Sparger : Propellers
o : Upflow
× : Downflow
(Downflow
Propeller :
Ring Sparger)
N = 450. rpm
A
(m²/m³)
14
13
12
11
10
9
8
1.
2.
3.
4.
5.
6.
7.
Q_G (vvm)

Fig.4.5.3a

sparger. Thus whilst at Q_G = 1.5 vvm there is scarcely anything to choose between the ring and tube spargers, at Q_G = 5.0, the ring develops a gas-liquid area 50.% greater than the tube.

It will be recalled that a maximum surface area was observed for the downflow disc turbine at a constant stirrer speed when using a single tube sparger (16). Quite evidently, there is no sign of such an effect for the propellers, although for a considerable portion of the gas range, the downflow disc remains the better option : at very low gas rates, the interfacial areas are alike (and small) but from then up to about Q_G = 4.25, the improvement in contact area is greater for the downflow disc (A is ~20.% larger than for either propeller). Beyond this peak though, A declines rapidly for the disc so that by Q_G = 5.0, the propellers are marginally better and become better still at even higher gas rates.

Amongst the results of section 4.5.1, it was found that the higher the stirrer speed, the less important the type of gas sparger. Fig.4.5.3b confirms this : at low impeller speeds, both propellers with the single tube sparger give much smaller interfacial areas than they do when a ring sparger is fitted. The gap narrows with increasing stirring rates, though rather more slowly than with the downflow disc turbine : only at about 600. rpm does the downflow propeller (with single tube) attain as good a gas dispersion as the upflow one with ring sparger.

The downflow propeller again produced larger surface areas than its upflow counterpart, though the difference between them is minimal for speeds up to ~450. rpm (at Q_G = 3.5) and certainly the curves imply that neither propeller makes the most of the gas supply in this operating range without some degree of bubble pre-dispersion (e.g. with a ring sparger).

Similar data had already been obtained for the downflow disc but with Q_G = 5.0 vvm. However this was

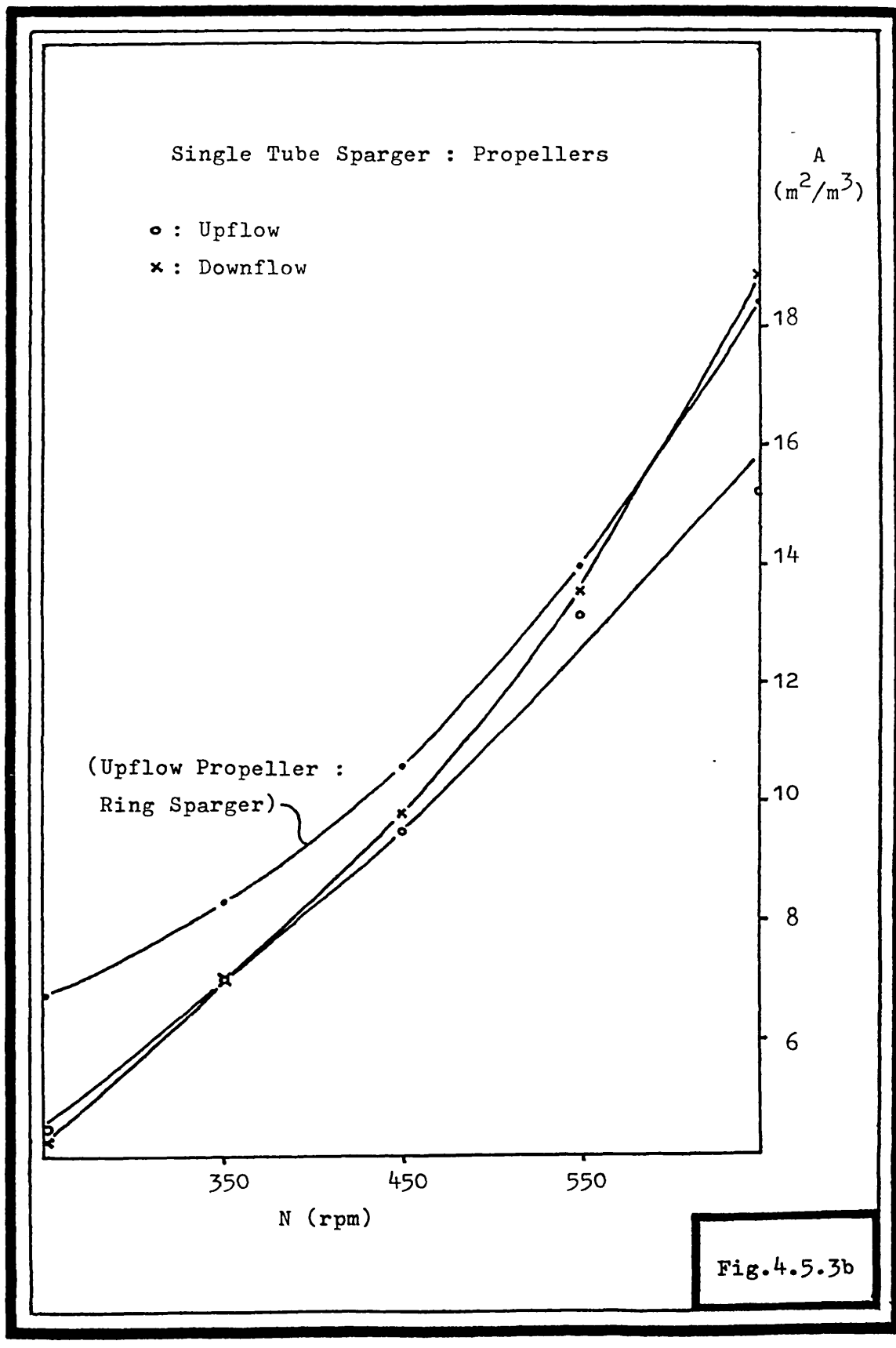

Single Tube Sparger : Propellers
o : Upflow
× : Downflow
A
(m²/m³)
18
16
14
12
10
8
6
(Upflow Propeller :
Ring Sparger)
350
450
550
N (rpm)

Fig.4.5.3b

subsequently found to be no better than Q_G = 3.5 in terms of interfacial area for this particular impeller (16), so the results should be comparable. In any case, the disc turbine creates progressively larger gas-liquid areas than the propellers but approximate equality is restored if one allows for the disc's greater power requirement.

Overall, the downflow impellers still generate larger interfacial areas than upflow ones but the difference is generally fairly small and the surface area values tend to be much lower than for comparable conditions with the ring sparger (except at very high stirrer speeds or low gas rates) simply because of the single tube's less effective method of gas introduction.

4.5.4 Correlation and Comparison of Results :

Taneja and Subbarao (3.b) proposed that Fl (= G/ND^3,- the gas flow number) may be used as a guide to the effectiveness of both solids suspension and gas dispersion, stating that both would be poor if Fl exceeds 0.05 .

Here : (i) propeller : D = 5.0 cm (0.5 dm)
(ii) disc turbine : D = 6.5 cm (0.65 dm)

(i) $Fl = G(l/min)/(N(rpm)(0.5)^3) = 8G/N$

The experimental conditions that yield the lowest (non-zero) value of Fl (whilst measuring A and N_{JS}) are :

$G = 6.0, N = 450. : Fl = 7.38 \times 10^{-2}$

(ii) $Fl = G(l/min)/(N(rpm)(0.65)^3) = 3.641G/N$

Again, for the lowest Fl,

$G = 6.0, N = 450. : Fl = 4.85 \times 10^{-2}$

i.e. whilst measuring N_{JS} and A, only for the disc turbine (at N = 450., Q_G = 1.5) was Fl less than 0.05 (and then only just).

Our observations demonstrate however, that for the systems studied, solids suspension (admittedly for quite buoyant solids) could be achieved at substantially higher gas flow numbers than 0.05 .

Smith et al (23) measured the gas hold-up (rather than A) vs Fl and obtained an exponential curve at very low Fl with a transition at Fl $\sim$ 0.03 (where large cavities form) to an approximately linear relationship : All our results would be expected to fall in this linear region and this seems to be the case : see Fig.4.5.4a.

Note : although the lower impeller is largely responsible for solids suspension, the same need not be true for interfacial area. Therefore, applying similar arguments to those in section 4.1.6, the Flow numbers in Fig.4.5.4a have all been based on D = 0.065 m.

The better performance of the downflow disc at higher speeds and/or larger gas rates is demonstrated, as is the importance of using the ring sparger (except at very low gas rates or very high stirrer speeds).

Fig.4.5.4a shows, then, ...

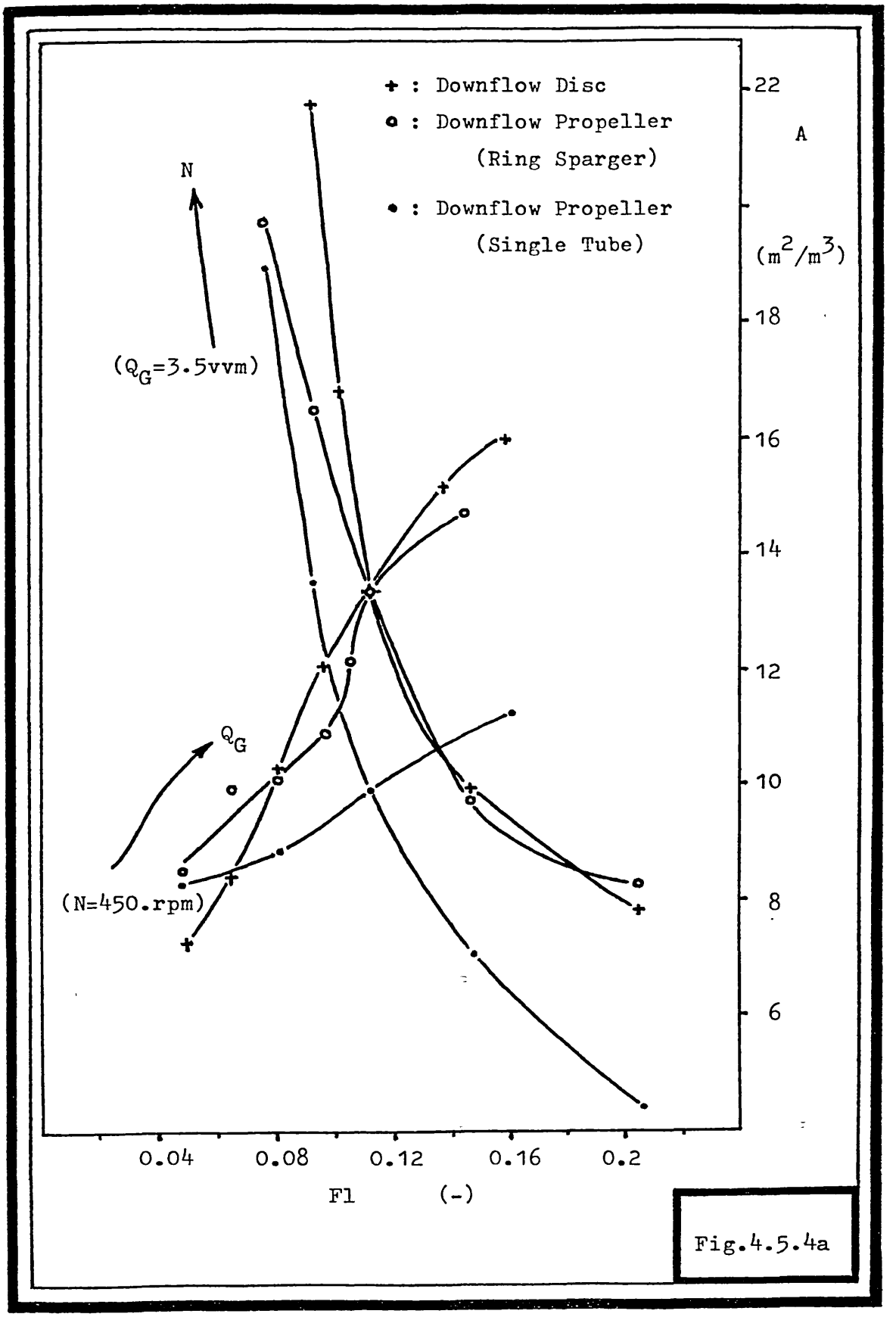

+ : Downflow Disc
o : Downflow Propeller
(Ring Sparger)
• : Downflow Propeller
(Single Tube)
N
(Q_G=3.5vvm)
Q_G
(N=450.rpm)
A
(m^2/m^3)
22
18
16
14
12
10
8
6
0.04
0.08
0.12
0.16
0.2
Fl (-)

Fig.4.5.4a

that low gas flow numbers do not, by themselves, ensure good gas dispersion : stirrer and gas sparger design must also be taken into account. It is also evident that a given gas flow number at a high gas rate accompanied by a high stirrer speed, produces a larger interfacial area than the same Fl at a low gas rate with low stirrer speed.

Interfacial area (or some other comparable parameter, such as bubble Sauter mean diameter) can be related to stirrer speed and gas flowrate in the form :

$$A = \text{constant} \times Q_G^b \times N^c$$

where, according to Greaves and Economides (3.e), the exponents b and c are generally found to be in the ranges : $0.0 < b < 1.0$ and $1.26 < c < 3.00$

Figs. 4.5.4b,c depict the dependence of surface area on N and Q_G for the ring sparger with the downflow disc turbine and the upflow propeller (results for the other two designs lie between these two extremes, generally somewhat nearer to the downflow disc lines). The slopes of these log-log graphs are the exponents b and c. The values of b at N = 450. rpm (0.38 for the upflow propeller, 0.71 for the downflow disc) are well within the range suggested above. The same is true for the stirrer speed exponent : $1.5 < c < 2.5$ for the impellers studied here at speeds in excess of ~400. rpm (Q_G = 3.5 vvm). However, below this rate of mixing, $0.6 < c < 0.74$. Presumably this is due to the presence of the ring sparger which is the dominant factor as regards gas dispersion at low stirrer speeds : This does not occur with the single tube sparger (Fig.4.5.4d) where any increase in stirrer speed, even at the lower end of the scale, results in much improved interfacial areas : $1.31 < c < 1.77$ for the propellers (at Q_G = 3.5). The exponent b (at a constant speed of N = 450. rpm) varies slightly with gas rate for the propellers (Fig.4.5.4e) but has an average value of 0.32 . (With the disc turbines and single tube sparger, b was found to be about double that for the propellers up to Q_G ~4.0, above which the interfacial areas decreased rapidly i.e. $b < 0$: 16).

The interfacial area cannot, therefore, be predicted with any reliability by choosing unique values of b and c because (although they fall within the range quoted in 3.e), b and c vary so widely according to N, Q_G and stirrer design. However, as has been stressed repeatedly, to make an economic comparison between impeller designs, it is necessary to compare the interfacial area (of which the product formation rate is a function) with the power requirement (i.e. running cost) for each stirrer.

This has been done by reading off values of power (P) vs N, Q_G from Figs.4.1.1a,b,c,d and Figs.4.1.2a-d, and comparing them with the interfacial areas (A) plotted in Figs.4.5.1a,b and Figs.4.5.2a,b. (Note that this required a certain amount of interpolation and (in a few cases) extrapolation of the power curves : a possible extra source of error).

Fig.4.5.4f shows surface area against power for the pitched blade disc turbines (at Q_G = 3.5 vvm). There is little difference between the two at low P (i.e. low speed) but the downflow starts to become significantly better at middle to high P. Both curves rise fairly steadily across the range investigated.

Fig.4.5.4g is the corresponding graph of A vs P for the propellers : both curves rise more steeply than the discs', initially, but taper off by comparison at higher power inputs. The upflow propeller is approximately the same as the upflow disc but is generally a little more economical. The downflow propeller is much better (by $\sim$ 20 %) than any of the others at low and intermediate power inputs but tails off : At high P, the downflow propeller is about the same as the two upflow impellers and the downflow disc becomes markedly better (by $\sim$ 15 %) at high P input.

Fig.4.5.4h shows log(A) vs log(P) : All four types of impeller have been plotted together. There is a fair amount of scatter but the overall trend is quite consistent, with $\log(A) \propto 0.41 \log(P)$.

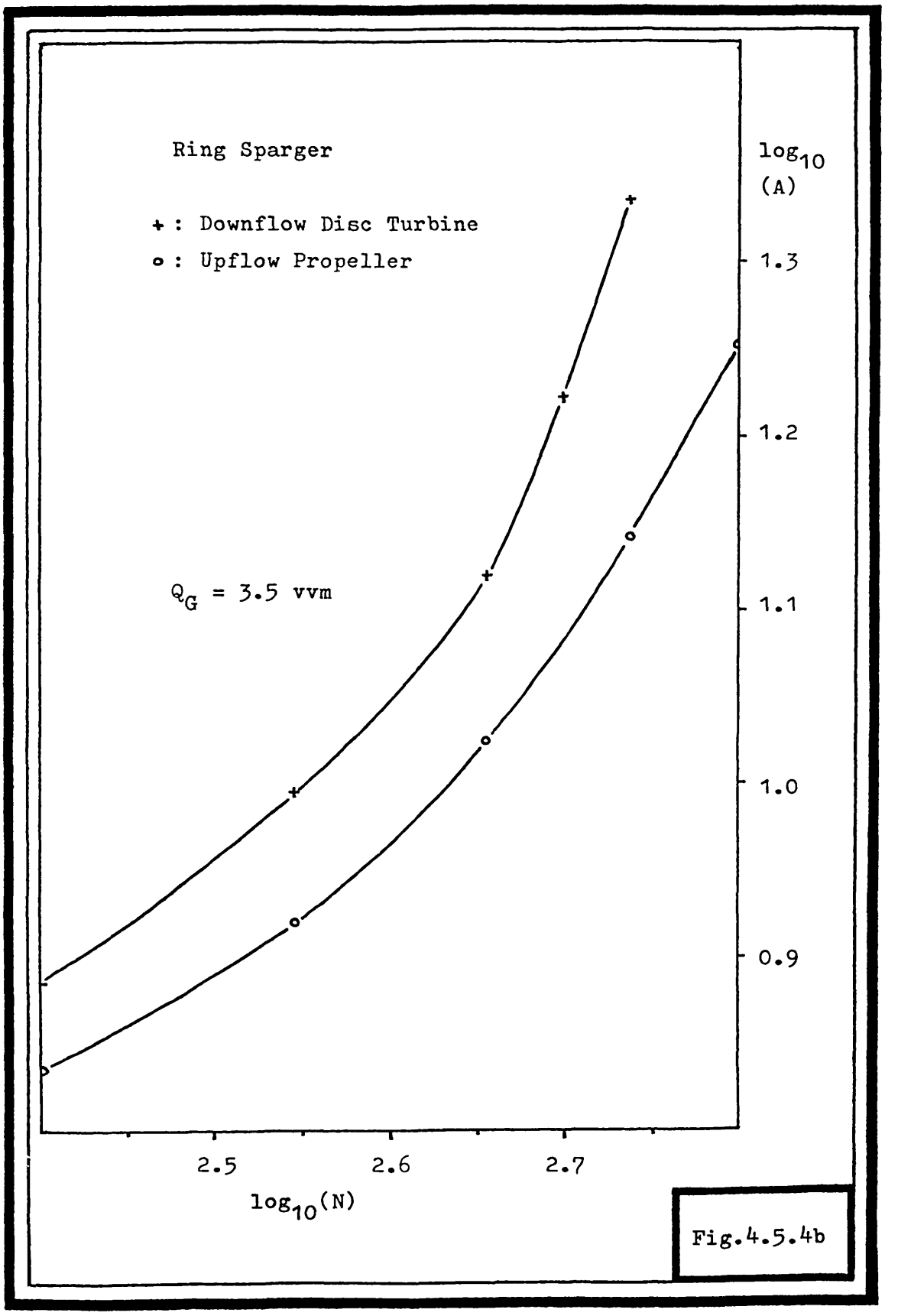

Ring Sparger
+ : Downflow Disc Turbine
o : Upflow Propeller
Q_G = 3.5 vvm
$\log_{10}$ (A)
1.3
1.2
1.1
1.0
0.9
2.5
2.6
2.7
$\log_{10}$(N)

Fig.4.5.4b

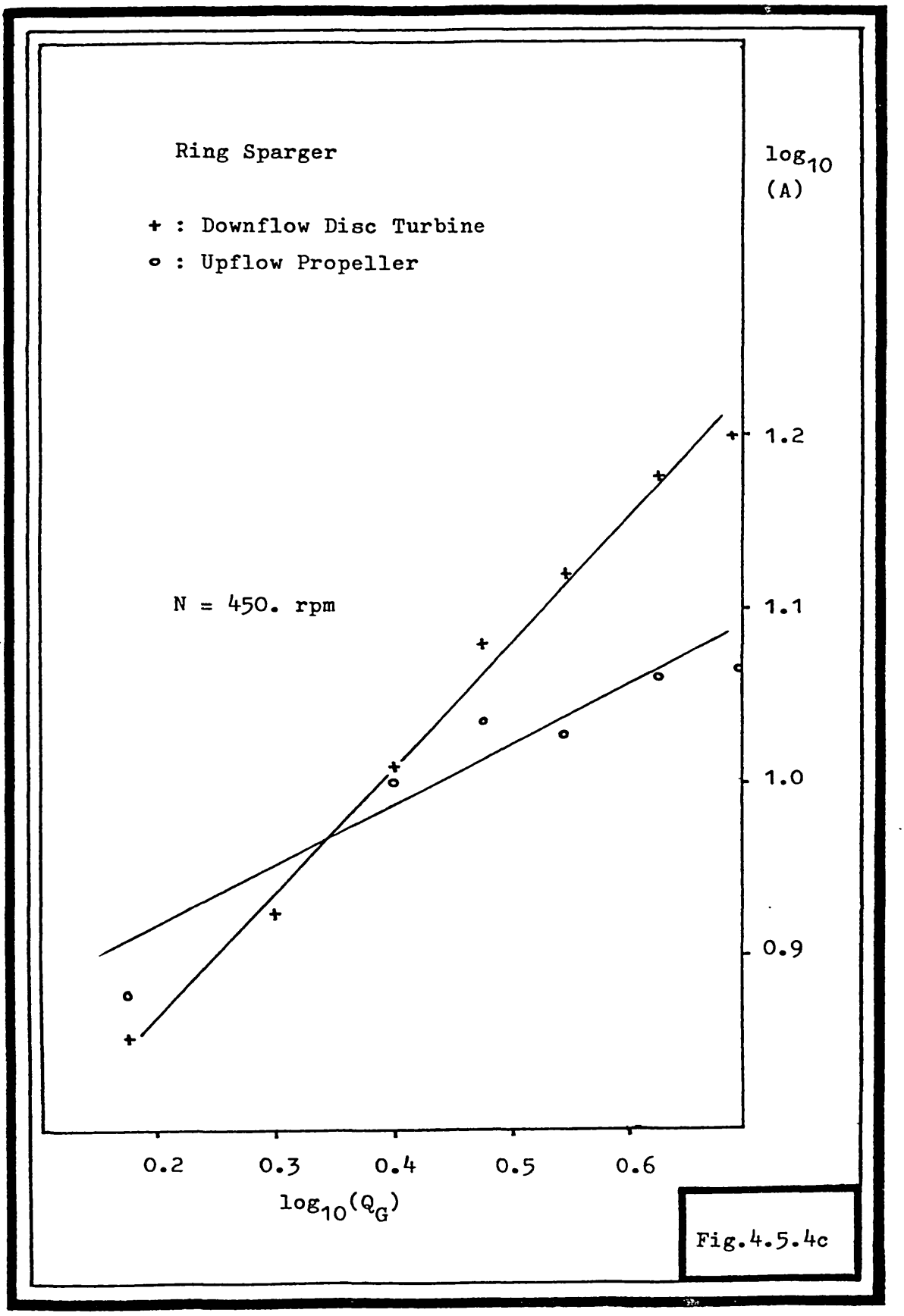

Ring Sparger
+ : Downflow Disc Turbine
o : Upflow Propeller
N = 450. rpm
log10 (A)
1.2
1.1
1.0
0.9
0.2
0.3
0.4
0.5
0.6
log10(QG)

Fig.4.5.4c

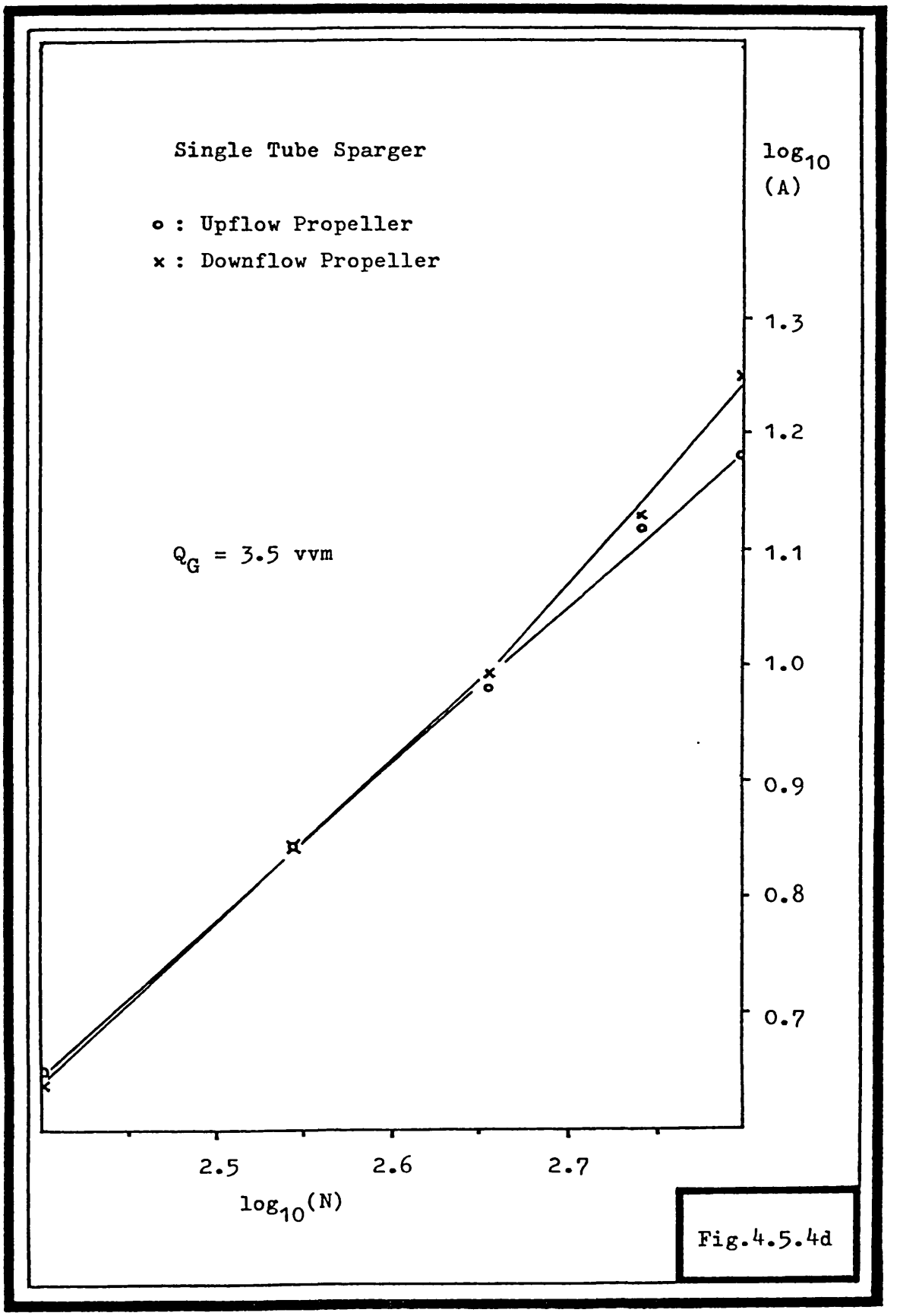

Single Tube Sparger
o : Upflow Propeller
x : Downflow Propeller
Q_G = 3.5 vvm
$\log_{10}$ (A)
1.3
1.2
1.1
1.0
0.9
0.8
0.7
2.5
2.6
2.7
$\log_{10}$(N)

Fig.4.5.4d

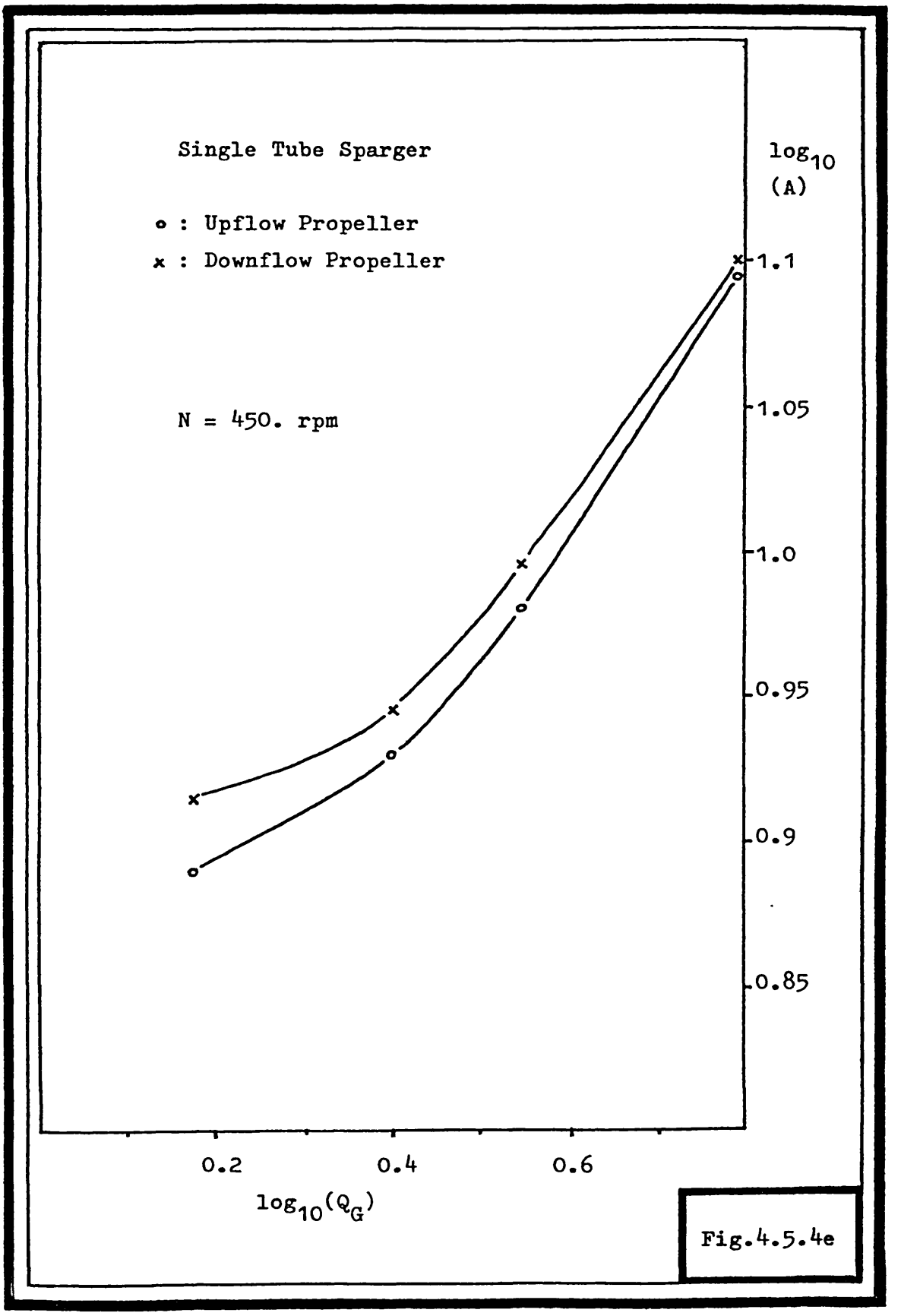

Single Tube Sparger
o : Upflow Propeller
x : Downflow Propeller
N = 450. rpm
log10 (A)
1.1
1.05
1.0
0.95
0.9
0.85
0.2
0.4
0.6
log10(QG)

Fig.4.5.4e

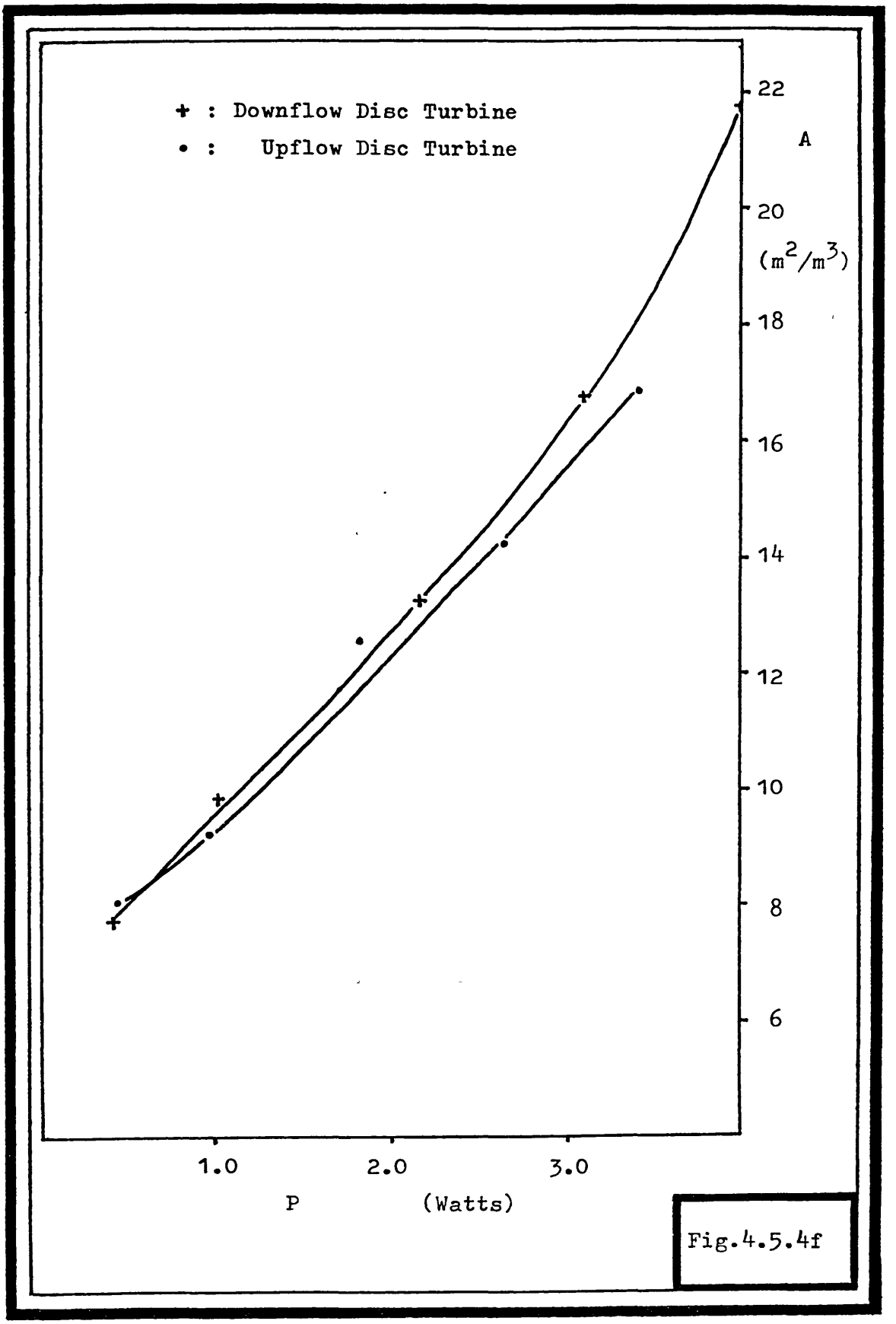

+ : Downflow Disc Turbine
• : Upflow Disc Turbine
22
20
18
16
14
12
10
8
6
A
(m²/m³)
1.0
2.0
3.0
P
(Watts)

Fig.4.5.4f

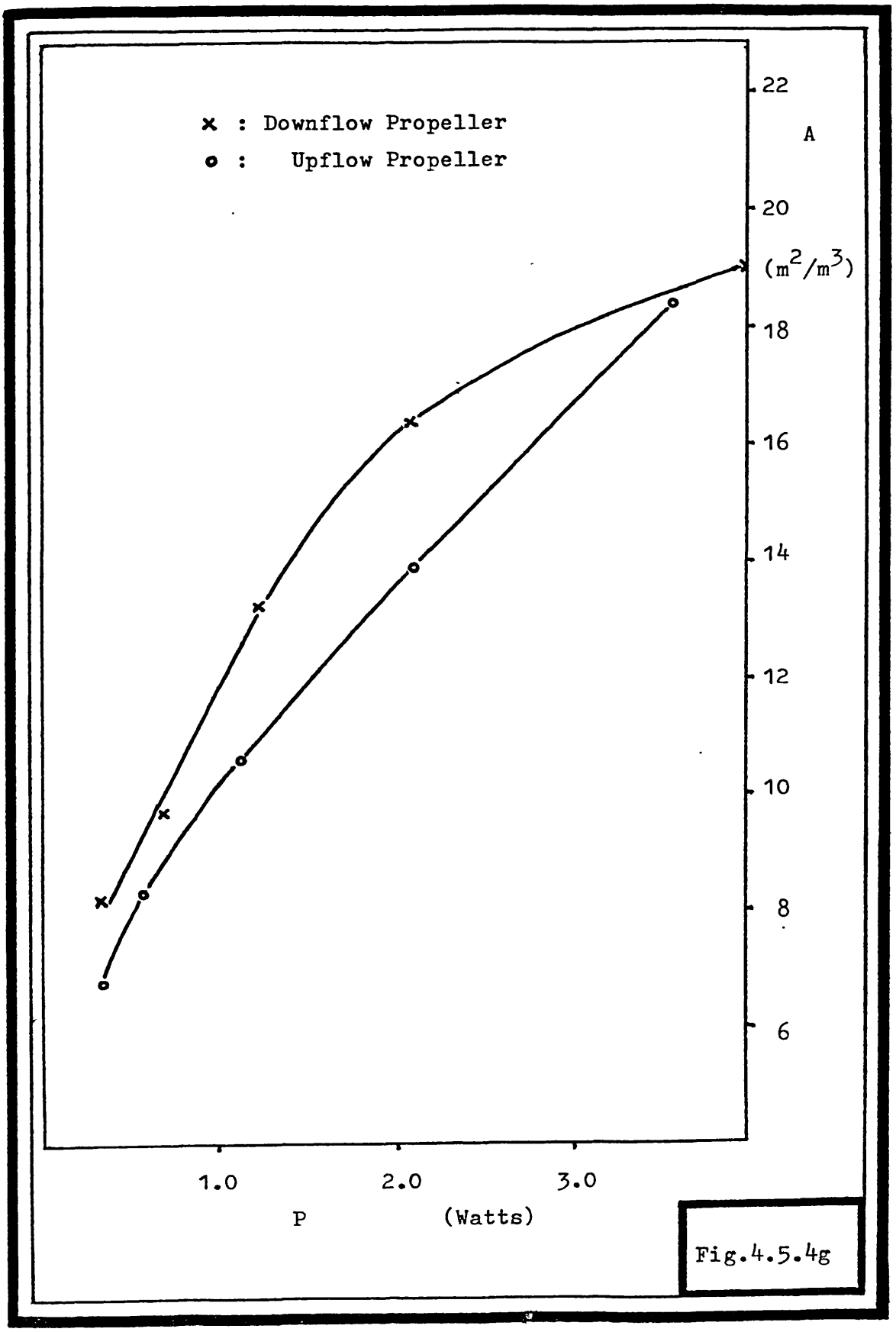

× : Downflow Propeller
o : Upflow Propeller
22
20
18
16
14
12
10
8
6
A
(m²/m³)
1.0
2.0
3.0
P
(Watts)

Fig.4.5.4g

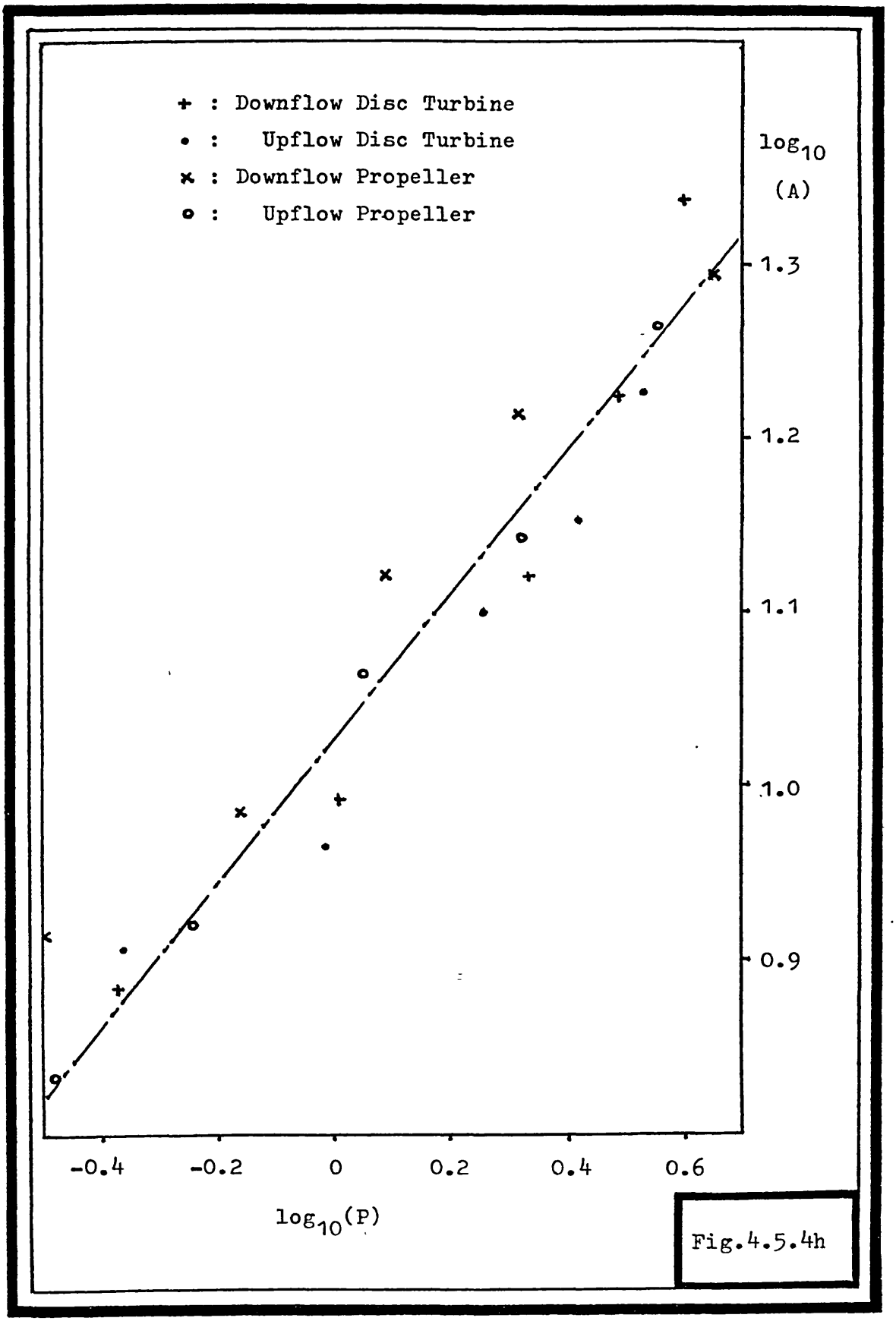

+ : Downflow Disc Turbine
• : Upflow Disc Turbine
× : Downflow Propeller
o : Upflow Propeller
log10 (A)
1.3
1.2
1.1
1.0
0.9
-0.4
-0.2
0
0.2
0.4
0.6
log10(P)

Fig.4.5.4h

5. CONCLUSIONS :

5.1 Power Consumption :

Energy requirement rises as a power function of stirrer speed but is lowered by the introduction of gas to the system : consistently with the mechanisms of drag-reducing cavity formation observed by Smith et al (see section 2.4).

Being of lower density than water, it was not surprising to find that, under all operating conditions, the xylene needed less energy to attain a given stirrer speed than an aqueous system.

Also as expected, the propellers were found to use less energy than the pitched blade disc turbines. Likewise, upflow arrangements (pumping cocurrently with the flow of gas) consumed slightly less power than downflow stirrers. This only minor difference in power consumption between up- and downflow is presumably due to the upper impeller (a flat blade disc turbine).

For both water alone and air-water, the Newton number became independent of Reynolds number for $Re \gtrsim 3. \times 10^4$ (with both Ne and Re based on liquid properties). - This value of Re and those of Ne in the unaerated system (varying from 5.5 for the upflow propeller to 7.5 for the downflow disc) compare favourably with the results of Kuboi and Nienow (24.c). The aerated Ne took on progressively lower values with increasing gas rate : between 2.1 and 4.0, depending on stirrer design, at $Q_G = 4.5$ vvm.

Given the rather complex mechanism of gas entrainment, cavity formation and dispersion as reviewed in section 2.4, perhaps predictably the data obtained did not give any clear correlation between the ratio of power consumption in an aerated liquid to that in the liquid alone (P_G/P_O) and stirrer speed, gas rate etc. but the equation of Michel and Miller, developed for a six blade turbine, works reasonably well.

5.2 Gas Sparger :

Previous work, on this project and elsewhere, has already dealt with the optimal positioning of a gas sparger in a stirred tank. Here, the experiments have compared results for a single tube sparger with those for a 12 hole, ring sparger. The interfacial areas generated by each are commented on in section 5.5, but in general, the ring produces much larger gas-liquid areas. It had been pointed out that a ring sparger (or other similar sparger design) might inhibit solids suspension by its presence (more than just a single tube would). In order to avoid this, the ring was made of narrow tubing and no significant inhibition of particle movement was observed.

A disadvantage of the ring sparger was the tendency of its inlet holes to become partially blocked, when testing amine-CO_2 reactions, restricting the flow of gas. (Clearly, a sintered plate would not have been appropriate for these systems, especially on such a comparatively small-scale apparatus, where its benefits would not be as great).

Section 2.3 explains why gas sparger power is a minor consideration in full-scale agitated tanks. As regards the possible contribution of the gas to mixing in the laboratory scale equipment, this must surely be small since it has been shown to be insufficient to suspend even fine sand grains (16) or more than a few polythene beads without the presence of mechanical agitation and the interfacial areas generated even at low (let alone zero) stirrer speeds, are only marginally greater than the free surface at the top of the tank : It is concluded that energy dissipated by gas bubbles rising through the tank is not significant in its effect c.f. the energy output from the impellers (even though, on this scale, the power input required to pump either is of similar magnitude).

5.3 Solids :

The three commonly employed suspension criteria were assessed for their suitability and the 'just suspended' condition was found to be the best for our purposes (: the 'suspension height' was attained too easily - prior to suspension en masse, whilst homogeneity was difficult to judge and probably never achieved).

3. mm polythene beads were suspended in xylene at various particle concentrations and gas rates, using the four different impeller designs. The same apparatus had previously been used in experiments on an air-water-sand slurry with only limited success : suspension only occurred at high stirrer speeds, small gas rates and fairly low particle concentrations for the downflow disc turbine; even then, the proportion of solids was always much greater in the lower regions of the vessel.

The organic system, with its lighter solids, was more representative of most industrial three phase reactors. (Note that because of their buoyancy, the organic solids could be suspended at stirrer speeds well below those required to produce a large gas-liquid interfacial area,- not the case for systems such as air-water-sand). Conditions approaching homogeneity could be achieved at high rates of mixing, in spite of the detrimental effect of gas upon the suspension :

The introduction of gas is known to create cavities behind the blades of an impeller (section 2.4) and hence reduce the effectiveness of pumping, thus diminishing the turbulent eddies and drag forces thought to be responsible for solids suspension. It was found that the initial introduction of gas has a substantial influence in making suspension difficult but, whilst further increases in gas flowrate made suspension harder still, they were not as important. Our results do not, therefore, agree entirely with those of Chapman et al (18), though it should be remembered that the operating conditions encountered here were rather different (: higher gas rates, lower particle

densities, different stirrer configurations). According to Chapman, upward pumping impellers are least affected by high gas flows in terms of suspension and downflow ones are most susceptible : this is confirmed by the results obtained here.

For the disc turbines, ΔN_{JS} (= $N_{JS}(G) - N_{JS}(G=0)$) was proportional to $\sim 0.4Q_G$ for $1.5 < Q_G < 5.0$. For the propellers, N_{JS} was only a weak function of gas flowrate for $Q_G > 1.5$ vvm.

The impeller speed necessary to suspend solids also depended on particle concentration, though (rather like gas flowrate) a small amount of solids added at low concentrations required a larger increase in stirrer speed than a proportionally greater quantity of particles added to a higher concentration.

The equation due to Zwietering (intended for solid-liquid systems) predicted that : $N_{JS} \propto X^{0.13}$. Most of the results here are close to this value (the unaerated downflow disc turbine being a notable exception).

The comparative ease with which the polythene beads (much larger and thus heavier than any of the sand used) were suspended, implies that relative density of solid to liquid is more important than individual particle size or mass ($N_{JS} \propto (\Delta\rho/\rho_L)^{0.45}$ according to Zwietering). Although shape has not been taken into account, other work has suggested it is not crucial unless the solids tend to interlock.

One of the main aims of this project was to investigate the merits of the four impeller designs and the results here have shown the downflow disc turbine to be considerably better at solids suspension than the other stirrer configurations. At zero to low gas rates, the upflow

disc turbine was second best but was otherwise the least effective. The propellers were less affected by increases in gas flowrate than the disc turbines, with the upflow propeller producing suspensions at slightly lower speeds than the downflow one.

5.4 Organic Systems :

In conjunction with the polythene solids in a xylene liquid phase, it had been hoped to find an appropriate reaction (to take the place of sodium sulphite oxidation) in order to measure gas-liquid interfacial areas by the chemical method.

The reaction between cyclohexylamine (CHA) and carbon dioxide had been used previously but, as had been predicted, it was found to be too fast when applied to a fairly efficient, stirred vessel. Two other amine-CO_2 reactions were tried in turn :

Diethanolamine (DEA) -CO_2 was somewhat slower but choked the vessel with crystals quite rapidly and the sample analysis (by chromatography) proved unreliable.

Di-isopropanolamine (DIPA) -CO_2, though slower than DEA and without either of its disadvantages, was still too fast for the criteria of a chemical method to be satisfied. Nevertheless, it was demonstrated that DIPA could be employed for qualitative comparisons between different operating conditions.

5.5 Interfacial Areas :

The two principal objectives of a slurry reactor are the suspension of the solid phase and the generation of a large gas-liquid interfacial area. The success or failure to achieve the latter was established by measuring the rate of oxidation of sodium sulphite in an aqueous solution.

Perhaps the most obvious way to produce a large surface area is to introduce a high gas flowrate (though of course, this makes the other priority : solids suspension, more difficult). However, earlier work on this project

showed that with the single tube sparger and disc turbines, beyond a certain value of gas flow, interfacial areas levelled off and even decreased as a result of impeller flooding. This did not seem to occur with the propellers. The change to a ring sparger gave much larger contact areas for all the stirrer designs with $A \propto Q_G$ to the power 0.38 to 0.71 for the ring sparger but only an exponent of 0.32 (on average) for the single tube sparger (all for N = 450. rpm).

Impeller speed is also an important factor, with even quite small increases bringing about significant improvements. For the single tube sparger, $A \propto N$ to the power 1.3 to 1.8 (at Q_G = 3.5). With the ring sparger, up to $\sim$400 rpm, interfacial area is determined largely by the (pre-dispersed) influx of gas and $A \propto$ only to $N^{\sim 0.7}$. Above that rate of mixing though, stirrer speed becomes more critical with $A \propto N$ raised to the power 1.5 (for upflow propeller) to 2.5 (for downflow disc).

The interfacial area appears to be a fairly consistent function of impeller power input : $A \sim\propto P^{0.4}$ for all of the stirrer designs examined (at Q_G = 3.5 vvm, across the whole range of stirrer speeds). Local variations mean that whilst there is little to choose between the stirrers at very low power inputs, in the intermediate range the downflow propeller is markedly more effective (by $\sim$ 20 % in terms of surface area generated for a given power supply). However, the downflow propeller's performance tails off in comparison with the others at the higher power range, leaving the downflow disc $\sim$15 % better than any of the other configurations.

The effect of solids is not clear cut. Theory suggests that particles of high momentum will have enough energy to cause the break-up of gas bubbles with a consequent rise in gas-liquid area. This was confirmed by the air-water-sand experiments (16) where A was increased by an average of 30. %. Conversely, it has been observed (e.g. by Lee et al : 24.d) that low momentum particles will decrease the interfacial area by reducing the degree of turbulence within a mixed vessel (see section 2.6 for a

more detailed review). However, this has not been seen here because, though the polythene beads used were light, they were also quite large. So whilst enhancement of the surface area was not expected, neither was its severe deterioration. This was to some extent confirmed by measuring the rate of the DIPA-CO_2 reaction in the agitated vessel, with and without solids present. However, it is questionable whether this method was sensitive enough to detect anything but a fairly large change in gas-liquid area.

As regards impeller design, it was found that the downflow arrangements made better use of increasing gas rates and growing stirrer speeds than the upflow ones, and that the pitched blade disc turbines tended to create larger interfacial areas than their corresponding propellers. As explained earlier on in this section, though, the discs (needing more power) were not necessarily the most economic option.

5.6 Optimum Conditions :

It is apparent that the best operating conditions may vary greatly from one process to another e.g. the complete suspension of solids may be essential or unimportant, blockage of narrow gas inlets may or may not be a danger etc. Nevertheless, certain general guidelines have emerged :

A high gas flowrate is preferable but it must be well-dispersed to make it worthwhile : conditions reminiscent of 'slugging' in a fluidised bed can occur, especially in more viscous liquids, resulting in a drop in interfacial area. Note that solids suspension is also deterred by even a small gas rate.

Pre-dispersion of gas entering the vessel (e.g. by installing a ring sparger or sintered plate) can greatly improve the gas-liquid surface area, particularly when the impeller speed is low. However, depending on the design of the gas sparger, the following disadvantages may be encountered :

- blockage by solids or product formation in the gas inlet holes,
- higher pressure drops in the gas line,
- inhibition of solids movement (and therefore their suspension) around the sparger.

The only certain way to achieve both a better gas dispersion and maintain a solids suspension is to have a higher stirrer speed, the only drawback being a consequent increase in power consumption : a balance has to be struck between the cost of energy and the prices of the chemicals (reactants and products) involved.

The remaining experimental variable is that of impeller design. Comparisons have been made between pitched blade disc turbines and propellers, and between upflow and downflow impellers. Under the conditions thought to be most suitable for effective operation (i.e. high, well-dispersed gas flowrates through a ring sparger at high impeller speeds) the two downflow stirrers produced much larger interfacial areas than the upflow ones. At the same stirrer speed, the

disc turbines also gave larger interfacial areas than the corresponding propellers.

However, as mentioned in sections 4.5.4 and 5.5, it is generally the power input (rather than speed) to interfacial area relationship that is decisive in economic terms. At very low power inputs, there is not much to choose between the various designs : $\sim$ 10.% variation, but such conditions correspond to a very poorly aerated tank with only limited solids suspension and are hence not thought to be of great relevance. More importantly, in the intermediate power range, the downflow propeller was the best option, whilst the downflow disc was best at higher power inputs (i.e. at large interfacial areas and with good solids suspension).

As far as solids suspension is concerned, the downflow disc was much better than the other three in the air-xylene-polythene slurry. The two propellers though, given an equal power input, were not much worse at high gas rates, with the upflow being slightly better than the downflow propeller. For air-water-sand (i.e. dense solids) of the two disc turbines, only the downflow was ever able to achieve complete suspension and preliminary experiments with the propellers showed them to be as ineffective as the upflow disc.

Overall therefore, the downflow disc is to be recommended with the downflow propeller a fairly close second. (Note however, that in certain circumstances, this order of preference might be reversed, e.g. if gas inlet blockage were to enforce the use of a larger bore, single tube sparger, or if the vessel was to be operated at intermediate power inputs with only gas and liquid phases.

5.7 Assessment of Method and Apparatus :

(i) The Quiescent Interface Cell :

This piece of equipment worked quite satisfactorily, with good temperature control. The only problem encountered, stemmed from the PTFE seal around the lower stirrer shaft which needed to be tightened frequently during operation to prevent leaks and required replacement after only a few hours use.

(ii) The Agitated Vessel :

The apparatus was adapted successfully for use with a ring sparger (as well as a single tube gas inlet) and up- and downflow propellers were made to compare with the two pitched blade disc turbines already available. Unfortunately, erosion of the PTFE impeller bearing at the base of the tank allowed small sand particles to become wedged between the stirrer shaft and its bearing, arresting the motion of the impeller and preventing the completion of the air-water-sand experiments with the propellers.

In other respects, the agitated tank ran well, with the power consumption and stirrer speed being monitored accurately. The ring gas sparger did have a tendency for some

of its inlet holes to become blocked, especially during the amine-CO_2 experiments.

(iii) The Sulphite Method :

This chemical method of measuring the gas-liquid interfacial area was used in past work on this project and continued to be of value here. Its major drawbacks are the limitations it places on the liquid viscosity and the type of particulate solids tested, e.g. for the former, glycerol cannot be added as the sulphite reaction would no longer take place at the gas-liquid interface. For the latter, an aqueous system (atypical of most slurries) restricts the choice of solids to particles which are not hydrophobic, yet are relatively light and easy to suspend.

Analysis of the samples by back-titration, though somewhat tedious, is reasonably satisfactory.

(iv) Amine-CO_2 Reactions :

Cyclohexylamine was shown to be far too fast for use as a chemical method and whilst diethanolamine was somewhat slower, its analysis became unreliable early on in each experimental run. Di-isopropanolamine was even slower, its analysis consistent, and was thus the most appropriate of the amines tested. However, its reaction with CO_2 was still too rapid for anything other than a qualitative comparison between operating conditions in the agitated vessel.

The attempted distillation of spent chemicals was unsuccessful due, it is thought, to the partial decomposition of the amines into components that polluted the distilled xylene and propanol.

5.8 Future Work :

(Note : Middleton (19.b) gives an excellent summary of the requirements of industrial research with respect to mixing technology in the immediate and long term future).

Given the results discussed in the previous sections, it should be apparent that several areas for further work suggest themselves :

(i) A wider search for an organic reaction that could be used for the chemical method of interfacial area

measurement, preferably one that can be carried out in a number of solvents of various viscosities and, if possible, does not involve highly toxic or very expensive compounds.

(ii) The collection of experimental data (minimum suspension stirrer speed, effect of gas flowrate etc.) for a greater range of particle sizes, (shapes) and densities.

(iii) Measurement of local bubble size distribution (and therefore gas hold-up and interfacial area) using a suitable physical method to help explain and predict the effects of different stirrer, gas sparger and tank designs.

(iv) Repetition of the experiments outlined above (in addition to those already performed) in larger vessels, to enable reliable scale-up rules to be developed : Although the sulphite method (or some appropriate counterpart) offers a fairly simple way of making quantitative comparisons between various designs and for gas dispersion scale-up criteria, as yet no entirely satisfactory model exists for the prediction of solids suspension, particularly in the presence of a gas. For suspension itself, Zwietering's equation (modified for three phases) seems the best so far, whilst for the distribution of solids in the tank, a balance between gravitational and turbulent mixing forces might be used, e.g. at steady state :

$$m_s n v_t = -m_s l \bar{v}' \left[\frac{dn}{dh}\right]$$ where : m_s = mass of a particle, n = number of particles, h = height in tank

$\bar{v}'$ = r.m.s. value of the random fluctuating velocity component

$*v_t$ = terminal settling velocity

l = mixing length (c.f. Prandtl mixing length in turbulent fluid flow or mean free path in kinetic theory of gases).

$$\therefore \ln\left[\frac{n}{n_o}\right] = -v_t(h-h_o)/(l\bar{v}')$$: if $l\bar{v}'$ is constant for a given geometry, N and Q_G.

$$* \ v_t = (4d_s(\rho_S-\rho_L)g/(3C_d\rho_L))^{\frac{1}{2}}$$

where C_d = drag coefficient (= 0.44 for turbulent flow)

APPENDIX : A 3.1.1

Calculation of Motor Power :

The power supplied by the air motor is determined by measuring the torque (T) on the shaft. This is done by measuring the extension of a calibrated spring, attached to the motor, which retards motion of the motor in its bearing. The power input is given by the product of the torque and angular speed of rotation (ω) :

$\omega = 2 \times \pi \times N/60$ (N : rpm)

and $T = F \times r$ (F : force N)

(r : radius 5.cm)

The spring is elastic and obeys Hooke's law, so the tension in it is given by :

$F = 0.327 \times E \times N$ (E : extension cm)

Thus the power consumption is :

$P = 1.712 \times 10^{-3} \times E \times N$ (Watts)

Gas Sparger Power :

According to Smith and Goossens (24.a), the power required is approximately that needed to compress the air (with efficiency, e, taken to be 0.6) :

$\therefore P = \rho_L gHG/e \qquad \rho_L gH = 10^3 \times 10 \times 0.5 = 5000 \text{ N/m}^2$

$G \sim 10 \text{ l/min} = 1.67 \times 10^{-4} \text{ m}^3/\text{s}$

$\therefore P = 0.833/e \sim 1.39 \text{ Watts}$

This compares well with the equation for a reversible polytropic process :

$$W = p_1 v_1 \left(\frac{n}{n-1}\right)\left[\left(\frac{p_2}{p_1}\right)^{\frac{n-1}{n}} - 1\right]$$

$n = 1.4$; $p_1 = 1.013 \times 10^5$, $p_2 = 1.063 \times 10^5 \text{ N/m}^2$

$v_2 \sim 1.67 \times 10^{-4} \text{ m}^3/\text{s}$ and $pv^n = \text{constant}$

$\therefore 1.063(1.67 \times 10^{-4})^{1.4} = 1.013(v_1)^{1.4}$

$\therefore v_1 = 1.725 \times 10^{-4} \text{ m}^3/\text{s}$

$\therefore$ Power = .8476 Watts; if e = 0.6, P = 1.413 Watts

APPENDIX : A 3.1.2

Sulphite Reaction : Variation of Rate with Temperature

The rate of reaction was measured as 9.89899×10^{-6} (mol/l min cm^2)

T	C_{Ai}	D_A	$k_2/(Co^{2+})$		
(°C)	(mol/cm^3atm)	(cm^2/s)	($(l/mol)^2 s^{-1}$)		
			pH = 7.5	8.0	8.5
15	6.8	1.36	0.25	-	2.0
20	6.4	1.60	0.45	0.85	4.0
30	5.8	2.10	1.2	2.5	4.0
33	5.7	2.25	1.5	3.0	5.0
	($x10^{-7}$)	($x10^{-5}$)		($x10^{10}$)	

Danckwerts (5.b)

Since :

$$N_{Ai} \text{ (mol/l s cm}^2\text{)} = (C_{Ai})^{1.5}(\tfrac{2}{3}k_2 D_A)^{0.5}$$

and from the table above, at 20°C :

$$C_{Ai} = 6.4 \times 10^{-7}, \quad D_A = 1.60 \times 10^{-5}$$

$$\therefore k_2(20^\circ C) = 9.7245 \times 10^9$$

Now $k_2(T)$ = constant x $\exp(-E_a/RT)$ and from the table above, at pH 8.5 :

$$\frac{k_2(33+273)}{k_2(15+273)} = \frac{5.0}{2.0} = 2.5 = \frac{\exp(-E_a/306\,R)}{\exp(-E_a/288\,R)}$$

$$\therefore \ln 2.5 = E_a(1/288 - 1/306)/R$$

$$\therefore E_a/R = \ln 2.5 \,/\, (1/288 - 1/306) = 4486.16$$

$$\therefore \frac{k_2(T)}{k_2(20+273)} = \frac{\exp(-4486.16/T)}{\exp(-4486.16/293)}$$

$$\therefore k_2(T) = 9.7245 \times 10^9 \times 4.4621 \times 10^6 \times \exp(-4486.16/T)$$

APPENDIX : A 3.1.2 (contd.)

$\therefore k_2(T) = 4.33917 \times 10^{16} \times \exp(-4486.16/T)$

- this gives k_2 for all temperatures (at pH 8.5 and a catalyst concentration of 9.3×10^{-4}M).

D_A and C_{Ai} taken from the table overleaf, were plotted against temperature and thus N_{Ai} could be calculated for any given temperature, as shown below :

T (^oC)	k_2 (l/mol s)	D_A (cm^2/s)	C_{Ai} (mol/cm^3)	N_{Ai} (mol/l s) (per cm^2 contact area)	N_{Ai} (mol/l min)
18	8.753	1.505	6.55	1.571	9.425
19	9.228	1.55	6.47	1.607	9.642
20	9.7245	1.60	6.40	1.649	9.89899
22	10.788	1.70	6.25	1.728	10.366
23	11.357	1.75	6.19	1.773	10.636
24	11.952	1.80	6.13	1.816	10.893
25	12.573	1.85	6.07	1.860	11.159
26	13.222	1.90	6.01	1.907	11.440
27	13.90	1.95	5.95	1.951	11.707
30	16.119	2.10	5.80	2.098	12.590
33	19.311	2.25	5.70	2.316	13.896
35	20.498	2.35	5.65	2.407	14.440
	($x10^9$)	($x10^{-5}$)	($x10^{-7}$)	($x10^{-7}$)	($x10^{-6}$)

APPENDIX : A 3.3.1

Analysis of Sulphite Samples :

The following solutions are made up :

(a) potassium iodate soln. (M.Wt. : 214. g)
1. g of potassium iodate is dissolved in 250. cm^3 of distilled water.

(b) sodium thiosulphate soln. (M.Wt. : 248.2 g)
37. g of sodium thiosulphate is dissolved in 1. litre of distilled water.

Standardisation : to 25. cm^3 of potassium iodate solution, some solid potassium iodide and 5. cm^3 of 1.M sulphuric acid are added. This is titrated against the thiosulphate to be standardised. Starch is added as an indicator for the end point (from purple/black to colourless).

(c) iodine soln. (M.Wt. : 253.8 g)
12.7 g of iodine crystals are added to a solution of 40. g of potassium iodide in 1. litre of water.

Standardisation : 25. cm^3 of iodine soln. is diluted with 100. cm^3 of distilled water. This is then titrated with the standardised thiosulphate, adding starch indicator.

(d) starch soln.
10. g of starch is made into a smooth paste with distilled water. This is poured into a litre of boiling water and left to cool. (Starch soln. deteriorates on keeping).

(e) sulphite soln. (M.Wt. : 126. g)
About 350. g of anhydrous sodium sulphite is made up to 4 litres for a 0.7M solution.

APPENDIX : 3.3.1 (contd.)

Standardisation Calculations :

KIO_3 : 4.0 g/l = (4/214.01)M = 0.018691 M

$KIO_3 \equiv 6\ Na_2SO_3$ $\therefore$ $V(IO_3) \times 0.01869$ $V(S_2O_3) \times M(S_2O_3)/6$

($V(IO_3) = 25.\ cm^3$) $\therefore$ $M(S_2O_3) = 6 \times 25 \times 0.01869/V(S_2O_3)$

$\therefore$ $M(S_2O_3) = 2.803605/V(S_2O_3)$

$I_2 \equiv 2\ S_2O_3^{2-}$ $\therefore$ $M(I_2) = \frac{1}{2}(M(S_2O_3) \times V(S_2O_3)/V(I_2))$

Sample Calculations :

The sample is added to an excess (20. ml) of iodine soln. and this mixture is then titrated with thiosulphate (to react with the excess iodine) : $V(S_2O_3)$ is noted.

This corresponds to a volume of iodine :

$eq.V(I_2) = M(S_2O_3) \times V(S_2O_3)/(M(I_2) \times 2)$

$\therefore$ The rest of the iodine was used up by the sulphite :

$eq.V(SO_3) = V(I_2) - eq.V(I_2)$ (= 20 - $eq.V(I_2)$)

where $M(SO_3) = eq.V(SO_3) \times M(I_2)$

(= moles of iodine used up by the sulphite)

APPENDIX : A 3.3.2

Analysis of Amine Samples :

		CHA	DEA	DIPA	
Sample Column	:	QS	Oronite	Oronite	
Reference Column	:	PS	PS	PS	
Carrier Gas	:	Helium	Helium	Helium	
Column Temp.	:	180°	180°	180°	(°C)
Injector Temp.	:	220°	200°	200°	"
Detector Temp.	:	125°	200°	200°	"

Note : H_A = height of peak on chromatograph chart recorder for component 'A'.

(i) Calculation of M_{CHA} :

As $t \longrightarrow \infty$, $M_{CHA} \longrightarrow 0$ and $(H_{CO2}/H_{CHA}) \longrightarrow 0.36$

$M_{CHA}(t) = M_{CHA}(t=0) - 2 \times M_{CO2}(t)$ (from the stoichiometry of the reaction)

For 10.% (v/v) CHA, $M_{CHA} = 0.872$

$\therefore M_{CHA}(t) = 0.872 - 2 \times \text{constant} \times (H_{CO2}/H_{CHA})$

As $t \longrightarrow \infty$, $0 = 0.872 - (2 \times \text{constant} \times 0.36)$

$\therefore$ constant $= (0.872/0.72) = 1.211$

$\therefore M_{CHA}(t) = 0.872 - 2.422(H_{CO2}/H_{CHA})$

(ii) Calculation of M_{DEA} :

CO_2 : 0.5 ml at RTP = 7.63 (= H_{CO2}) at R = 320

i.e. 0.5 ml = (7.63 x 320/16) at R = 16

= 152.6 i.e. 1 ml = 305.2

Given H_{CO2}, $V_{CO2} = (H_{CO2}/305.2)$ ml in the sample.

APPENDIX : A 3.3.2 (contd.)

(ii) (contd.)

DEA : H_{DEA} in a standard sample (10.%v/v) = 0.874

$\therefore V_{CO2} = (H_{CO2}/305.2) \times (0.874/H_{DEA})$ ml gas/ 5 μl sample

$\therefore V_{CO2} = 10^{-3} \times 10^{6} \times 1/5 \times (H_{CO2}/305.2) \times (0.874/H_{DEA})$

$= 0.57274(H_{CO2}/H_{DEA})$ litres CO_2/ litre of sample

$M_{CO2} = (V_{CO2}/24)$, $\therefore M_{CO2} = 0.023864(H_{CO2}/H_{DEA})$

$$M_{DEA}(t) = M_{DEA}(t=0) - 2 \times M_{CO2}(t)$$
$$= M_{DEA}(t=0) - 0.047728(H_{CO2}/H_{DEA})$$

DEA : ρ = 1.1, M.Wt. = 105.14, Concentration = 100. ml/litre

$\therefore M_{DEA}(t=0) = 1.1 \times 100/105.14 = 1.0462$

$\therefore M_{DEA}(t) = 1.0462 - 0.04773(H_{CO2}/H_{DEA})$

(iii) Calculation of M_{DIPA} :

CO_2 : 0.5 ml at RTP = 6.7678* at R = 640

i.e. 0.5 ml = (6.7678 x 640/16) at R = 16

= 270.71 i.e. 1 ml = 541.42

Given H_{CO2}, $V_{CO2} = (H_{CO2}/541.42)$ ml in sample.

* : CO_2 calibration varied over a period of time as the oronite column started to deteriorate : recalibration was carried out to re-measure H_{CO2} for $\frac{1}{2}$ ml CO_2 and re-calculate the coefficient of (H_{CO2}/H_{DIPA}) in the equation for $M_{DIPA}(t)$.

APPENDIX : A 3.3.2 (contd.)

(iii) (contd.)

DIPA : H_{DIPA} in a standard sample (10.%v/v) = 1.637

$\therefore V_{CO2} = (H_{CO2}/541.42) \times (1.637/H_{DIPA})$ ml gas/ 5 µl sample

$\therefore V_{CO2} = 10^{-3} \times 10^{6} \times 1/5 \times (H_{CO2}/541.42) \times (1.637/H_{DIPA})$

$= 0.6047(H_{CO2}/H_{DIPA})$ litres CO_2/ litre of sample

$M_{CO2} = (V_{CO2}/24)$, $\therefore M_{CO2} = 0.025196(H_{CO2}/H_{DIPA})$

$$M_{DIPA}(t) = M_{DIPA}(t=0) - 2 \times M_{CO2}(t)$$
$$= M_{DIPA}(t=0) - 0.05039(H_{CO2}/H_{DIPA})$$

DIPA : ρ = 1.0, M.Wt. = 133.19, Concentration = 100. ml/litre

$\therefore M_{DIPA}(t=0) = 1.0 \times 100/133.19 = 0.7508$

$\therefore M_{DIPA}(t) = 0.7508 - 0.05039(H_{CO2}/H_{DIPA})$

APPENDIX : A 3.4

Safety : compiled from (11.), (20.) and (21.)

NAME :	CHA	DEA	DIPA
Chemical Formula :	$(C_6H_{11})NH_2$	$HN(CH_2CH_2OH)_2$	$HN(CH_2CHOHCH_3)_2$
Molecular Weight :	99.2	105.14	133.19
Density :	0.865	1.10(20°)	0.989
M.Pt.(°C) :	-	28°	42°
B.Pt. " :	134°	269.1°(dec.)	248.2°
Viscosity (cP) :	-	380(30°)	198(45°)
Water Solubility :	v.sol.	v.sol.	v.sol.
TLV (ppm) :	10(skin)	-	-
TLV (mg/m^3) :	40	-	-

NAME :	xylenes	n-propanol	iso-propanol
Chemical Formula :	$CH_3(C_6H_4)CH_3$	$CH_3CH_2CH_2OH$	$CH_3CHOHCH_3$
Molecular Weight :	106.2	60.1	60.1
Density :	0.86	0.804	0.804
M.Pt.(°C) :	$^{-}27.1°$-13.2°	$^{-}127°$	$^{-}85.8°$
B.Pt.(°C) :	138°-144°	97.2°	82.3°
Viscosity (cP) :	0.6-0.8	2.23	2.2
Water Solubility :	insol.	sol.	sol.
lel (v/v%) :	1.1	2.1	2.3
uel (") :	7.0	13.5	12.7
TLV (ppm) :	100	200(skin)	400(skin)
TLV (mg/m^3) :	435	500	980

APPENDIX : A 3.4 (contd.)

(i) Cyclohexylamine :

- Flammable (moderate fire hazard),
- Harmful vapour (strong, ammoniacal, fishy odour),
- Irritating to skin, eyes and respiratory system.

Precautions :

- Avoid breathing vapour,
- Prevent contact with skin and eyes.

Toxic effects :

- Difficulty in breathing,
- Burns eyes and skin,
- Absorption causes nausea and vomiting.

(ii) Diethanolamine :

- Slight fire hazard,
- Slight irritant.

(iii) Diisopropanolamine :

- Slight fire hazard.

(iv) n-Propanol (propan-1-ol) :

- Highly flammable,
- Eye and respiratory system irritant,
- Narcotic at high concentrations.

Precautions :

- Avoid breathing vapour,
- Avoid contact with eyes.

Toxic effects :

- Similar to ethanol but greater.

APPENDIX : A 3.4 (contd.)

(v) iso-Propanol (propan-2-ol) :

- Highly flammable,
- Harmful vapour,
- Irritating to eyes and respiratory system.

Precautions :

- Avoid breathing vapour,
- Prevent contact with eyes.

Toxic effects :

- Liquid damages eyes severely,
- Headache, dizziness, nausea, vomiting and, at high concentrations, narcosis, anaesthesia and coma.

(vi) Xylenes :

- Flammable,
- Harmful vapour,
- Harmful by skin absorption.

Precautions :

- Avoid breathing vapour,
- Avoid contact with skin and eyes.

Toxic effects :

- Vapour causes dizziness, headache and nausea,
- Vapour and liquid irritate eyes and mucous membrane,
- Poisoning if absorbed through skin or ingested.

In all cases, FIRE PREVENTION : use CO_2, dry chemical or foam extinguishers.

APPENDIX : B 4.1

Two Phase Results : Power Consumption

(Ring sparger, Air-Water) (Downflow Disc Turbine)

G (l/min)	N (rpm)	L (cm)	E (cm)	P (Watts)
0	250	11.05	1.75	0.749
	300	11.5	2.2	1.130
	350	12.2	2.9	1.738
	400	13.1	3.8	2.602
6	250	10.4	1.1	0.471
	300	10.95	1.65	0.847
	350	11.75	2.45	1.468
	400	12.45	3.15	2.157
8	250	10.35	1.05	0.449
	300	10.8	1.5	0.770
	350	11.3	2.0	1.198
	400	11.9	2.6	1.780
	450	12.7	3.4	2.619
12	250	10.3	1.0	0.428
	300	10.6	1.3	0.668
	350	11.05	1.75	1.049
	400	11.6	2.3	1.575
	450	12.3	3.0	2.311
18	250	10.3	1.0	0.428
	300	10.6	1.3	0.668
	350	10.95	1.65	0.989
	400	11.3	2.0	1.370
	450	11.85	2.55	1.965
	500	12.4	3.1	2.654

APPENDIX : B 4.1 (contd.)

(Downflow Disc Turbine)

G (l/min)	N (rpm)	L (cm)	E (cm)	P (Watts)
25	250	10.25	0.95	0.407
	300	10.5	1.2	0.616
	350	10.85	1.55	0.929
	400	11.25	1.95	1.335
	450	11.7	2.4	1.903
	500	12.2	2.9	2.482
	550	12.75	3.45	3.249

(Upflow Disc Turbine)

G (l/min)	N (rpm)	L (cm)	E (cm)	P (Watts)
6	250	10.4	1.1	0.471
	300	10.8	1.5	0.770
	350	11.3	2.0	1.198
	400	11.95	2.65	1.815
	450	12.8	3.5	2.696
8	250	10.35	1.05	0.449
	300	10.7	1.4	0.719
	350	11.05	1.75	1.049
	400	11.5	2.2	1.507
	450	12.1	2.8	2.157
	500	12.75	3.45	2.953
12	250	10.3	1.0	0.428
	300	10.6	1.3	0.668
	350	10.95	1.65	0.989
	400	11.3	2.0	1.370
	450	11.7	2.4	1.849
	500	12.15	2.85	2.440

APPENDIX : B 4.1 (contd.)

(Upflow Disc Turbine)

G (l/min)	N (rpm)	L (cm)	E (cm)	P (Watts)
18	250	10.3	1.0	0.428
	300	10.55	1.25	0.642
	350	10.85	1.55	0.929
	400	11.2	1.9	1.301
	450	11.6	2.3	1.772
	500	12.0	2.7	2.311
25	250	10.25	0.95	0.407
	300	10.53	1.23	0.632
	350	10.75	1.45	0.869
	400	11.1	1.8	1.233
	450	11.5	2.2	1.695
	500	11.9	2.6	2.226
	550	12.3	3.0	2.825

(Downflow Propeller)

G (l/min)	N (rpm)	L (cm)	E (cm)	P (Watts)
0	250	10.55	1.25	0.535
	300	10.95	1.65	0.847
	350	11.5	2.2	1.318
	400	12.1	2.8	1.917
	450	12.9	3.6	2.773
6	250	10.15	0.85	0.364
	300	10.25	0.95	0.488
	350	10.55	1.25	0.749
	400	10.85	1.55	1.061
	450	11.3	2.0	1.541
	500	11.9	2.6	2.226
	550	12.6	3.3	3.107

APPENDIX : B 4.1 (contd.)

(Downflow Propeller)

G (l/min)	N (rpm)	L (cm)	E (cm)	P (Watts)
8	250	10.1	0.8	0.342
	300	10.2	0.9	0.462
	350	10.5	1.2	0.719
	400	10.8	1.5	1.027
	450	11.1	1.8	1.387
	500	11.45	2.15	1.840
	550	11.9	2.6	2.448
	600	12.5	3.2	3.287
12	250	10.05	0.75	0.321
	300	10.2	0.9	0.462
	350	10.45	1.15	0.689
	400	10.7	1.4	0.959
	450	10.95	1.65	1.271
	500	11.3	2.0	1.712
	550	11.7	2.4	2.260
	600	12.1	2.8	2.876
	650	12.6	3.3	3.672
18	250	10.05	0.75	0.321
	300	10.2	0.9	0.462
	350	10.4	1.1	0.659
	400	10.6	1.3	0.890
	450	10.8	1.5	1.156
	500	11.0	1.7	1.455
	550	11.25	1.95	1.836
	600	11.55	2.25	2.311
	650	11.95	2.65	2.949
	700	12.45	3.15	3.775

APPENDIX : B 4.1 (contd.)

(Downflow Propeller)

G (l/min)	N (rpm)	L (cm)	E (cm)	P (Watts)
25	250	10.0	0.7	0.300
	300	10.2	0.9	0.462
	350	10.4	1.1	0.659
	400	10.6	1.3	0.890
	450	10.8	1.5	1.156
	500	11.0	1.7	1.455
	550	11.25	1.95	1.836
	600	11.5	2.2	2.260
	650	11.9	2.6	2.893
	700	12.3	3.0	3.595

(Upflow Propeller)

G (l/min)	N (rpm)	L (cm)	E (cm)	P (Watts)
0	250	10.55	1.25	0.535
	300	11.0	1.7	0.873
	350	11.5	2.2	1.318
	400	12.1	2.8	1.917
	450	12.8	3.5	2.696
6	250	10.1	0.8	0.342
	300	10.2	0.9	0.462
	350	10.4	1.1	0.659
	400	10.65	1.35	0.924
	450	11.05	1.75	1.348
	500	11.6	2.3	1.969
	550	12.2	2.9	2.731

APPENDIX : B 4.1 (contd.)

(Upflow Propeller)

G (l/min)	N (rpm)	L (cm)	E (cm)	P (Watts)
8	250	10.1	0.8	0.342
	300	10.15	0.85	0.437
	350	10.3	1.0	0.599
	400	10.55	1.25	0.856
	450	10.9	1.6	1.233
	500	11.3	2.0	1.712
	550	11.75	2.45	2.307
	600	12.3	3.0	3.082
12	250	10.05	0.75	0.321
	300	10.1	0.8	0.411
	350	10.25	0.95	0.569
	400	10.5	1.2	0.822
	450	10.8	1.5	1.156
	500	11.15	1.85	1.584
	550	11.5	2.2	2.072
	600	11.9	2.6	2.671
	650	12.3	3.0	3.338
18	250	10.05	0.75	0.321
	300	10.1	0.8	0.411
	350	10.23	0.93	0.557
	400	10.45	1.15	0.788
	450	10.7	1.4	1.079
	500	11.0	1.7	1.455
	550	11.33	2.03	1.911
	600	11.7	2.4	2.465
	650	12.05	2.75	3.060
	700	12.5	3.2	3.835

APPENDIX : B 4.1 (contd.)

(Upflow Propeller)

G (l/min)	N (rpm)	L (cm)	E (cm)	P (Watts)
25	250	9.95	0.65	0.278
	300	10.05	0.75	0.385
	350	10.2	0.9	0.539
	400	10.43	1.13	0.774
	450	10.65	1.35	1.040
	500	10.87	1.57	1.344
	550	11.2	1.9	1.789
	600	11.55	2.25	2.311
	650	11.85	2.55	2.838
	700	12.2	2.9	3.475

(Ring Sparger, Air-Xylene) (Downflow Disc Turbine)

G (l/min)	N (rpm)	L (cm)	E (cm)	P (Watts)
0	250	10.65	1.35	0.578
	300	11.1	1.8	0.924
	350	11.85	2.55	1.528
	400	12.7	3.4	2.328
6	250	10.1	0.8	0.342
	300	10.5	1.2	0.616
	350	11.15	1.85	1.109
	400	11.85	2.55	1.746
	450	12.5	3.2	2.465
8	250	10.1	0.8	0.342
	300	10.4	1.1	0.565
	350	10.9	1.6	0.959
	400	11.5	2.2	1.507
	450	12.2	2.9	2.234

APPENDIX : B 4.1 (contd.)

(Downflow Disc Turbine)

G (l/min)	N (rpm)	L (cm)	E (cm)	P (Watts)
12	250	10.05	0.75	0.321
	300	10.3	1.0	0.514
	350	10.7	1.4	0.839
	400	11.2	1.9	1.301
	450	11.8	2.5	1.926
	500	12.5	3.2	2.739
18	250	10.05	0.75	0.321
	300	10.25	0.95	0.488
	350	10.6	1.3	0.779
	400	10.95	1.65	1.130
	450	11.3	2.0	1.541
	500	11.65	2.35	2.012
	550	12.05	2.75	2.589
	600	12.5	3.2	3.287
25	250	10.0	0.7	0.300
	300	10.2	0.9	0.462
	350	10.5	1.2	0.719
	400	10.85	1.55	1.061
	450	11.15	1.85	1.425
	500	11.5	2.2	1.883
	550	11.9	2.6	2.448
	600	12.3	3.0	3.082

(Upflow Disc Turbine)

G	N	L	E	P
0	250	10.75	1.45	0.621
	300	11.35	2.05	1.053
	350	12.1	2.8	1.678
	400	12.95	3.65	2.500

APPENDIX : B 4.1 (contd.)

(Upflow Disc Turbine)

G (l/min)	N (rpm)	L (cm)	E (cm)	P (Watts)
6	250	10.15	0.85	0.364
	300	10.5	1.2	0.616
	350	10.95	1.65	0.989
	400	11.45	2.15	1.472
	450	12.0	2.7	2.080
	500	12.75	3.45	2.953
8	250	10.15	0.85	0.364
	300	10.4	1.1	0.565
	350	10.75	1.45	0.869
	400	11.2	1.9	1.301
	450	11.7	2.4	1.849
	500	12.33	3.03	2.594
12	250	10.1	0.8	0.342
	300	10.35	1.05	0.539
	350	10.63	1.33	0.979
	400	11.0	1.7	1.164
	450	11.45	2.15	1.656
	500	11.9	2.6	2.226
	550	12.4	3.1	2.919
18	250	10.05	0.75	0.321
	300	10.35	1.05	0.539
	350	10.55	1.25	0.749
	400	10.85	1.55	1.061
	450	11.25	1.95	1.502
	500	11.6	2.3	1.969
	550	12.0	2.7	2.542
	600	12.45	3.15	3.236

APPENDIX : B 4.1 (contd.)

(Upflow Disc Turbine)

G (l/min)	N (rpm)	L (cm)	E (cm)	P (Watts)
25	250	10.05	0.75	0.321
	300	10.3	1.0	0.514
	350	10.5	1.2	0.719
	400	10.75	1.45	0.993
	450	11.1	1.8	1.387
	500	11.45	2.15	1.840
	550	11.8	2.5	2.354
	600	12.2	2.9	2.979

(Downflow Propeller)

G (l/min)	N (rpm)	L (cm)	E (cm)	P (Watts)
0	250	9.85	0.55	0.235
	300	10.4	1.1	0.565
	350	10.9	1.6	0.959
	400	11.5	2.2	1.507
	450	12.2	2.9	2.234
6	250	9.73	0.43	0.184
	300	9.83	0.53	0.272
	350	10.05	0.75	0.449
	400	10.5	1.2	0.822
	450	10.93	1.63	1.256
	500	11.43	2.13	1.823
	550	12.0	2.7	2.542
8	250	9.73	0.43	0.184
	300	9.83	0.53	0.272
	350	10.0	0.7	0.419
	400	10.3	1.0	0.685

APPENDIX : B 4.1 (contd.)

(Downflow Propeller)

G (l/min)	N (rpm)	L (cm)	E (cm)	P (Watts)
8	450	10.6	1.3	1.002
	500	10.95	1.65	1.412
	550	11.45	2.15	2.024
	600	11.95	2.65	2.722
12	250	9.73	0.43	0.184
	300	9.8	0.5	0.257
	350	10.0	0.7	0.419
	400	10.2	0.9	0.616
	450	10.5	1.2	0.924
	500	10.83	1.53	1.310
	550	11.2	1.9	1.789
	600	11.6	2.3	2.363
	650	12.0	2.7	3.005
18	250	9.73	0.43	0.184
	300	9.8	0.5	0.257
	350	9.95	0.65	0.389
	400	10.15	0.85	0.582
	450	10.45	1.15	0.886
	500	10.75	1.45	1.241
	550	11.05	1.75	1.648
	600	11.4	2.1	2.157
	650	11.7	2.4	2.671
	700	12.05	2.75	3.296
25	250	9.75	0.45	0.193
	300	9.83	0.53	0.272
	350	9.95	0.65	0.389
	400	10.15	0.85	0.582
	450	10.4	1.1	0.847
	500	10.7	1.4	1.198

APPENDIX : B 4.1 (contd.)

(Downflow Propeller)

G (l/min)	N (rpm)	L (cm)	E (cm)	P (Watts)
25	550	10.95	1.65	1.554
	600	11.2	1.9	1.952
	650	11.5	2.2	2.448
	700	11.85	2.55	3.056

(Upflow Propeller)

G (l/min)	N (rpm)	L (cm)	E (cm)	P (Watts)
0	250	9.95	0.65	0.278
	300	10.45	1.15	0.591
	350	11.0	1.7	1.019
	400	11.6	2.3	1.575
	450	12.2	2.9	2.234
6	250	9.73	0.43	0.184
	300	9.85	0.55	0.282
	350	10.2	0.9	0.539
	400	10.55	1.25	0.856
	450	10.9	1.6	1.233
	500	11.45	2.15	1.840
	550	12.0	2.7	2.542
8	250	9.73	0.43	0.184
	300	9.85	0.55	0.282
	350	10.15	0.85	0.509
	400	10.35	1.05	0.719
	450	10.7	1.4	1.079
	500	11.1	1.8	1.541
	550	11.5	2.2	2.072
	600	11.95	2.65	2.722

APPENDIX : B 4.1 (contd.)

(Upflow Propeller)

G (l/min)	N (rpm)	L (cm)	E (cm)	P (Watts)
12	250	9.7	0.4	0.171
	300	9.83	0.53	0.272
	350	10.07	0.77	0.461
	400	10.3	1.0	0.685
	450	10.53	1.23	0.948
	500	10.83	1.53	1.310
	550	11.3	2.0	1.883
	600	11.6	2.3	2.362
	650	11.93	2.63	2.927
18	250	9.7	0.4	0.171
	300	9.8	0.5	0.257
	350	10.03	0.73	0.437
	400	10.2	0.9	0.616
	450	10.45	1.15	0.886
	500	10.75	1.45	1.241
	550	11.1	1.8	1.695
	600	11.37	2.07	2.126
	650	11.75	2.45	2.726
	700	12.0	2.7	3.236
25	250	9.7	0.4	0.171
	300	9.8	0.5	0.257
	350	10.0	0.7	0.419
	400	10.2	0.9	0.616
	450	10.43	1.13	0.871
	500	10.7	1.4	1.198
	550	10.97	1.67	1.572
	600	11.2	1.9	1.952
	650	11.55	2.25	2.504
	700	11.8	2.5	2.996

APPENDIX : C 4.2

Three Phase Results : Suspension Conditions

(Ring sparger, Air-Xylene-Polythene beads)

(Downflow Disc Turbine)

M (g)	G (l/min)	N_{JS} (rpm)	*	M (g)	G (l/min)	N_{JS} (rpm)
25	0	60	*	200	0	120
	6	260	*		6	275
	10	285	*		10	310
	14	320	*		14	335
	20	350	*		20	370
			*			
50	0	80	*	300	0	130
	6	265	*		6	280
	10	295	*		10	315
	14	325	*		14	335
	20	355	*		20	370
			*			
100	0	100	*	400	0	150
	6	270	*		6	285
	10	300	*		10	320
	14	330	*		14	340
	20	360	*		20	375
			*			
150	0	110	*	500	0	165
	6	275	*		6	290
	10	305	*		10	325
	14	330	*		14	345
	20	365	*		20	380

APPENDIX : C 4.2 (contd.)

(Upflow Disc Turbine)

M (g)	G (l/min)	N_{JS} (rpm)	*	M (g)	G (l/min)	N_{JS} (rpm)
25	0	240	*	200	0	270
	6	355	*		6	435
	10	385	*		10	490
	14	410	*		14	510
	20	425	*		20	540
			*			
50	0	250	*	300	0	270
	6	380	*		6	455
	10	405	*		10	500
	14	440	*		14	520
	20	465	*		20	550
			*			
100	0	255	*	400	0	275
	6	400	*		6	475
	10	435	*		10	510
	14	470	*		14	530
	20	500	*		20	560
			*			
150	0	260	*	500	0	275
	6	420	*		6	495
	10	465	*		10	520
	14	490	*		14	535
	20	520	*		20	570

APPENDIX : C 4.2 (contd.)

(Downflow Propeller)

M (g)	G (l/min)	N_{JS} (rpm)	*	M (g)	G (l/min)	N_{JS} (rpm)
25	0	320	*	200	0	400
	6	410	*		6	500
	10	370	*		10	460
	14	400	*		14	470
	20	420	*		20	495
			*			
50	0	365	*	300	0	410
	6	450	*		6	510
	10	405	*		10	475
	14	440	*		14	485
	20	460	*		20	505
			*			
100	0	380	*	400	0	415
	6	470	*		6	520
	10	435	*		10	495
	14	450	*		14	510
	20	480	*		20	520
			*			
150	0	390	*	500	0	425
	6	490	*		6	535
	10	455	*		10	520
	14	460	*		14	525
	20	490	*		20	535

APPENDIX : C 4.2 (contd.)

(Upflow Propeller)

M (g)	G (l/min)	N_{JS} (rpm)	*	M (g)	G (l/min)	N_{JS} (rpm)
25	0	275	*	200	0	320
	6	340	*		6	425
	10	330	*		10	415
	14	350	*		14	425
	20	370	*		20	440
			*			
50	0	290	*	300	0	330
	6	370	*		6	450
	10	345	*		10	435
	14	370	*		14	445
	20	385	*		20	460
			*			
100	0	305	*	400	0	340
	6	390	*		6	470
	10	365	*		10	460
	14	395	*		14	470
	20	400	*		20	480
			*			
150	0	310	*	500	0	355
	6	415	*		6	485
	10	395	*		10	480
	14	410	*		14	490
	20	420	*		20	500

APPENDIX : D 4.3.1

Quiescent Interface Cell : CHA - CO_2

S = 39.6 cm^2, G = 20. l/min (18 air, 2 CO_2)

Runs 1,2,3,4,5 : 10.% CHA, 20.% propanol, 70.% xylene

	t (mins)	H_{CO2} x	H_{CHA} y	(x/y)	M_{CHA} (mol/l)
Run 1	0	0.03	4.6	0.007	0.855
	10	0.39	4.35	0.090	0.654
	20	0.75	4.93	0.152	0.504
	30	1.09	5.0	0.218	0.344
Run 2	0	0.04	4.76	0.008	0.853
	10	0.6	5.0	0.120	0.581
	25	1.05	5.02	0.209	0.366
	40	1.38	5.22	0.264	0.233
	60	1.75	5.14	0.340	0.048
Run 3	0	0.21	4.42	0.048	0.756
	10	0.64	4.8	0.133	0.550
	20	0.99	4.7	0.208	0.368
	30	1.14	4.48	0.254	0.257
	40	1.53	5.08	0.301	0.143
	50	1.85	5.3	0.349	0.027
Run 4	0	0.24	5.0	0.048	0.756
	10	0.6	4.98	0.120	0.581
	20	0.92	4.87	0.189	0.414
	30	1.23	4.72	0.261	0.240
	40	1.41	4.77	0.296	0.155
	50	1.82	5.24	0.347	0.031
Run 5	0	0.18	4.28	0.042	0.770
	10	0.58	5.0	0.116	0.591
	20	0.95	5.04	0.188	0.417
	30	1.31	5.19	0.252	0.262
	40	1.58	5.15	0.307	0.128

APPENDIX : D 4.3.2

Quiescent Interface Cell : DEA - CO_2

S = 39.6 cm^2, G = 20. l/min (18 air, 2 CO_2)

Runs 1,2,3 : 10.% DEA, 20.% propanol, 70.% xylene

Runs 4,5 : 10.% DEA, 90.% propanol

	t (mins)	H_{CO2} x	H_{DEA} y	(x/y)	M_{DEA} (mol/l)
Run 1	0	0.30	0.85	0.353	1.029
	5	1.55	0.91	1.703	0.965
	10	3.53	1.27	2.780	0.914
	15	3.40	0.90	3.778	0.866
	20	2.19	0.54	4.056	0.853
	30	3.77	0.50	7.540	0.686
Run 2	0	0.04	0.77	0.052	1.044
	10	1.83	0.83	2.205	0.941
	20	3.11	0.80	3.888	0.861
	30	2.86	0.56	5.107	0.802
	40	3.20	0.43	7.442	0.691
	50	3.33	0.40	8.325	0.649
Run 3	0	0.42	0.70	0.600	1.018
	15	2.52	0.72	3.500	0.879
	30	3.17	0.56	5.661	0.776
	45	3.52	0.44	8.00	0.664
	60	2.94	0.24	12.250	0.462
	90	2.01	0.14	14.357	0.361

APPENDIX : D 4.3.2 (contd.)

	t (mins)	H_{CO2} x	H_{DEA} y	(x/y)	M_{DEA} (mol/l)
Run 4	0	0.07	0.88	0.080	1.042
	20	2.09	0.92	2.272	0.938
	40	3.31	0.84	3.940	0.858
	55	3.12	0.74	4.216	0.845
	70	4.36	0.95	4.589	0.827
Run 5	0	0.01	0.83	0.012	1.046
	15	1.62	0.92	1.761	0.962
	30	3.18	1.00	3.180	0.894
	45	4.33	1.06	4.085	0.851
	60	3.60	0.80	4.500	0.831

APPENDIX : D 4.3.3

Quiescent Interface Cell : DIPA - CO_2

S = 39.6 cm^2, G = 20. l/min (18 air, 2 CO_2)

Runs 1,2,3,4,5 : 10.% DIPA, 20.% propanol, 70.% xylene

Run 6 : 10.% DIPA, 90.% propanol

	t (mins)	H_{CO2} x	H_{DIPA} y	(x/y)	M_{DIPA} (mol/l)
Run 1	0	0.02	1.59	0.013	0.750
	10	1.05	1.61	0.652	0.718
	20	2.09	1.70	1.229	0.689
	30	3.24	1.76	1.841	0.658
	40	4.30	1.77	2.429	0.628
	50	5.15	1.85	2.784	0.611
Run 2	0	0.65	1.49	0.436	0.729
	10	1.56	1.58	0.987	0.701
	20	2.49	1.66	1.500	0.675
	30	3.52	1.73	2.035	0.648
	40	4.53	1.77	2.559	0.622
	50	5.36	1.75	3.063	0.596
	60	6.38	1.86	3.430	0.578
	70	7.11	1.87	3.802	0.559
Run 3	0	0.06	1.58	0.038	0.749
	15	1.46	1.69	0.864	0.707
	30	2.76	1.75	1.577	0.671
	45	3.79	1.55	2.445	0.628
	60	4.64	1.32	3.515	0.574
	75	6.88	1.86	3.699	0.564
Run 4	0	0.06	1.84	0.033	0.749
	15	1.63	1.94	0.840	0.709
	25	2.73	1.99	1.372	0.682
	35	3.88	2.03	1.911	0.655

APPENDIX : D 4.3.3 (contd.)

	t (mins)	H_{CO2} x	H_{DIPA} y	(x/y)	M_{DIPA} (mol/l)
Run 5	0	0.13	1.83	0.071	0.747
	15	1.84	1.96	0.939	0.704
	35	4.39	2.00	2.195	0.640
	55	7.28	2.17	3.355	0.582
	75	9.71	2.27	4.278	0.535
	95	12.09	2.39	5.059	0.496
	115	13.33	2.47	5.397	0.479
	140	15.15	2.50	6.060	0.445
Run 6	0	0.01	1.58	0.006	0.751
	10	0.40	1.64	0.244	0.739
	20	0.88	1.79	0.492	0.726
	30	1.35	1.78	0.758	0.713
	40	1.78	1.86	0.957	0.703
	60	2.73	1.77	1.542	0.673
	80	3.63	1.87	1.941	0.653
	100	4.42	1.98	2.232	0.638

APPENDIX : E 4.4.1

Agitated Vessel : CHA - CO_2

Runs 1,2,3,4 : 10.% CHA, 20.% propanol, 70.% xylene

Run 1 : N = 500 rpm, G = 10 l/min, Upflow Propeller

Run 2 : N = 450 rpm, G = 20 l/min, Upflow Propeller

Run 3 : N = 450 rpm, G = 10 l/min, Downflow Disc Turbine

Run 4 : N = 450 rpm, G = 10 l/min, Downflow Propeller

(p_{Air} = 0.9, p_{CO2} = 0.1)

	t (mins)	H_{CO2} x	H_{CHA} y	(x/y)	M_{CHA} (mol/l)
Run 1	0	0.01	4.73	0.002	0.867
	3	0.15	4.52	0.033	0.792
	6	0.27	4.46	0.061	0.724
	10	0.49	4.71	0.104	0.620
	15	0.69	4.66	0.148	0.514
	20	0.89	4.66	0.191	0.409
	25	1.03	4.70	0.219	0.342
	30	1.21	4.87	0.248	0.271
Run 2	0	0.01	4.84	0.002	0.867
	3	0.28	4.53	0.062	0.722
	6	0.56	4.44	0.126	0.567
	10	0.94	4.68	0.201	0.385
	15	1.19	4.79	0.248	0.271
Run 3	0	0.03	4.26	0.007	0.855
	3	0.15	4.00	0.038	0.780
	6	0.24	4.35	0.055	0.739
	10	0.41	4.59	0.089	0.656
	15	0.66	4.81	0.137	0.540
	20	0.82	4.51	0.182	0.431
	25	1.09	4.90	0.222	0.334
	30	1.22	4.81	0.254	0.257

APPENDIX : E 4.4.1 (contd.)

	t (mins)	H_{CO2} x	H_{CHA} y	(x/y)	M_{CHA} (mol/l)
Run 4	0	0.04	4.15	0.010	0.848
	3	0.21	4.98	0.042	0.770
	6	0.33	4.61	0.072	0.698
	10	0.56	5.09	0.110	0.606
	15	0.81	5.06	0.160	0.484
	20	1.04	5.48	0.190	0.412
	25	1.12	4.79	0.234	0.305
	30	1.29	4.67	0.276	0.203

APPENDIX : E 4.4.2

Agitated Vessel : DEA - CO_2

Run 1 : 10.% DEA, 20.% propanol, 70.% xylene

: N = 450 rpm, G = 20 l/min, Downflow Disc Turbine

(p_{Air} = 0.9, p_{CO2} = 0.1)

	t (mins)	H_{CO2} x	H_{DEA} y	(x/y)	M_{DEA} (mol/l)
Run 1	0	0.13	0.77	0.169	1.038
	5	2.41	0.52	4.635	0.825
	10	1.69	0.22	7.682	0.680
	15	1.58	0.11	14.364	?
	20	1.57	0.065	24.154	?
	30	0.315	0.035	9.0	0.617 (?)

APPENDIX : E 4.4.3

Agitated Vessel : DIPA - CO_2

Runs 1,2,3,4 : 10.% DIPA, 90.% propanol, G = 10. l/min
(9 Air, 1 CO_2)

Run 1 : N = 350 rpm, Downflow Disc Turbine
Run 2 : N = 250 rpm, " " "
Run 3 : N = 350 rpm, " " " , M = 100. g
Run 4 : N = 250 rpm, Upflow Propeller

CO_2 re-calibration : R = 640, 0.5 ml CO_2 = 6.31

$\therefore M_{DIPA} = 0.7508 - 0.054048(H_{CO2}/H_{DIPA})$

	t (mins)	H_{CO2} x	H_{DIPA} y	(x/y)	M_{DIPA} (mol/l)
Run 1	0	0.12	1.82	0.066	0.747
	10	3.53	1.89	1.868	0.650
	20	6.19	1.91	3.241	0.576
	30	7.53	1.72	4.378	0.514
	40	8.36	1.87	4.471	0.509
	50	8.35	1.89	4.418	0.512
	60	8.27	1.85	4.470	0.509
Run 2	0	0.19	1.75	0.109	0.745
	5	1.59	1.74	0.914	0.701
	10	2.95	1.81	1.630	0.663
	15	4.23	1.84	2.299	0.627
	20	5.15	1.82	2.830	0.598
	30	6.63	1.63	4.067	0.531
	40	7.77	1.80	4.317	0.518
	50	7.69	1.79	4.296	0.519

APPENDIX : E 4.4.3 (contd.)

	t (mins)	H_{CO2} x	H_{DIPA} y	(x/y)	M_{DIPA} (mol/l)
Run 3	0	0.26	1.60	0.163	0.742
	5	2.16	1.80	1.200	0.686
	10	3.46	1.77	1.955	0.645
	15	4.81	1.81	2.657	0.607
	20	5.81	1.84	3.158	0.580
	30	6.61	1.81	3.652	0.553
	40	7.12	1.83	3.891	0.541
	50	7.54	1.89	3.989	0.535
Run 4	0	0.20	1.61	0.124	0.744
	5	1.69	1.78	0.949	0.700
	10	2.98	1.82	1.637	0.662
	15	3.89	1.78	2.185	0.633
	20	4.86	1.83	2.656	0.607
	30	6.62	1.87	3.540	0.559
	40	6.69	1.84	3.636	0.554
	50	7.12	1.88	3.787	0.546

APPENDIX : F 4.5.1

Agitated Vessel : Air - Sulphite Reaction

(Ring Sparger) (Downflow Disc Turbine)

Run 1 : G = 10. l/min, N = 450 rpm

: $M(S_2O_3)$ = 0.1549, $M(I_2)$ = 0.0503

t	T	pH	$V(S_2O_3)$	$eqV(I_2)$	$eqV(SO_3)$	$M(SO_3)$
0	18°	8.5	2.96	4.56	15.44	0.776
15	22		3.64	5.61	14.39	0.723
30	26		4.51	6.95	13.05	0.656
45	30		5.88	9.06	10.94	0.550
60	34°	8.33	7.37	11.36	8.64	0.434

Run 2 : G = 6. l/min, N = 450 rpm

: $M(S_2O_3)$ = 0.1552, $M(I_2)$ = 0.0505

t	T	pH	$V(S_2O_3)$	$eqV(I_2)$	$eqV(SO_3)$	$M(SO_3)$
0	18°	8.5	4.12	6.33	13.67	0.690
15			4.62	7.10	12.90	0.651
30			5.21	8.01	11.99	0.605
45	24		5.81	8.93	11.07	0.559
55			6.45	9.92	10.08	0.509
65	28°	8.37	7.14	10.98	9.02	0.455

Run 3 : G = 14. l/min, N =450 rpm

: $M(S_2O_3)$ = 0.1550, $M(I_2)$ = 0.0503

t	T	pH	$V(S_2O_3)$	$eqV(I_2)$	$eqV(SO_3)$	$M(SO_3)$
0	16.5	8.5	4.18	6.44	13.56	0.682
10			4.76	7.34	12.66	0.637
20	21		5.44	8.38	11.62	0.584
30			6.20	9.56	10.44	0.525
40	26.5		7.10	10.94	9.06	0.456
50	30°	8.2	8.23	12.68	7.32	0.368

APPENDIX : F 4.5.1 (contd.)

(Downflow Disc Turbine)

Run 4 : G = 19.5 l/min, N = 450 rpm

: $M(S_2O_3)$ = 0.1545, $M(I_2)$ = 0.0504

t	T	pH	$V(S_2O_3)$	$eqV(I_2)$	$eqV(SO_3)$	$M(SO_3)$
0	16°	8.5	4.22	6.46	13.54	0.683
10	18		4.98	7.63	12.37	0.624
20	20		5.77	8.84	11.16	0.563
30	24		6.87	10.52	9.48	0.478
40	29.5		8.13	12.45	7.55	0.381
50	32.5	8.15	9.44	14.46	5.54	0.279

Run 5 : G = 17. l/min, N = 450 rpm

: $M(S_2O_3)$ = 0.1551, $M(I_2)$ = 0.05199

t	T	pH	$V(S_2O_3)$	$eqV(I_2)$	$eqV(SO_3)$	$M(SO_3)$
0	21°	8.5	4.44	6.62	13.38	0.695
10	23.5		5.26	7.84	12.16	0.632
20	27		6.22	9.28	10.72	0.557
30	30.5		7.41	11.05	8.95	0.465
40	35°	8.26	8.72	13.01	6.99	0.364

Run 6 : G = 8. l/min, N = 450 rpm

: $M(S_2O_3)$ = 0.1553, $M(I_2)$ = 0.0505^a, 0.0525^b, 0.0516^c, 0.0528^d

t	T	pH	$V(S_2O_3)$	$eqV(I_2)$	$eqV(SO_3)$	$M(SO_3)$
0	20°	8.5	a4.32	6.65	13.35	0.674
10	23		b5.24	7.75	12.25	0.643
20	26		c5.54	8.33	11.67	0.603
30			d6.75	9.93	10.07	0.532
40	30°	8.35	d7.76	11.41	8.59	0.454

APPENDIX : F 4.5.1 (contd.)

(Downflow Disc Turbine)

Run 7 : G = 14. l/min, N = 350 rpm

: $M(S_2O_3)$ = 0.1554, $M(I_2)$ = 0.0565[a], 0.0574[b], 0.0571[c], 0.0583[d], 0.0587[e]

t	T	pH	$V(S_2O_3)$	$eqV(I_2)$	$eqV(SO_3)$	$M(SO_3)$
0	17.5	8.5	a5.70	7.84	12.16	0.688
10	19.5		b6.42	8.69	11.31	0.650
20	21.5		c6.84	9.31	10.69	0.611
30	23.5		d7.64	10.19	9.81	0.572
40	26°	8.36	e8.46	11.21	8.79	0.516

Run 8 : G = 14. l/min, N = 250 rpm

: $M(S_2O_3)$ = 0.1552, $M(I_2)$ = 0.0523

t	T	pH	$V(S_2O_3)$	$eqV(I_2)$	$eqV(SO_3)$	$M(SO_3)$
0	18°	8.5	4.37	6.48	13.52	0.707
10	19		4.73	7.02	12.98	0.679
20	20		5.11	7.58	12.42	0.649
30	21		5.50	8.16	11.84	0.619
40	22.5	8.47	5.94	8.81	11.19	0.585

Run 9 : G = 14. l/min, N =550 rpm

: $M(S_2O_3)$ = 0.1552, $M(I_2)$ = 0.0520

t	T	pH	$V(S_2O_3)$	$eqV(I_2)$	$eqV(SO_3)$	$M(SO_3)$
0	18°	8.5	4.42	6.59	13.41	0.698
10	21		5.50	8.20	11.80	0.614
20	27		6.67	9.95	10.05	0.523
30	32		8.34	12.44	7.56	0.394
40	38°	8.22	9.91	14.78	5.22	0.272

APPENDIX : F 4.5.1 (contd.)

(Downflow Disc Turbine)

Run 10 : G = 14. l/min, N = 500 rpm

: $M(S_2O_3)$ = 0.1549, $M(I_2)$ = 0.0523

t	T	pH	$V(S_2O_3)$	$eqV(I_2)$	$eqV(SO_3)$	$M(SO_3)$
0	19°	8.5	4.71	6.97	13.03	0.682
10	22		5.57	8.25	11.75	0.615
20	26		6.62	9.80	10.20	0.534
30	31		8.03	11.89	8.11	0.424
40	33.5	8.3	9.41	13.93	6.07	0.318

Run 11 : G = 12. l/min, N = 450 rpm

: $M(S_2O_3)$ = 0.1551, $M(I_2)$ = 0.0522

t	T	pH	$V(S_2O_3)$	$eqV(I_2)$	$eqV(SO_3)$	$M(SO_3)$
0	16.5	8.5	4.85	7.21	12.79	0.668
10	19		5.37	7.98	12.02	0.627
20	22		6.07	9.02	10.98	0.573
30	25		6.88	10.22	9.78	0.510
40	28°	8.37	7.86	11.68	8.32	0.434

APPENDIX : F 4.5.1 (contd.)

(Downflow Disc Turbine)

Run	N (rpm)	G (l/min)	R_A (mol/lmin) (x10^{-3})	S (cm^2)	
1	450	10	4.47	410	a
2	450	6	2.83	286	
3	450	14	5.23	529	
4	450	19.5	6.0	637	b
5	450	17	6.3	603	c
6	450	8	3.55	334	d
7	350	14	3.9	394	
8	250	14	3.05	308	
9	550	14	8.6	869	
10	500	14	6.7	670	e
11	450	12	4.75	480	

Where possible, the rate of reaction at T = 20.^{o}C was used, otherwise, the rate at some other, convenient temperature has been employed, with allowances made as described in Appendix A 3.1.2 :

a : T = 24^{o} N_A = 10.893 x 10^{-6} (mol/l min cm^2)

b : T = 18 N_A = 9.425 " "

c : T = 22.25 N_A = 10.441 " "

d : T = 23 N_A = 10.636 " "

e : T = 20.5 N_A = 10.007 " "

APPENDIX : F 4.5.1 (contd.)

(Ring Sparger) (Upflow Disc Turbine)

Run 1 : G = 6. l/min, N = 450 rpm

: $M(S_2O_3)$ = 0.1557, $M(I_2)$ = 0.0520

t	T	pH	$V(S_2O_3)$	$eqV(I_2)$	$eqV(SO_3)$	$M(SO_3)$
0	17.5	8.5	4.22	6.32	13.68	0.711
10	19		4.65	6.96	13.04	0.678
20	21		5.11	7.65	12.35	0.642
30	23		5.61	8.40	11.60	0.603
40	25°	8.42	6.18	9.25	10.75	0.559

Run 2 : G = 10. l/min, N = 450 rpm

: $M(S_2O_3)$ = 0.1552, $M(I_2)$ = 0.0519

t	T	pH	$V(S_2O_3)$	$eqV(I_2)$	$eqV(SO_3)$	$M(SO_3)$
0	17.5	8.5	4.43	6.62	13.38	0.695
10	20		4.87	7.28	12.72	0.661
20	22.5		5.48	8.19	11.81	0.613
30	25		6.20	9.27	10.73	0.557
40	27.5	8.41	6.96	10.40	9.60	0.498

Run 3 : G = 16. l/min, N = 450 rpm

: $M(S_2O_3)$ = 0.1558, $M(I_2)$ = 0.0520

t	T	pH	$V(S_2O_3)$	$eqV(I_2)$	$eqV(SO_3)$	$M(SO_3)$
0	18°	8.5	4.45	6.67	13.33	0.693
10	20		5.12	7.68	12.32	0.640
20	23		6.05	9.07	10.93	0.568
30	26		6.68	10.01	9.99	0.519
40	29°	8.39	7.73	11.59	8.41	0.437

APPENDIX : F 4.5.1 (contd.)

(Upflow Disc Turbine)

Run 4 : G = 14. l/min, N = 450 rpm

: $M(S_2O_3)$ = 0.1553, $M(I_2)$ = 0.0516

t	T	pH	$V(S_2O_3)$	$eqV(I_2)$	$eqV(SO_3)$	$M(SO_3)$
0	18°	8.5	4.53	6.82	13.18	0.680
10	20		5.03	7.57	12.43	0.642
20	22.5		5.82	8.76	11.24	0.580
30	25		6.65	10.01	9.99	0.516
40	28	8.43	7.56	11.38	8.62	0.445

Run 5 : G = 14. l/min, N = 350 rpm

: $M(S_2O_3)$ = 0.1556, $M(I_2)$ = 0.0523

t	T	pH	$V(S_2O_3)$	$eqV(I_2)$	$eqV(SO_3)$	$M(SO_3)$
0	17°	8.5	4.55	6.77	13.23	0.692
10	19		4.92	7.32	12.68	0.664
20	20		5.38	8.00	12.00	0.628
30	22		5.93	8.82	11.18	0.585
40	23.5	8.43	6.52	9.70	10.30	0.539

Run 6 : G = 14. l/min, N = 550 rpm

: $M(S_2O_3)$ = 0.1548, $M(I_2)$ = 0.0524

t	T	pH	$V(S_2O_3)$	$eqV(I_2)$	$eqV(SO_3)$	$M(SO_3)$
0	18°	8.5	4.49	6.64	13.36	0.700
10	20		5.33	7.88	12.12	0.635
20	23		6.18	9.14	10.86	0.569
30	27		7.18	10.61	9.39	0.491
40	32°	8.33	8.66	12.80	7.20	0.377

APPENDIX : F 4.5.1 (contd.)

(Upflow Disc Turbine)

Run 7 : G = 14. l/min, N = 250 rpm

: $M(S_2O_3)$ = 0.1553, $M(I_2)$ = 0.0525

t	T	pH	$V(S_2O_3)$	$eqV(I_2)$	$eqV(SO_3)$	$M(SO_3)$
0	16.5	8.5	4.53	6.70	13.30	0.698
10	17.5		4.89	7.23	12.77	0.670
20	19		5.26	7.78	12.22	0.641
30	20		5.67	8.39	11.61	0.610
40	21.5	8.47	6.13	9.07	10.93	0.574

Run 8 : G = 14. l/min, N = 500 rpm

: $M(S_2O_3)$ = 0.1557, $M(I_2)$ = 0.0523

t	T	pH	$V(S_2O_3)$	$eqV(I_2)$	$eqV(SO_3)$	$M(SO_3)$
0	17.5	8.5	4.61	6.86	13.14	0.688
10	20.5		5.32	7.91	12.09	0.633
20	24		6.19	9.20	10.80	0.565
30	28		7.30	10.86	9.14	0.479
40	32°	8.33	8.68	12.91	7.09	0.371

Run 9 : G = 8. l/min, N = 450 rpm

: $M(S_2O_3)$ = 0.1553, $M(I_2)$ = 0.0522

t	T	pH	$V(S_2O_3)$	$eqV(I_2)$	$eqV(SO_3)$	$M(SO_3)$
0	18.5	8.5	4.71	7.01	12.99	0.678
10	20.5		5.11	7.60	12.40	0.647
20	23		5.71	8.50	11.50	0.600
30	25.5		6.53	9.72	10.28	0.537
40	28°	8.42	7.24	10.77	9.23	0.482

APPENDIX : F 4.5.1 (contd.)

(Upflow Disc Turbine)

Run 10 : G = 12. l/min, N = 450 rpm

: $M(S_2O_3)$ = 0.1556, $M(I_2)$ = 0.0522

t	T	pH	$V(S_2O_3)$	$eqV(I_2)$	$eqV(SO_3)$	$M(SO_3)$
0	18°	8.5	4.54	6.77	13.23	0.690
10	20		5.12	7.64	12.36	0.645
20	22.5		5.72	8.53	11.47	0.598
30	25		6.49	9.68	10.32	0.538
40	28°	8.41	7.41	11.05	8.95	0.467

Run 11 : G = 18. l/min, N = 450 rpm

: $M(S_2O_3)$ = 0.1553, $M(I_2)$ = 0.0519

t	T	pH	$V(S_2O_3)$	$eqV(I_2)$	$eqV(SO_3)$	$M(SO_3)$
0	18.5	8.5	4.61	6.90	13.10	0.680
10	20.5		5.30	7.93	12.07	0.626
20	23		6.01	8.99	11.01	0.571
30	26.5	8.41	6.85	10.25	9.75	0.506

APPENDIX : F 4.5.1 (contd.)

(Upflow Disc Turbine)

Run	N (rpm)	G (l/min)	R_A (mol/lmin) $(x10^{-3})$	S (cm^2)	
1	450	6	3.6	364	
2	450	10	4.1	414	
3	450	16	5.3	550	a
4	450	14	5.0	503	b
5	350	14	3.6	369	c
6	550	14	6.5	674	d
7	250	14	3.2	323	
8	500	14	5.5	570	e
9	450	8	3.9	388	f
10	450	12	4.6	463	g
11	450	18	5.45	542	h

a : T = 19^o N_A = 9.642 x 10^{-6} (mol/l min cm^2)

b : T = 20.25 N_A = 9.943 " "

c : T = 19.5 N_A = 9.757 " "

d : T = 19 N_A = 9.642 " "

e : T = 19 N_A = 9.642 " "

f : T = 20.75 N_A = 10.056 " "

g : T = 20.25 N_A = 9.943 " "

h : T = 20.75 N_A = 10.056 " "

APPENDIX : F 4.5.2

Agitated Vessel : Air - Sulphite Reaction

(Ring Sparger) (Downflow Propeller)

Run 1 : G = 10. l/min, N = 450 rpm

: $M(S_2O_3)$ = 0.1551, $M(I_2)$ = 0.0520

t	T	pH	$V(S_2O_3)$	$eqV(I_2)$	$eqV(SO_3)$	$M(SO_3)$
0	17.5	8.5	4.51	6.73	13.27	0.690
10	19		4.92	7.34	12.66	0.658
20	21		5.39	8.04	11.96	0.622
30	23		6.05	9.02	10.98	0.571
40	25°	8.4	6.76	10.08	9.92	0.516

Run 2 : G = 6. l/min, N = 450 rpm

: $M(S_2O_3)$ = 0.1552, $M(I_2)$ = 0.0521

t	T	pH	$V(S_2O_3)$	$eqV(I_2)$	$eqV(SO_3)$	$M(SO_3)$
0	18°	8.5	4.40	6.55	13.45	0.701
10	19		4.80	7.15	12.85	0.670
20	20.5		5.21	7.76	12.24	0.638
30	23		5.69	8.47	11.53	0.601
40	24.5	8.45	6.13	9.13	10.87	0.567

Run 3 : G = 14. l/min, N = 450 rpm

: $M(S_2O_3)$ = 0.1551, $M(I_2)$ = 0.0520

t	T	pH	$V(S_2O_3)$	$eqV(I_2)$	$eqV(SO_3)$	$M(SO_3)$
0	18°	8.5	4.34	6.47	13.53	0.704
10	20		5.00	7.45	12.55	0.653
20	22.5		5.72	8.52	11.48	0.597
30	25		6.51	9.70	10.30	0.536
40	28°	8.4	7.38	11.00	9.00	0.468

APPENDIX : F 4.5.2 (contd.)

(Downflow Propeller)

Run 4 : G = 18. l/min, N = 450 rpm

: $M(S_2O_3)$ = 0.1550, $M(I_2)$ = 0.0519

t	T	pH	$V(S_2O_3)$	$eqV(I_2)$	$eqV(SO_3)$	$M(SO_3)$
0	19°	8.5	4.31	6.43	13.57	0.704
10	23		5.08	7.58	12.42	0.645
20	25		6.09	9.09	10.91	0.566
30	29.5		7.17	10.70	9.30	0.483
40	33°	8.25	8.39	12.52	7.48	0.388

Run 5 : G = 14. l/min, N = 250 rpm

: $M(S_2O_3)$ = 0.1553, $M(I_2)$ = 0.0520

t	T	pH	$V(S_2O_3)$	$eqV(I_2)$	$eqV(SO_3)$	$M(SO_3)$
0	19°	8.5	4.38	6.54	13.46	0.701
10	20		4.80	7.16	12.84	0.668
20	21		5.21	7.78	12.22	0.636
30	22		5.70	8.51	11.49	0.598
40	24°	8.46	6.08	9.07	10.93	0.568

Run 6 : G = 14. l/min, N = 350 rpm

: $M(S_2O_3)$ = 0.1553, $M(I_2)$ = 0.0520

t	T	pH	$V(S_2O_3)$	$eqV(I_2)$	$eqV(SO_3)$	$M(SO_3)$
0	18°	8.5	4.40	6.57	13.43	0.699
10	19		4.84	7.22	12.78	0.665
20	21		5.31	7.93	12.07	0.628
30	22.5		5.88	8.78	11.22	0.584
40	24°	8.46	6.39	9.54	10.46	0.544

APPENDIX : F 4.5.2 (contd.)

(Downflow Propeller)

Run 7 : G = 14. l/min, N = 550 rpm

: $M(S_2O_3)$ = 0.1549, $M(I_2)$ = 0.0523

t	T	pH	$V(S_2O_3)$	$eqV(I_2)$	$eqV(SO_3)$	$M(SO_3)$
0	16°	8.5	4.58	6.79	13.21	0.691
10	18		5.34	7.91	12.09	0.632
20	21.5		6.18	9.16	10.84	0.567
30	24.5		7.10	10.52	9.48	0.496
40	29°	8.34	8.21	12.16	7.84	0.410

Run 8 : G = 14. l/min, N = 650 rpm

: $M(S_2O_3)$ = 0.1549, $M(I_2)$ = 0.0513[a], 0.0523[b], 0.0518[c]

t	T	pH	$V(S_2O_3)$	$eqV(I_2)$	$eqV(SO_3)$	$M(SO_3)$
0	18°	8.5	a4.49	6.78	13.22	0.678
10	22		b5.75	8.52	11.48	0.600
20	26		c6.95	10.40	9.60	0.497
30	32.5		b8.64	12.80	7.20	0.376
40	39°	8.1	-			

Run 9 : G = 12. l/min, N = 450 rpm

: $M(S_2O_3)$ = 0.1549, $M(I_2)$ = 0.0519

t	T	pH	$V(S_2O_3)$	$eqV(I_2)$	$eqV(SO_3)$	$M(SO_3)$
0	16°	8.5	4.57	6.52	13.18	0.684
10	17.5		5.04	7.52	12.48	0.647
20	19.5		5.60	8.36	11.64	0.604
30	21.5		6.16	9.19	10.81	0.561
40	24°	8.41	6.78	10.12	9.88	0.513

APPENDIX : F 4.5.2 (contd.)

(Downflow Propeller)

Run 10 : G = 8. l/min, N = 450 rpm

: $M(S_2O_3)$ = 0.1549, $M(I_2)$ = 0.0520

t	T	pH	$V(S_2O_3)$	$eqV(I_2)$	$eqV(SO_3)$	$M(SO_3)$
0	14.5	8.5	5.03	7.50	12.50	0.650
10	16		5.46	8.14	11.86	0.616
20	17.5		5.90	8.79	11.21	0.582
30	19		6.39	9.52	10.48	0.544
40	21°	8.42	6.92	10.31	9.69	0.503

Run 11 : G = 13. l/min, N = 450 rpm

: $M(S_2O_3)$ = 0.1550, $M(I_2)$ = 0.0522

t	T	pH	$V(S_2O_3)$	$eqV(I_2)$	$eqV(SO_3)$	$M(SO_3)$
0	17°	8.5	4.47	6.64	13.36	0.697
10	19		5.04	7.48	12.52	0.653
20	21.5		5.67	8.42	11.58	0.604
30	23.5		6.39	9.49	10.51	0.549
40	26°	8.42	7.07	10.50	9.50	0.496

APPENDIX : F 4.5.2 (contd.)

(Downflow Propeller)

Run	N (rpm)	G (l/min)	R_A (mol/lmin)	S (cm^2)	
1	450	10	3.97	401	
2	450	6	3.3	337	
3	450	14	5.1	529	a
4	450	18	5.9	583	b
5	250	14	3.25	328	
6	350	14	3.83	387	
7	550	14	6.5	656	
8	650	14	7.8	788	
9	450	12	4.3	434	
10	450	8	3.9	394	
11	450	13	4.8	485	
			($x10^{-3}$)		

a : $T = 19^{o}$ $N_A = 9.642 \times 10^{-6}$ (mol/l min cm^2)

b : $T = 21$ $N_A = 10.119$ " "

APPENDIX : F 4.5.2 (contd.)

(Ring Sparger) (Upflow Propeller)

Run 1 : G = 10. l/min, N = 450 rpm

: $M(S_2O_3)$ = 0.1549, $M(I_2)$ = 0.0522

t	T	pH	$V(S_2O_3)$	$eqV(I_2)$	$eqV(SO_3)$	$M(SO_3)$
0	20°	8.5	4.61	6.83	13.17	0.688
10	21.5		5.07	7.52	12.48	0.652
20	23.5		5.61	8.32	11.68	0.610
30	25.5		6.28	9.31	10.69	0.558
40	27.5	8.43	6.93	10.27	9.73	0.508

Run 2 : G = 6. l/min, N =450 rpm

: $M(S_2O_3)$ = 0.1549, $M(I_2)$ = 0.0523

t	T	pH	$V(S_2O_3)$	$eqV(I_2)$	$eqV(SO_3)$	$M(SO_3)$
0	19°	8.5	4.53	6.71	13.29	0.695
10	20		4.92	7.29	12.71	0.664
15	21		5.17	7.66	12.34	0.645
30	22.5		5.71	8.46	11.54	0.603
40	23.5	8.46	6.10	9.04	10.96	0.573

Run 3 : G = 20. l/min, N = 450 rpm

: $M(S_2O_3)$ = 0.1550, $M(I_2)$ = 0.0520

t	T	pH	$V(S_2O_3)$	$eqV(I_2)$	$eqV(SO_3)$	$M(SO_3)$
0	18°	8.5	4.95	7.38	12.62	0.656
10	20		5.50	8.20	11.80	0.613
20	22		6.13	9.14	10.86	0.564
30	24.5		6.90	10.29	9.71	0.504
40	27.5	8.36	7.92	11.81	8.19	0.425

APPENDIX : F 4.5.2 (contd.)

(Upflow Propeller)

Run 4 : G = 14. l/min, N = 450 rpm

: $M(S_2O_3)$ = 0.1553, $M(I_2)$ = 0.0521

t	T	pH	$V(S_2O_3)$	$eqV(I_2)$	$eqV(SO_3)$	$M(SO_3)$
0	18°	8.5	4.44	6.62	13.38	0.697
10	20		5.01	7.47	12.53	0.652
20	22		5.52	8.23	11.77	0.613
30	24		6.16	9.19	10.81	0.563
40	26°	8.41	6.85	10.22	9.78	0.509

Run 5 : G = 14. l/min, N = 550 rpm

: $M(S_2O_3)$ = 0.1552, $M(I_2)$ = 0.0522

t	T	pH	$V(S_2O_3)$	$eqV(I_2)$	$eqV(SO_3)$	$M(SO_3)$
0	19°	8.5	4.48	6.66	13.34	0.697
10	21		5.19	7.71	12.29	0.642
20	23.5		6.06	9.00	11.00	0.574
30	28		7.01	10.42	9.58	0.501
40	31.5	8.41	8.19	12.17	7.83	0.409

Run 6 : G = 14. l/min, N = 350 rpm

: $M(S_2O_3)$ = 0.1556, $M(I_2)$ = 0.0523

t	T	pH	$V(S_2O_3)$	$eqV(I_2)$	$eqV(SO_3)$	$M(SO_3)$
0	19°	8.5	4.41	6.56	13.44	0.702
10	20.5		4.88	7.26	12.74	0.666
20	22		5.34	7.95	12.05	0.630
30	24		5.90	8.78	11.22	0.587
40	26°	8.43	6.51	9.69	10.31	0.539

APPENDIX : F 4.5.2 (contd.)

(Upflow Propeller)

Run 7 : G = 14. l/min, N = 250 rpm

: $M(S_2O_3)$ = 0.1562, $M(I_2)$ = 0.0525

t	T	pH	$V(S_2O_3)$	$eqV(I_2)$	$eqV(SO_3)$	$M(SO_3)$
0	20°	8.5	4.42	6.58	13.42	0.704
10	21		4.74	7.05	12.95	0.679
20	22		5.29	7.87	12.13	0.636
30	23		5.56	8.27	11.73	0.615
40	24.5	8.47	6.05	9.00	11.00	0.577

Run 8 : G = 14. l/min, N = 650 rpm

: $M(S_2O_3)$ = 0.1552, $M(I_2)$ = 0.0517

t	T	pH	$V(S_2O_3)$	$eqV(I_2)$	$eqV(SO_3)$	$M(SO_3)$
0	17°	8.5	4.44	6.66	13.34	0.690
10	21		5.35	8.03	11.97	0.619
20	25		6.74	10.11	9.89	0.511
30	30		8.21	12.32	7.68	0.397
40	35	8.3	9.43	14.15	5.85	0.303

Run 9 : G = 17. l/min, N = 450 rpm

: $M(S_2O_3)$ = 0.1130, $M(I_2)$ = 0.0521

t	T	pH	$V(S_2O_3)$	$eqV(I_2)$	$eqV(SO_3)$	$M(SO_3)$
0	18.5	8.5	4.67	6.93	13.07	0.684
10	20.5		5.24	7.78	12.22	0.640
20	23		5.87	8.72	11.28	0.591
30	25		6.58	9.77	10.23	0.536
40	28°	8.4	7.44	11.05	8.95	0.469

APPENDIX : F 4.5.2 (contd.)

(Upflow Propeller)

Run 10 : G = 12. l/min, N = 450 rpm

: $M(S_2O_3)$ = 0.1134, $M(I_2)$ = 0.0522

t	T	pH	$V(S_2O_3)$	$eqV(I_2)$	$eqV(SO_3)$	$M(SO_3)$
0	20°	8.5	6.07	6.60	13.40	0.699
10	22.5		6.80	7.39	12.61	0.658
20	24.5		7.62	8.28	11.72	0.611
30	26.5		8.50	9.24	10.76	0.561
40	28.5	8.41	9.58	10.41	9.59	0.500

Run	N (rpm)	G (l/min)	R_A (mol/lmin)	S (cm^2)	
1	450	10	4.2	400	a
2	450	6	3.0	303	
3	450	20	4.6	465	
4	450	14	4.2	424	
5	550	14	5.5	556	
6	350	14	3.3	333	
7	250	14	2.75	272	b
8	650	14	7.1	736	c
9	450	17	4.5	461	d
10	450	12	4.7 ($x10^{-3}$)	437	e

a : T = 22.5 $N_A = 10.502 \times 10^{-6}$ (mol/l min cm^2)

b : T = 21 N_A = 10.119 " "

c : T = 19 N_A = 9.642 " "

d : T = 19.5 N_A = 9.757 " "

e : T = 23.5 N_A = 10.758 " "

APPENDIX : F 4.5.3

Agitated Vessel : Air - Sulphite Reaction

(Single Tube Sparger) (Downflow Propeller)

Run 1 : G = 20. l/min, N =450 rpm

: $M(S_2O_3)$ = 0.1548, $M(I_2)$ = 0.0523

t	T	pH	$V(S_2O_3)$	$eqV(I_2)$	$eqV(SO_3)$	$M(SO_3)$
0	22°	8.5	4.81	7.13	12.87	0.673
10	24		5.24	7.76	12.24	0.639
20	25		5.81	8.61	11.39	0.595
30	27		6.50	9.63	10.37	0.542
40	29	8.39	7.17	10.62	9.38	0.490

Run 2 : G = 6. l/min, N = 450 rpm

: $M(S_2O_3)$ = 0.1549, $M(I_2)$ = 0.0522

t	T	pH	$V(S_2O_3)$	$eqV(I_2)$	$eqV(SO_3)$	$M(SO_3)$
0	22.5	8.5	4.67	6.92	13.08	0.683
10	23.5		5.12	7.59	12.41	0.648
20	25		5.45	8.08	11.92	0.623
30	26		5.79	8.58	11.42	0.596
40	27.5	8.43	6.20	9.19	10.81	0.565

Run 3 : G = 14. l/min, N = 450 rpm

: $M(S_2O_3)$ = 0.1558, $M(I_2)$ = 0.0524

t	T	pH	$V(S_2O_3)$	$eqV(I_2)$	$eqV(SO_3)$	$M(SO_3)$
0	22.5	8.5	4.45	6.62	13.38	0.701
10	24		5.00	7.44	12.56	0.658
20	26		5.60	8.33	11.67	0.611
30	27.5		6.19	9.20	10.80	0.565
40	29.5	8.39	6.78	10.08	9.92	0.519

APPENDIX : F 4.5.3 (contd.)

(Downflow Propeller)

Run 4 : G = 10. l/min, N = 450 rpm

: $M(S_2O_3)$ = 0.1552, $M(I_2)$ = 0.0522

t	T	pH	$V(S_2O_3)$	$eqV(I_2)$	$eqV(SO_3)$	$M(SO_3)$
0	21°	8.5	4.71	7.00	13.00	0.679
10	22.5		5.00	7.43	12.57	0.656
20	24		5.42	8.05	11.95	0.624
30	25.5		5.99	8.90	11.10	0.579
40	27°	8.41	6.53	9.70	10.30	0.538

Run 5 : G = 25. l/min, N = 450 rpm

: $M(S_2O_3)$ = 0.1558, $M(I_2)$ = 0.0521

t	T	pH	$V(S_2O_3)$	$eqV(I_2)$	$eqV(SO_3)$	$M(SO_3)$
0	27.5	8.5	4.50	6.72	13.28	0.692
10	30		-			
20	32.5		6.14	9.17	10.83	0.565
30	35.5		7.11	10.62	9.38	0.489
40	38°	8.32	8.12	12.13	7.87	0.410

Run 6 : G = 14. l/min, N = 350 rpm

: $M(S_2O_3)$ = 0.1548, $M(I_2)$ = 0.0522

t	T	pH	$V(S_2O_3)$	$eqV(I_2)$	$eqV(SO_3)$	$M(SO_3)$
0	23.5	8.5	4.57	6.78	13.22	0.690
10	24		4.78	7.09	12.91	0.674
20	25		5.09	7.55	12.45	0.650
30	25.5		5.48	8.12	11.88	0.620
40	26.5	8.45	5.89	8.73	11.27	0.588

APPENDIX : F 4.5.3 (contd.)

(Downflow Propeller)

Run 7 : G = 14. l/min, N = 650 rpm

: $M(S_2O_3)$ = 0.1555, $M(I_2)$ = 0.0523

t	T	pH	$V(S_2O_3)$	$eqV(I_2)$	$eqV(SO_3)$	$M(SO_3)$
0	24°	8.5	4.57	6.80	13.20	0.690
10	28		5.60	8.33	11.67	0.610
20	33		6.82	10.14	9.86	0.515
30	38.5		8.35	12.42	7.58	0.397
40	43.5	8.23	9.94	14.78	5.22	0.273

Run 8 : G = 14. l/min, N = 550 rpm

: $M(S_2O_3)$ = 0.1551, $M(I_2)$ = 0.0521

t	T	pH	$V(S_2O_3)$	$eqV(I_2)$	$eqV(SO_3)$	$M(SO_3)$
0	24.5	8.5	4.51	6.72	13.28	0.692
10	27		5.20	7.74	12.26	0.638
20	30		6.04	8.99	11.01	0.573
30	33.5		7.05	10.50	9.50	0.495
40	37.5	8.39	8.14	12.12	7.88	0.410

Run 9 : G = 14. l/min, N = 250 rpm

: $M(S_2O_3)$ = 0.1551, $M(I_2)$ = 0.0521

t	T	pH	$V(S_2O_3)$	$eqV(I_2)$	$eqV(SO_3)$	$M(SO_3)$
0	25°	8.5	4.46	6.64	13.35	0.695
10	25.5		4.81	7.16	12.84	0.668
20	26		4.92	7.33	12.67	0.660
30	26.5		5.12	7.62	12.38	0.644
40	27°	8.48	5.43	8.09	11.91	0.620

APPENDIX : F 4.5.3 (contd.)

(Downflow Propeller)

Run	N (rpm)	G (l/min)	R_A (mol/lmin)	S (cm^2)	
1	450	20	5.25	448	a
2	450	6	3.5	329	b
3	450	14	4.4	394	c
4	450	10	3.85	353	d
5	450	25	6.35	504	e
6	350	14	3.2	280	f
7	650	14	9.5	756	g
8	550	14	6.5	536	h
9	250	14	2.0 ($X10^{-3}$)	173	i

a : T = 27^{o}, $N_A = 11.707 \times 10^{-6}$ (mol/l min cm^2)

b : T = 23 $N_A = 10.636$ " "

c : T = 25 $N_A = 11.159$ " "

d : T = 24 $N_A = 10.893$ " "

e : T = 30 $N_A = 12.590$ " "

f : T = 26 $N_A = 11.440$ " "

g : T = 30.5 $N_A = 12.753$ " "

h : T = 28.5 $N_A = 12.131$ " "

i : T = 26.5 $N_A = 11.573$ " "

APPENDIX : F 4.5.3 (contd.)

(Single Tube Sparger) (Upflow Propeller)

Run 1 : G = 10. l/min, N = 450 rpm

: $M(S_2O_3)$ = 0.1557, $M(I_2)$ = 0.0522

t	T	pH	$V(S_2O_3)$	$eqV(I_2)$	$eqV(SO_3)$	$M(SO_3)$
0	19°	8.5	4.60	6.86	13.14	0.686
10	21		5.00	7.46	12.54	0.655
20	22.5		5.41	8.07	11.93	0.623
30	24		5.91	8.81	11.19	0.584
40	25.5	8.45	6.36	9.49	10.51	0.549

Run 2 : G = 6. l/min, N = 450 rpm

: $M(S_2O_3)$ = 0.1553, $M(I_2)$ = 0.0519

t	T	pH	$V(S_2O_3)$	$eqV(I_2)$	$eqV(SO_3)$	$M(SO_3)$
0	21°	8.5	4.57	6.84	13.16	0.683
10	22		5.00	7.49	12.52	0.649
20	23.5		5.42	8.11	11.89	0.617
30	25		5.77	8.64	11.36	0.589
40	26.5	8.45	6.31	9.45	10.55	0.548

Run 3 : G = 20. l/min, N = 450 rpm

: $M(S_2O_3)$ = 0.1553, $M(I_2)$ = 0.0519

t	T	pH	$V(S_2O_3)$	$eqV(I_2)$	$eqV(SO_3)$	$M(SO_3)$
0	21.5	8.5	4.56	6.83	13.17	0.683
10	23		5.12	7.66	12.34	0.640
20	25		5.67	8.49	11.51	0.597
30	27		6.35	9.51	10.49	0.544
40	29°	8.38	7.06	10.57	9.43	0.489

APPENDIX : F 4.5.3 (contd.)

(Upflow Propeller)

Run 4 : G = 25. l/min, N = 450 rpm

: $M(S_2O_3)$ = 0.1558, $M(I_2)$ = 0.0519

t	T	pH	$V(S_2O_3)$	$eqV(I_2)$	$eqV(SO_3)$	$M(SO_3)$
0	28.5	8.5	4.32	6.48	13.52	0.702
10	30.5		5.02	7.53	12.47	0.647
20	32.5		5.76	8.64	11.36	0.590
30	35		6.66	9.99	10.01	0.520
40	38°	8.31	7.65	11.48	8.52	0.443

Run 5 : G = 14. l/min, N = 450 rpm

: $M(S_2O_3)$ = 0.1557, $M(I_2)$ = 0.0522

t	T	pH	$V(S_2O_3)$	$eqV(I_2)$	$eqV(SO_3)$	$M(SO_3)$
0	23°	8.5	4.40	6.57	13.43	0.701
10	24.5		4.97	7.42	12.58	0.656
20	26.5		5.47	8.16	11.84	0.617
30	28		6.08	9.07	10.93	0.570
40	30°	8.4	6.66	9.94	10.06	0.525

Run 6 : G = 14. l/min, N = 350 rpm

: $M(S_2O_3)$ = 0.1551, $M(I_2)$ = 0.0520

t	T	pH	$V(S_2O_3)$	$eqV(I_2)$	$eqV(SO_3)$	$M(SO_3)$
0	22.5	8.5	4.58	6.84	13.16	0.684
10	23		4.93	7.36	12.64	0.657
20	24		5.32	7.94	12.06	0.627
30	25		5.76	8.60	11.40	0.592
40	26°	8.46	6.16	9.19	10.81	0.561

APPENDIX : F 4.5.3 (contd.)

(Upflow Propeller)

Run 7 : G = 14. l/min, N = 550 rpm

: $M(S_2O_3)$ = 0.1550, $M(I_2)$ = 0.0520

t	T	pH	$V(S_2O_3)$	$eqV(I_2)$	$eqV(SO_3)$	$M(SO_3)$
0	23°	8.5	4.40	6.56	13.44	0.698
10	25.5		5.17	7.71	12.29	0.639
20	28		5.94	8.86	11.14	0.579
30	31.5		6.85	10.22	9.78	0.508
40	34°	8.37	8.00	11.93	8.07	0.419

Run 8 : G = 14. l/min, N = 650 rpm

: $M(S_2O_3)$ = 0.1552, $M(I_2)$ = 0.0520

t	T	pH	$V(S_2O_3)$	$eqV(I_2)$	$eqV(SO_3)$	$M(SO_3)$
0	22°	8.5	4.60	6.87	13.13	0.683
10	25		5.35	7.99	12.01	0.625
20	29		6.37	9.51	10.49	0.546
30	34		7.76	11.58	8.42	0.438
40	38°	8.35	9.30	13.88	6.12	0.318

Run 9 : G = 14. l/min, N = 250 rpm

: $M(S_2O_3)$ = 0.1555, $M(I_2)$ = 0.0521

t	T	pH	$V(S_2O_3)$	$eqV(I_2)$	$eqV(SO_3)$	$M(SO_3)$
0	21.5	8.5	4.59	6.85	13.15	0.685
10	22		4.80	7.16	12.84	0.669
20	22.5		5.02	7.49	12.51	0.652
30	23		5.25	7.84	12.16	0.634
40	23.5	8.44	5.50	8.21	11.79	0.614

APPENDIX : F 4.5.3 (contd.)

(Upflow Propeller)

Run	N (rpm)	G (l/min)	R_A (mol/lmin)	S (cm^2)	
1	450	10	3.7	340	a
2	450	6	3.3	310	b
3	450	20	5.0	437	c
4	450	25	7.35	496	d
5	450	14	4.3	381	e
6	350	14	3.05	280	f
7	550	14	5.95	527	g
8	650	14	6.85	607	h
9	250	14	1.9 ($x10^{-3}$)	179	i

a : T = 24° $N_A = 10.893 \times 10^{-6}$ (mol/l min cm^2)

b : T = 23 $N_A = 10.636$ " "

c : T = 26 $N_A = 11.440$ " "

d : T = 35.25 $N_A = 14.81$ " "

e : T = 25.5 $N_A = 11.293$ " "

f : T = 24 $N_A = 10.893$ " "

g : T = 25.5 $N_A = 11.293$ " "

h : T = 25.5 $N_A = 11.293$ " "

i : T = 23 $N_A = 10.636$ " "

REFERENCES :

1. German Chemical Engineering :

(a) Vol.1 No.3 p.191-198 (1978)
U.Onken,W.Schalk

(b) Vol.1 No.4 p.212-218 (1978)
W.Weisweiler,S.Rösch

(c) Vol.1 No.6 p.347-351 (1978)
H.Kürten,P.Zehner

(d) Vol.2 No.4 p.220-227 (1979)
H.Kürten,P.Zehner

(e) Vol.3 No.5 p.303-312 (1980)
J.-A.Wiedmann,A.Steiff,P.-M.Weinspach

(f) Vol.4 No.2 p.113-123 (1981)
H.Höcker,G.Langer,U.Werner

(g) Vol.4 No.3 p.125-136 (1981)
J.-A.Wiedmann,A.Steiff,P.-M.Weinspach

(h) Vol.5 No.5 p.314-323 (1982)
N.Rübiger,A.Vogelpohl

(i) Vol.5 No.6 p.342-350 (1982)
A.Steiff,P.-M.Weinspach

(j) Vol.6 No.2 p.105-112 (1983)
R.Buchholz,J.Tsepetonides,J.Steinemann,U.Onken

(k) Vol.6 No.2 p.119-128 (1983)
K.Kipke

REFERENCES :

2. Chemical Engineering Science :
(a) Vol.17 p.411-421 (1962)
S.Yagi,H.Inoue

(b) Vol.21 p.777-790 (1966)
V.Linek

(c) Vol.24 p.481-496 (1969)
V.Linek,J.Mayrhoferova

(d) Vol.35 p.1717-1723 (1980)
C.Alvarez-Fuster,N.Midoux,A.Laurant,J.Charpentier

(e) Vol.37 p.813-844 (1982)
J.Joshi,A.Pandit,M.Sharma

(f) Vol.28 p.1031-1037 (1973)
K.van't Riet,J.Smith

3. Proceedings of the Third European Conference on Mixing :
Vol.1 (April 1979)
(a) Paper D1 : R.Herringe

(b) Paper D3 : D.Subbarao,V.Taneja

(c) Paper F3 : J.Bryant,S.Sadeghzadeh

(d) Paper F4 : N.Midoux,J.Charpentier

(e) Paper F5 : M.Greaves,C.Economides

4. Chemical Engineering Progress :
(a) Vol.51 p.85-94 (1955)
T.Vermeulen,G.Williams,G.Langlois

REFERENCES :

5. Gas-Liquid Reactions : P.Danckwerts (1970)
(McGraw-Hill)
(a) Chapter 5 : p.96-151

(b) Chapter 10 : p.238-263

6. Mixing : Principles and Applications : S.Nagata (1975)
(Wiley and Sons)
(a) Chapter 8 : p.335-367

(b) Chapter 6 : p.249-296

(c) Chapter 10 : p.391-449

7. (a) Investigation of the Speed of Absorption with Chemical Reaction on a Sieve Plate : R.Pohorecki (Badania szybkości absorpcji z reakcją chemiczną, na półce sitowej) (1970)
(Wydawnictwa Politechniki Warszawskiej, praca naukowa : Chemia Nr.5)

(b) Private communication : R.Pohorecki

8. Journal of Analytical Chemistry of the U.S.S.R. :
Vol.24 p.963-965 (1969)
Y.Eremin,K.Kiseleva

9. A Text Book of Quantitative Inorganic Analysis :
A.Vogel (1951) 2nd Ed. (Longmans)

10. Physical Aspects of Bubble Dispersions in Liquids :
T.Reith (1968) thesis (Delft University)

11. International Critical Tables :
(McGraw-Hill)

REFERENCES :

12. Transactions of the Rheological Society :
Vol.21 p.1-18 (1977)
J.White,S.Chankraiphon,Y.Ide

13. Chemie Ingenieur Technik :
(a) Vol.41 p.1270-1276 (1969)
M.Zlokarnik,H.Judat

(b) Vol.52 p.362-363 : synopsis (1980)
MS 796 (19 pages)
H.Hofer,A.Mersmann

14. NATO ASI on Mass Transfer with Chemical Reaction in Multi-Phase Systems : Turkey (August 1981)
(a) Gas-Liquid Mass Transfer Parameters :
(review article) J.Charpentier,B.Morsi

(b) Reaction Engineering Problems in Slurry Reactors :
(pamphlet) H.Hofmann

15. British Chemical Engineering :
(a) Vol.15 p.522-528 (1970)
M.Sharma,P.Danckwerts

16. Agitated Three Phase Reactors : A.Kruszewski (1981)
(University of London) M.Sc. thesis

17. Chemical Engineering Journal :
(a) Vol.13 p.7-12 (1977)
H.Hikita,S.Asai,H.Ishikawa,M.Honda

REFERENCES :

18. Chemical Engineering Research and Development,
Transactions of the I.Chem.E. :
Particle-Gas-Liquid Mixing in Stirred Vessels :
(review article)
C.Chapman,A.Nienow,M.Cooke,J.Middleton
Vol.61 No.2 (March 1983)
part I : p.71-81
part II : p.82-95
Vol.61 No.3 (May 1983)
part III : p.167-181
part IV : p.182-185

19. I.Chem.E. Jubilee Symposium : (April 1982)
Symposium Series No.73 : Fluid Mixing
(a) Solid-Liquid Mixing : a state of the art summary
p.J1-J3 A.Nienow

(b) An Industrial View of Mixing Research :
p.J8-J12 J.Middleton

20. Hazards in the Chemical Laboratory :
(London, The Chemical Society)
2nd Ed. : Editor : G.Muir (March 1977)
3rd Ed. : " " : L.Bretherick (April 1981)

21. Dangerous Properties of Industrial Materials :
(Reinhold) 2nd Ed. (1963) N.Irving Sax

REFERENCES :

22. Transactions of the I.Chem.E. :
Vol.52 p88-104 (1974)
W.Bruijn,K.van't Riet,J.Smith

23. I.Chem.E. Symposium : (1981)
Symposium Series No.64 : Fluid Mixing
p.J1-J14
M.Warmoeskerken,J.Feijen,J.Smith

24. Proceedings of the Fourth European Conference on Mixing
(April 1982)
(a) Paper C2 : J.Smith,L.Goossens

(b) Paper G1 : M.Warmoeskerken,J.Smith

(c) Paper G2 : R.Kuboi,A.Nienow

(d) Paper H4 : J.Lee,S.Ali,P.Tasakorn